European Polymer Journal 164 (2022) 110974

Contents lists available at ScienceDirect

European Polymer Journal

journal homepage: www.elsevier.com/locate/europolj

Freeze/thawed polyvinyl alcohol hydrogels: Present, past and future

Hossein Adelnia [a,b], Reza Ensandoost [d], Shehzahdi Shebbrin Moonshi [a], Jaber Nasrollah Gavgani [e], Emad Izadi Vasafi [f], Hang Thu Ta [a,b,c,*]

[a] Queensland Micro- and Nanotechnology, Griffith University, Brisbane, Queensland 4111, Australia
[b] Australian Institute for Bioengineering and Nanotechnology, the University of Queensland, Brisbane, Queensland 4072, Australia
[c] School of Environment and Science, Griffith University, Brisbane, Queensland 4111, Australia
[d] Department of Polymer Engineering, Islamic Azad University-Shahreza Branch, 86145-311 Shahreza, Iran
[e] Department of Polymer Engineering and Color Technology, Amirkabir University of Technology, P.O. Box 15875-4413, Tehran, Iran
[f] Iran Polymer and Petrochemical Institue, P.O. Box: 14965-115, Tehran, Iran

ARTICLE INFO

Keywords:
Poly(vinyl alcohol) hydrogels
freeze-thawing (F-T)
Crystallization
Nanocomposites
Biomedical applications

ABSTRACT

A comprehensive review of polyvinyl alcohol (PVA) hydrogels prepared by the freezing/thawing (F-T) process is presented. We discuss their preparation, gelation mechanisms, handling of physical/mechanical properties, physicochemical characteristics, and various applications. PVA gelation through repeated F-T occurs without an externally added crosslinking agent due to the molecular structure and ability of PVA solutions to crystallize, resulting in ultrapure hydrogels. Gelation factors such as F-T cycle number, maximum and minimum temperature used, cycle duration, as well as molecular characteristics of the employed PVA samples, such as the average molecular weight, and the degree of hydrolysis, enable precise tuning of crystallization, hydrogen bonding as well as the final hydrogel properties. Incorporation of a second polymer and/or nanoparticles, which respectively results in interpenetrating polymer networks and nanocomposites, further facilitates obtaining desirable final properties to customize the gels for variety of applications. Facile customizability of the properties along with biocompatibility of PVA has led to the development of diverse prosthetic materials ranging from vascular stents, cartilages, and even contact lenses. In addition, PVA hydrogels have also been under investigation for drug delivery vehicles, and wound dressings. Furthermore, PVA hydrogels may possess a variety of other interesting features such as autonomous self-healing ability and programmed shape memory characteristic. As such PVA hydrogels can be used as components in actuators. Applications of the F-T PVA hydrogels in ionically conductive- and photonic crystal-based sensors are also discussed.

1. Introduction

Hydrogels are three-dimensional polymers produced by chemical and/or physical reactions which produce “tie points” formed by covalent or ionic bonds, strong entanglements, crystallites or hydrogen bonds. They are prepared from linear or branched water-soluble polymers to form the corresponding hydrogels. Depending on the chemical structure, they can be divided into ionic (also referred to as polyelectrolytes) and non-ionic classes [1]. In the former, free ions disrupt chain conformation due to charge screening/shielding and counter-ion interaction, leading to the deterioration of gel properties and swelling. Such an effect is however less severe in non-ionic hydrogels [e.g., poly(vinyl alcohol) (PVA)] [2]. Thus, immense attention has been directed toward this class of polymers and gels.

Poly(vinyl alcohol) (PVA) is an important and versatile non-ionic hydrophilic polymer that has drawn much attention as hydrogel,

Abbreviations: AgNPs, silver nanoparticles; β-CD-DA, β-cyclodextrin aldehyde; DC, Direct current; DMSO, dimethyl sulfoxide; ECM, extracellular matrix; F-T, freezing/thawing; GNPs, graphene nanoplatelets; GO, graphene oxide; HACC, 2-hydroxypropyltrimethyl ammonium chloride chitosan; HAp, hydroxyapatite; hCHs, human chondrocytes; HPG, Hydroxypropyl guar; IPN, Interpenetrating polymer networks; LCST, lower critical solubility temperature; LED, light emitting diode; MC3T3-E1, mouse osteoblastic; MRC-5, human fibroblast; MSCs, mesenchymal stem; MVTR, moisture vapor transmission rate; NIH 3T3, mouse embryonic fibroblast; NIR, Near infrared; NPs, nanoparticles; PAACA, poly 6-acrylamidohexanoic acid; PEDOT:PSS, (poly(3,4-ethylenedioxythiophene):polystyrene sulfonate); PEG, Polyethylene glycol; PHEMA, poly(hydroxyethyl methacrylate; poly(NIPAAm), Poly(N-isopropylacrylamide); PVA, polyvinyl alcohol; RGD, Arg-Gly-Asp; rGO, reduced graphene oxide; SV40, human osteoblast; TiO2, Titanium dioxide.

* Corresponding author at: Queensland Micro- and Nanotechnology, Griffith University, Brisbane, Queensland 4111, Australia.
E-mail address: h.ta@griffith.edu.au (H.T. Ta).

https://doi.org/10.1016/j.eurpolymj.2021.110974
Received 14 October 2021; Received in revised form 21 December 2021; Accepted 22 December 2021
Available online 29 December 2021

among other uses, due to its non-toxicity [3–8]. Generally, there are two methods for the preparation of PVA gels viz, chemical and physical methods. Chemically cross-linked PVA hydrogels can be achieved through multifunctional aldehyde molecules such as glutaraldehyde [9,10], glyoxal [11], borate-containing species [12,13] as well as irradiation techniques (e.g., gamma) [14,15]. Nonetheless, the use of a chemical crosslinker could be accompanied with adverse effects such as undesirable reactions with other components (if any) [5,16].

Physically crosslinked PVA hydrogels are typically preferred candidates for diverse applications, especially in bio-related areas due to its high level of purity and simplicity in gelation under mild conditions [17–23]. The earliest attempts for the development of PVA physical hydrogels were succeeded by Peppas in 1975 [24] who demonstrated that PVA solutions turn into gels upon repetitive freezing–thawing (F-T) cycles as a result of phase separation and crystallization [5,24–28]. Since then, many other studies have been completed by his and other groups. Specifically, what distinguishes this class of gels from others is the facile customization of properties, ultra-purity, biocompatibility, and high mechanical strength. Accordingly, since its discovery, an exponentially growing interest has been directed towards different aspects of these gels ranging from its preparation to application (Fig. 1).

In light of such an ever-growing interest, here we provide a comprehensive review on the F-T PVA hydrogels. Previous reviews on these gels in terms of preparation, properties, and biomedical application were made by Chang et al. in 2000 [29], and then by Wan et. al in 2014 [30]. Considering the significant progress and given that there is no comprehensive review on these gels since 2014, in this review, mechanism, tuning the properties, characteristics, and applications are updated. Additionally, the recently discovered features of the gels such as inherent self-healability as well as programmed shape memory is discussed in detail. The effects of various parameters on the mechanical strength and swelling of the gels are explained on the basis of gelation mechanism, which provides a clear guidance for customizing the properties. The introduction of nanoparticles or a second polymer has conferred attractive features to the gels, offering the potential to design bioactive gels soft enough for vascular stents or hard enough for cartilages. Finally, emerging and potential applications of the gels such as wound dressing, drug delivery, and sensors are discussed.

2. Synthesis of PVA and preparation of solutions and F-T hydrogels of PVA

Industrially, PVA is synthesized by the hydrolysis of hydrophobic polyvinyl acetate as direct radical polymerization of vinyl alcohol is not feasible due to the instability of the monomer (Fig. 2) [29]. Polyvinyl acetate itself is synthesized through polymerization of vinyl acetate in water-based emulsions or in solution (e.g., methanol or ethyl acetate as a solvent). The emulsion form is incorporated with certain additives and utilized as wood glue, whereas the solution form in methanol is typically used for PVA synthesis in industry. PVA synthesis involves the alkali hydrolysis of polyvinyl acetate in methanol which is referred to as the saponification process. The by-product is sodium acetate which is removed by washing processes. The degree of acetate to alcohol substitution, referred to as the degree of hydrolysis, largely determines PVA properties which will be discussed later (Fig. 2).

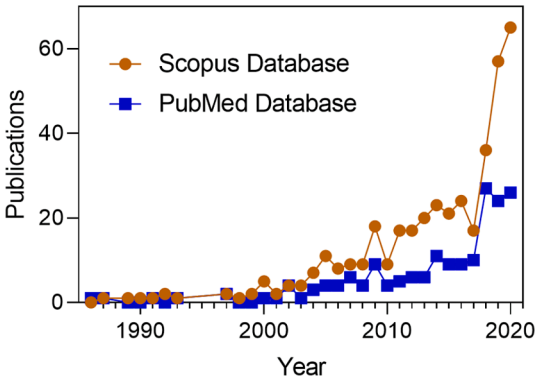

Fig. 1. Results of Scopus and PubMed database search using "polyvinyl alcohol freeze thaw" keyword from 1986 until 2020 obtained in June 2021.

As fabrication of PVA hydrogel by the F-T method requires the complete dissolution of PVA, a brief discussion on the preparation of PVA solution is made below. Clearly, the higher the degree of hydrolysis and molecular weight, the harder the dissolution process, which is attributed to inter- and intramolecular H-bonding as well as a high degree of crystallinity. Under such cases, PVA dissolution is recommended to be carried out in hot ($T > 80$℃) or boiling water for a long time under intense stirring preferably with a mechanical stirrer rather than a magnetic one which may not be suitable for highly viscous solutions. As the PVA concentration increases (generally > 15 wt%), its dissolution becomes even more challenging due to the increased viscosity which causes the powders or granules to stick together and form lumps which can be addressed through gradual addition of PVA to water. One should also note that due to poor flowability, highly concentrated PVA solutions (>30–40 wt%) may not be processed and molded easily.

In a typical hydrogel preparation through the F-T, a homogenous PVA solution is poured into a mold and frozen at −20 °C. The sample is kept under frozen state for a few hours and then thawed at room temperature [31]. This cycle is carried out several times (generally ranging from 3 to 9 times) to ensure that a strong and stable gel is achieved. Depending on the cycle duration, the F-T process may take up to several days, and thus the mold should be sealed to prevent water loss and shrinkage of the gel over time [32]. The temperatures of the F-T process, as well as the durations can vary significantly, and these effects are discussed below.

It is noteworthy to mention that due to the strong tendency of PVA for crystallization in solution state especially when the degree of hydrolysis and concentration are high, long-term storage of the solution even at room temperature may give rise to the formation of visible strands and slight turbidity which are indicative of crystallization and initiation of gelation. Therefore, prolonged storage of concentrated solutions (>15 wt%) can result in weak gels which will not meet the requirement of many applications [5]. Therefore, after a long-term storage and prior to any use, the solution is recommended to be incubated at elevated temperature (>60℃) for a few hours to disrupt weak crystalline regions, thereby regaining the solution uniformity.

2.1. Mechanism and properties of the F-T PVA hydrogels

The properties of PVA hydrogels prepared by F-T can be substantially influenced by the parameters of the gelation process such as duration, temperature, and cycle number of F-T, as well as molecular weight, concentration, and degree of PVA hydrolysis. Gel strength and swelling capacity which basically are inversely related to each other, are generally evaluated in the literature as key indicators of hydrogel properties. The higher the gelation points/junctions in the structure, the stronger the gel, and as a result crosslinking density is increased which is associated with less space for water to be absorbed. Before discussing how the properties are influenced by different parameters, the mechanism of the PVA gel formation by the F-T method is briefly explained below

Phase separation of water (under frozen state, i.e., ice) and PVA chains together with PVA crystallization are key and complementing factors in the gelation process. In the freezing step, phase separation is intensified as the ice crystals push PVA chains towards each other and then the PVA-rich phase is formed, which is separated from the water phase [28]. As the F-T cycles continue, the polymer-rich regions are further enriched with more chains, and they are expelled into closer contact with each other, facilitating H-bonding as well as crystallization (Fig. 3).

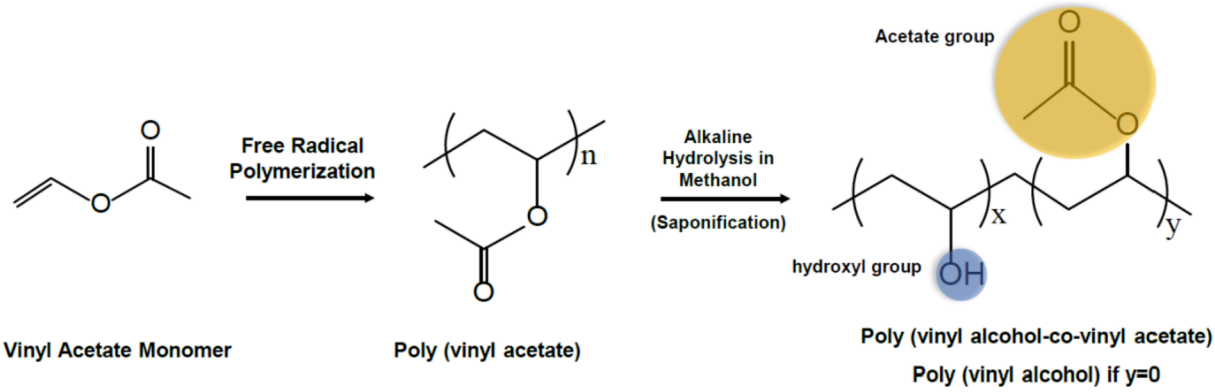

Fig. 2. Schematic illustration of PVA synthesis, and chemical structure. Due to the instability of vinyl alcohol monomer, the synthesis of PVA is carried out through alkaline hydrolysis (KOH or NaOH) of poly(vinyl acetate) in methanol which is referred to as saponification. Poly(vinyl acetate) itself is synthesized by radical polymerization through either emulsion or solution methods. Partial hydrolysis gives copolymers of vinyl alcohol and vinyl acetate, which has lower tendency for crystallinity due to bulky acetate groups. $x + y = n$ [3].

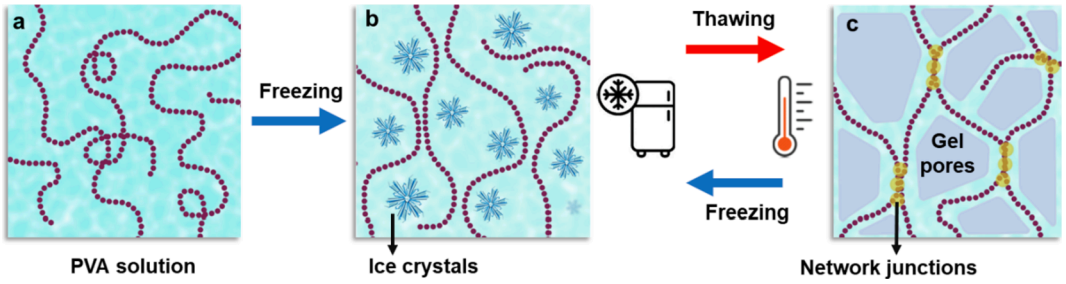

Fig. 3. Schematic illustration of the preparation of PVA hydrogels by F-T method. (a) PVA chains in solution, (b) freezing step leads to entrapment of PVA chains between ice crystals due to phase separation, and (c) under thawing, the gel network is formed as the ice crystals are transformed to the pores of hydrogels. The more the cycle number, the more chains are incorporated into the PVA crystallites, thereby strengthening the gel.

The chains form ordered arrays in the polymer-rich phase due to the high tendency of PVA for crystallization. These crystalline areas are then locked to each other due to strong inter- and intra-molecular H-bonding, providing the network with structural integrity. As the movement of macromolecules is usually a slow process, not all PVA chains are involved in the gelation in the first cycle. Therefore, more cycling (which increases the PVA crystallinity) ensures the participation of larger content of PVA into the gel structure, yielding stronger and more stable gels [20,33]. The ice crystal domains after thawing are regarded as pores of the gel surrounded by a water-impermeable PVA skeleton (Fig. 3) [28,34]. Crystallization and phase separation complements each other in the F-T process. It was found that the former and the latter mostly occur at early cycles (1 to 3), and at least in the sixth cycle, respectively [20,28]. The effect of phase separation was elucidated by assessing the evolution of porous morphology as the F-T cycles proceed [35]. Study on the rheological behavior of PVA solution during the F-T further verified the stated mechanism and demonstrated transformation of the gel microstructure [36]. Due to its key role, recent studies have focused on inducing further crystallization through stretching the specimen either during [37] or in between [38] F-T cycles. Significant improvements in mechanical properties were achieved as stretching improves the PVA chain ordering/arrangement similar to that of thermoplastics [39,40]. In the following sections, the effects of gelation parameters and molecular characteristics of PVA on the hydrogel properties are discussed in detail. Briefly, the parameters that improve crystallinity and H-bonding can enhance the gel properties (Fig. 4a).

2.2. Effects of the F-T cycle number

As mentioned above, the higher the number of cycles, the more PVA chains are pushed toward polymer-rich regions and therefore become involved in the phase separation, crystallization, and gelation. Consequently, mechanical strength, elasticity, water-resistance, and hydrogel stability are improved [28,41–43]. It was found that the modulus of the gels significantly increases up to 10 cycles while after that, the increase was not very significant [29]. These results can be described by slow macromolecular motions and crystallization process [43]. Another study, however, indicated that the compressive modulus becomes independent of the F-T cycle number after 6 cycles [20]. Regardless of the PVA concentration, there is a linear relationship between the F-T number and modulus (Fig. 4b) [20,44]. Thickness of the PVA skeleton, turbidity and pore size is increased with increasing F-T cycles (Fig. 4c) [28,35,44,45]. More F-T cycles continuously increase the pore size as seen in Fig. 4c, d. It is worthwhile to mention that the gelation may occur even after 1 cycle under certain conditions (high Mw and concentration of PVA). However, as the network is still immature and partially developed, the gels may experience significant weight loss when exposed to water. This is attributed to the dissolution of un-crosslinked chains and or disintegration of weak parts of the network [43]. Additionally, at low F-T cycles, the gels have high adhesion ability which is reduced by increasing the F-T cycles [46].

2.3. Effect of F-T time, rate and temperature

Duration and temperatures of the freezing and thawing steps are important parameters, which have significant effect on the final properties. Although −20 °C for 8 to 12 h is generally adopted for the freezing step, it was reported that lower freezing temperatures as well as longer freezing times increase the crystallinity of the hydrogel, and provide the gels with higher strength and stiffness [45,47]. Pizano et al. [48] demonstrated that lower freezing temperature or longer freezing step in PVA-chitosan hydrogels gave rise to higher number but smaller

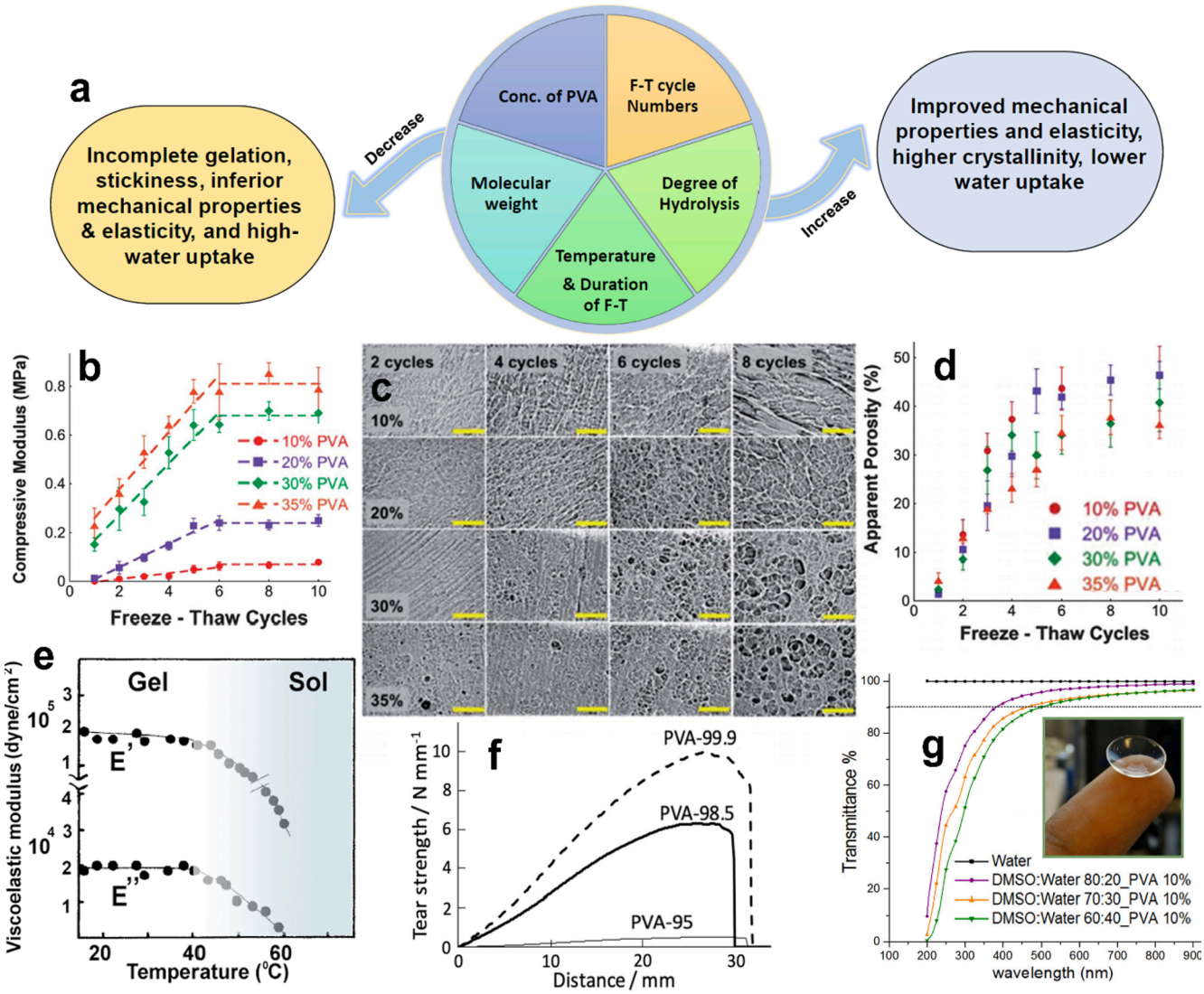

Fig. 4. Tuning the physical and mechanical properties of the F-T PVA hydrogels. (a) Effect of gelation parameters on final properties of the F-T PVA hydrogel. **(b)** Compressive modulus of the hydrogels with different concentrations (10, 20, 30, and 35 wt%) as a function of F-T cycles [20]. **(c)** SEM micrographs of the corresponding hydrogels (The scale bars = 80 μm) [20]. **(d)** Apparent porosity of F-T PVA hydrogels in the hydrated state shows that structural remodeling occurs by increasing F-T cycle number and PVA concentration [20]. **(e)** Viscoelastic modulus of the hydrogels as a function of temperature shows initiation of gel to sol transition at approx. 45 °C. This temperature is dependent upon other gelation parameters. [42]. **(f)** Tear strength of the gels shows that PVA hydrolysis degree has a great impact on the gel strength [58]. **(g)** UV–vis transmission spectra of the F-T PVA gels prepared in different DMSO:water ratios. The gels effectively absorb light in the UV range, while having high transmittance in the visible region. The inset shows the photograph of a typical prepared gel [65].

pores. A higher duration of freezing also led to lower swelling and permeation. The need for a long freezing time could be attributed to the slow movement of polymer chains and the fact that PVA crystallization is a time-consuming process.

The rates of temperature decrement or increment, respectively in the freezing and thawing steps play an important role in PVA crystallization. Slower rate in both steps can improve PVA crystallization and enhance the properties [49–52]. Lowering the thawing rate had a more significant impact than the freezing rate [49]. The thawing rate of>10 °C/min was not recommended for PVA gels [52]. The thawing rate as low as 0.2 °C/min in comparison with 1 °C/min was found to yield higher elastic modulus [53]. To the best of our knowledge, there is little or no control on the rate of both steps virtually in all studies of the literature as the specimen is simply placed in and out of the freezer, and thus control over the rates of F-T cycles is highly recommended given their effects.

It is also very important to note that the temperature at which the gels are stored/used/applied should not exceed high temperatures (>60 ℃) which can lead to melting of crystallite phase, dissociation of H-bonding, and eventually gel-to-sol transition (Fig. 4e) [42,54,55]. Although this transition may limit their application, the gels have been indicated to maintain sufficiently good structural stability under physiological conditions (pH 7.4, T: 37 °C). Besides, this transition could be exploited for the design of smart materials just as it is served for shape recovery in shape memory gels which will be discussed later in section 5.

2.4. Effect of PVA concentration

The concentration of PVA solution can be regarded as a main tool for tuning the final properties of the gel. Clearly, the higher the PVA concentration, the stronger the gel. Generally, a concentration of 5% or lower hardly gives rise to hydrogels. Also, a concentration lower than 10 wt% results in mechanically weak hydrogels. Typically the minimum concentration of 10 wt% is used in the literature, although the properties strongly depend on the other parameters (e.g., molecular weight, F-T cycles, etc.) [41,45]. The mechanical properties, as well as stability upon swelling are improved significantly and continuously at higher PVA

concentration which is attributed both to higher PVA contribution to the gel and to increased crystallization (Fig. 4b) [29,41,43,44,47]. Concentrated PVA solutions lead to larger crystallites and a higher degree of crystallinity [33]. It also leads to reduced water uptake and larger pore size (Fig. 4c) [28,33,56]. As mentioned, PVA concentration cannot exceed higher than 30–40 wt% (depending on M_w) as it yields a highly viscous and gel-like solution that does not flow easily and has difficult processability.

2.5. Effect of hydrolysis degree

The degree of hydrolysis can strongly affect the properties of the resulting hydrogels [3]. By increasing the degree of hydrolysis, more hydroxyl groups which are responsible for the formation of H-bonding strengthen the gel structure and stabilize the network integrity. On the other hand, acetate groups in the polymer backbone contribute to chemical heterogeneity along the chain, leading to disruption of chain ordering in the crystallization process [16]. Furthermore, acetate as compared to hydroxyl is a bulkier group, restricting chain ordering and crystallinity (Fig. 2) [28]. Takamura et al. [57] demonstrated the overwhelming superiority of fully hydrolyzed (98.5%) PVA over the partially hydrolyzed (88%) PVA in terms of gel strength. They also showed that partially hydrolyzed PVA was incapable of gelation below 12 wt%. The same behavior was also reported in another study by Nagakawa et al. [58]. Overall, it can be concluded that to prepare a PVA hydrogel with high strength, fully hydrolyzed PVA needs to be utilized (Fig. 4f) [47,59].

2.6. Effect of molecular weight of PVA

Molecular weight is one of the most important parameters affecting the properties of any polymeric material. Clearly, the higher the molecular weight, the stronger the PVA hydrogels. It was shown that PVA with relatively low molecular weight did not give a stable gel. However, when the molecular weight increased, mechanically tough hydrogels with improved rheological properties were obtained [60,61]. When PVA with different molecular weights (M_n: 30, 70, and 130 kDa) was tested after one cycle of the F-T, only the sample with M_n of 130 kDa was gelled [62]. Although most studies suggest the use of high molecular weight, Hassan et al. [43] demonstrated that PVA with low to intermediate molecular weights (M_w: 35 and 66 kDa) has higher long-term stability (6 months) during swelling at 37 °C when compared to the gels prepared from 88 kDa PVA. The 88 kDa PVA was shown to result in a smaller number of crystallites with larger lamellar thickness and broader crystal size distribution due to secondary crystallization [43]. It was proposed that long chain length of the 130 kDa PVA increased the chain rearrangement in the long term, which altered the gel properties.

2.7. Effect of Co-Solvent

Although PVA hydrogels have commonly been developed in water, other solvents such as dimethyl sulfoxide (DMSO) or ethylene glycol alone or in combination with water can also be employed for such purpose [62,63]. DMSO was found to be a better solvent for PVA compared to water as it led to a more extended chain conformation, and thus higher solution viscosity (3.25 dL/g for DMSO compared to 0.93 dL/g for water) [63,64]. DMSO has particularly been the subject of interest as several studies indicated that its addition to water can significantly improve the transparency of the resulting PVA hydrogels [55,63,65–68]. Hence, such high transparency could be exploited for contact lens application which will be discussed in section 7.5. It is important to note that typically after 2F-T cycles of PVA solution in water, the hydrogels become highly opaque [20].

Achieving high transparency is attributed to the formation of small fibril-like crystallites and small pores (<3 μm), both contributing to a better transmittance of light [47,63,69]. These are the direct consequences of anti-freezing property of DMSO-water mixture, which has surprisingly low freezing points, with the lowest value of −140 ℃ at 0.3 mol fraction of DMSO [70]. Small pore size is also due to the fact that the mixed solvent is no longer solidified/crystallized and thus pores are formed only as a result of phase separation rather than the forces induced by the growing solvent crystallites which are typically large [65].

The optimum DMSO content in terms of transmittance was determined to be 60 to 80 wt% (Fig. 4g) [65,66]. Importantly, DMSO removal by dialysis after the gel formation did not influence the transparency. Interestingly, a study showed that increasing PVA concentration resulted in more transparent hydrogels (30 wt% of DMSO) [68]. More interestingly, Gupta et al. [33,71] ruled out the use of DMSO as co-solvent as well as sub-zero temperature (-20 °C) by developing transparent F-T PVA hydrogels at 0 °C in the freezing step (8 h freezing, 16 h thawing at RT or 37 °C, 15 to 45 cycles of the F-T). The disadvantage of these hydrogels is the need for high number of F-T cycles (up to 45 cycles).

Contradictory results have been reported on the effect of DMSO on mechanical properties. Yusong et al. [68] indicated that gel strength decreased significantly by increasing DMSO content from 0 to 40 wt%. However, Hou et al. [66] observed a decreasing followed by an increasing trend of the tensile strength, respectively from 0 to 20 wt%, and from 20 to 100 wt%. These controversies may be explained by the high dependency of the solution properties on a certain mole fraction of DMSO as strong complexation of water-DMSO has been observed at 25 and 33 mol.% of DMSO [72–74].

Aside from transparency, if DMSO is left un-extracted, the gels will possess anti-freezing property. Though advantageous in some applications, DMSO toxicity necessitates its removal for biomedical applications. Anti-freezing feature can also be achieved by other co-solvents such as ethylene glycol or glycerol [75]. Glycerol has also emerged as a useful co-solvent to improve transparency and crosslinking degree (i.e., lower swelling ratio). Introduction of glycerol provided the F-T PVA hydrogels with an excellent moisturizing property, which effectively prevents water evaporation and gel drying [75,76].

3. Hybrid of F-T PVA hydrogels with polymers and/or nanoparticles

3.1. Semi-Interpenetrating networks (Semi-IPNs) based on F-T PVA hydrogels

Interpenetrating polymer networks (IPN) are a class of materials composed of at least two chemically distinct, but highly compatible polymers that are uniformly mixed in each other in molecular scales without any type of phase separation. The IPNs are classified into semi-IPNs and full IPNs, where respectively only one, and all polymers are cross-linked (Fig. 5a). Incorrect use of these terms in the literature is rampant and may cause controversies.

The F-T PVA hydrogels are useful platforms for the preparation of semi-IPNs from a variety of water-soluble polymers including those whose crosslinking/gelation is difficult and requires toxic agents. Such semi-IPNs simultaneously present the features of both PVA and the second polymer. The lack of need to any cross-linker, yields highly pure hybrid hydrogels and entraps the second polymer by chain entanglement. Since the second polymer in semi-IPNs is not chemically bonded, it is most likely to be released especially if there is no favorable interaction (e.g., H-bonding) with PVA. However, due to large size of macromolecules, and low diffusion rate, the release rate could be very slow, and may be considered even negligible for the short-term applications.

The second polymer especially at high concentrations may disrupt PVA chain ordering, adversely affecting the crystallinity, and eventually lowering the gelation and mechanical properties as reported in several cases such as sodium alginate [77], hyaluronic acid [78] collagen [79], Salecan [80], and gelatin [81]. For instance, the incorporation of 30% of

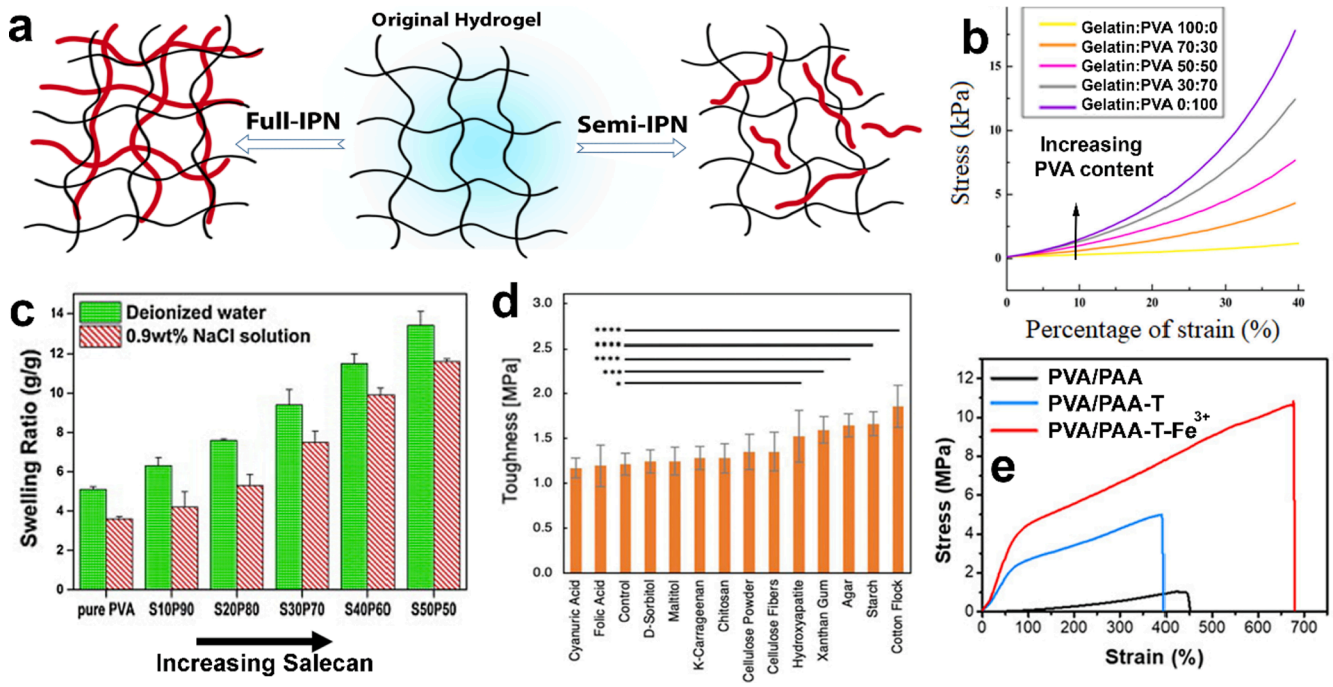

Fig. 5. (Semi)-IPNs based on the F-T PVA hydrogels (a) Schematic representation of semi-IPNs and full IPNs. **(b)** Tensile curve of gelatin/PVA semi-IPN hydrogels at different gelatin:PVA ratios shows that gelatin deteriorates the mechanical properties [81]. **(c)** Equilibrium swelling ratio of PVA and Salecan/PVA hydrogels in pure water and saline (0.9 wt% NaCl), shows that Salecan increases water uptake [80]. **(d)** Toughness of F-T PVA-based hydrogels by incorporation different additives (4 wt%). *$p < 0.05$, **$p < 0.01$, ***$p < 0.001$, ****$p < 0.0001$ [84]. **(e)** Stress–strain curves of PVA/poly(acrylic acid) (PAA) hydrogels. PVA/PAA, PVA/PAA-T, and PVA/PAA-T–Fe^{3+}, respectively stand for untreated, annealed, and annealed iron (Fe^{+}) doped hydrogels [85].

gelatin decreased the mechanical strength by ca. 25% (Fig. 5b) [81]. The decreased PVA crystallization and thus gelation are accompanied with high water uptake as reported in cases of Salecan (Fig. 5c) [80], and silk fibroin [82]. Likewise, high content of polyamidoamine-based dendrimers increased the ratio and rate of swelling of semi-IPN gels [83].

To avoid deterioration of the gel strength, lower content of the second polymer (<10 wt) should be used if it can satisfy the requirement of the given application. For instance, Koshut et al. [84] displayed that 4 wt % of various types of bio-friendly additives did not significantly affect the crystallinity. Starch was found to be the most effective additive in terms of toughness without affecting swelling for the F-T PVA hydrogels among various types of tested additives (Fig. 5d). Interestingly, the second polymer may even be exploited for the enhancement of gel strength. For instance, 7 wt% of poly(acrylic acid) remarkably improved the properties of the F-T PVA hydrogels when the gels were annealed and treated with iron cations (Fe^{3+}) (Fig. 5e) [85]. The latter forms strong complex between hydroxyl groups of PVA and carboxylic groups of PVA, reinforcing the network. Overall, in light of these studies, one should consider the inclusion of the second polymer cautiously as its high content could be detrimental to mechanical strength.

3.2. (Nano)Composites of F-T PVA hydrogels

As most common inorganic nanoparticles (NPs) have high stiffness and hardness, their introduction to the relatively soft PVA hydrogels can eventuate into a significant improvement of mechanical properties, provided that the NPs are uniformly dispersed in the PVA matrix [86]. Apart from mechanical properties, variety of NPs possess attractive features that may be exploited simply by their addition to the gels. For example, hydroxyapatite (HAp) and silver nanoparticles (AgNPs), which respectively possess osteoconductivity and anti-bacterial properties have attracted a great deal of interest in biomedical applications (section 7.2, and 10.4). Similarly, the introduction of graphene and chitosan has been studied either alone or in combination to provide the F-T PVA based gels improved mechanical properties and further antimicrobial activity, respectively [87–91].

Almost all widely used NPs have abundant polar surface functional groups, making the surface hydrophilic enough to be compatible with PVA. Therefore, this contributes to their homogenous dispersion in the matrix without the need for further surface treatment and functionalization. However, in some cases, the small size of the NPs could be still a challenge as they have high surface energy, leading to aggregation.

It has been found that the PVA hydrogels due to their reducing and stabilizing capabilities can be employed as micro-reactors for the synthesis of AgNPs, significantly improving colloidal stability.[86,87,91]. The same approaches have also been adopted for the synthesis of iron oxide NPs [92], and HAp [93], and gold NPs[94]. Interestingly, Golabdar et al. [86] recently revealed that PVA itself has both reducing and stabilizing abilities. Simple heating of silver nitrate solution in the presence of PVA yielded stable AgNPs. Similarly a spontaneous reduction of ionic gold to atomic one (Au^{III} to Au^{0}) was reported in the presence of PVA [94]. This is in contrast to the, previous studies where either high voltage electrochemistry, chitosan, and sodium borohydride ($NaBH_4$) were necessarily applied for AgNPs synthesis [87,91]. The as-prepared mixture of PVA/AgNPs without further purification was directly subjected to F-T and gelled. Because of their metal nature, AgNPs can also endow the composites with electrical conductivity [86]. Although AgNPs like other NPs improve mechanical properties, they do not noticeably impact PVA crystallinity [86,95,96].

Clay-based nanosheets are also of great interest due to inexpensiveness, and abundance. Depending on their chemical and crystalline structure, they are divided into a variety of subgroups, such as sepiolite [97], montmorillonite [98], laponite [99], halloysite nanotubes [100], etc. The addition of clay-based nanomaterials into PVA hydrogels have led to a lower melting temperature, higher re-swelling ratio, better elasticity, improved thermal stability and mechanical properties. [98,99,101–107]. Exfoliation of the clay nanosheets is a key requirement for fabrication of effective hydrogel nanocomposites which can be met by the stabilizing effect of PVA without the need to use any other agent [99]. Such nanocomposite hydrogels have been tested for the

removal of cadmium ions [99,101], methylene blue [102], for subsurface irrigation [104], and for wound dressing [105] with promising results.

The addition of boron nitride nanosheets to PVA was found to improve thermal diffusivity and conductivity [108]. The nanosheets were modified with hydroxyl groups to improve their dispersibility in PVA matrix, leading to an effective load transfer at a very low concentration. Cerium oxide NPs exhibit pro- or anti-oxidative properties depending on pH and thus they were incorporated to the F-T PVA-chitosan hydrogels for wound healing application [109]. The NPs increased the porosity and swelling, while providing anti-bacterial activity. PVA-based ferrogels were prepared by infusion of iron ions into the gels first, followed by co-precipitation [92]. The composite gels were employed for slow release of ibuprofen.

Among almost all NPs, graphene oxide (GO) and its derivatives have attracted more attention for the development of tough and functional nanocomposites [110–112]. They consist of thin 2D layered sheets of sp^2 carbon atoms arranged in honeycomb structures. The monolayer GO possess extremely high modulus (0.2 to 1 TPa [113]), strength (up to 130 GPa [114]), flexibility as well as a high specific surface area (300–800 m^2/g) which is rich in oxygen-containing functional groups such as hydroxyls, carboxylic acids, and epoxides [115–117]. These polar groups can establish strong interaction with PVA, resulting in a homogenous dispersion of GO and excellent mechanical properties as summarized in Table 1. Such GO-PVA interactions were shown to give rise to gelation even without the F-T cycles under certain conditions (GO and PVA conc. higher than 0.25, and 5 mg/mL, respectively) [118]. Therefore, GO sheets can function as 2D macromolecule for crosslinking of PVA as indicated by other studies as well [119,120].

Liu et al. [111] showed that the addition of as low as 0.8 wt% of GO to the F-T hydrogels enhanced the tensile strength, compressive strength, and elongation at break by 132%, 36%, and 50%, respectively

Table 1
Mechanical properties of nanocomposites of the F-T PVA hydrogels with GO.

PVA M_W (kDa)/ Conc. (wt. %)	GO (wt.%)	Other materials	Tensile modulus (MPa)/strength (MPa)	Elongation at break (%)	Compressive modulus (MPa)/ strength (MPa)	Remark	Ref
n.a/n.a	2 wt%	Sodium alginate	n.d/3–6.5	n.d	n.d/1.5–4/n.d	2 wt% of GO increased the compression and tensile modulus by 4 and 2 times. GO also reduced the swelling ratio. Alginate was gelled with calcium solution either before or after F-T. The double network hydrogels showed shape-recovery and self-healing properties. It was found that if alginate is gelled first, denser structures, lower swelling ratio, and higher mechanical properties are achieved. Good removal of methylene blue (a cationic dye) was also achieved due to the presence of alginate (anionic biopolymer).	[31]
74.8/5 wt/v %	0.1 wt/v %	Sodium alginate	n.d/0.15–0.24	ca. 68–75	n.d	After F-T, sodium alginate was also crosslinked by calcium solution. The hydrogels had an effective adsorption towards methylene blue The GO addition increased the modulus and strength, while decreasing the elongation at break.	[126]
n.a/9	1–3		n.d	n.d	Up to 0.23 /3–25	2, 2′-(Ethylenedioxy)-diethanethiol was used as a crosslinker for GO. The incorporation of crosslinked GO improved the mechanical properties and led to a favourable cell adhesion and proliferation.	[110]
n.a/10.8	0.8	–	n.d/1.5–3.5	110–165	n.d/1.0–1.4	The addition of GO to the hydrogels improved the mechanical properties greatly. The hydrogel showed no cytotoxicity against osteoblast cells.	[111]
89–98/15	0.56-to 1.7%		n.d/n.d	400–850	0.2–0.9/n.d	β-cyclodextrin GO was modified with a silane coupling agent, yielding GO with amine (NH_2) functional groups. The amine groups were then reacted with aldehyde groups of β-cyclodextrin aldehyde (employed as a crosslinker for the modified GO), yielding GO networks. Introduction of the GO-based network to PVA significantly improved modulus and elongation at break simultaneously. The hydrogel showed no cytotoxicity against mouse embryonic fibroblast (NIH 3 T3) and human chondrocytes (hCHs).	[123]
88/10	0.005–0.2		n.d/0.25–0.52	405–547	n.d/0.081–0.091/n.d	The F-T hydrogels were further crosslinked with boric acid, which lowered the PVA crystallite size, and led to higher water uptake. Tensile and compression properties were evaluated showing a significant improvement even for elongation at break. It was stated that GO sheets are aligned under extension.	[127]
DP = 1700/ 15	0 to 0.2		n.d/0.6–1.4	n.d	n.d/0.45–0.95/n.d	Improved mechanical properties as well as decreased friction coefficient due to interactions between the GO-PVA. The friction coefficient was stable over time and lower as compared to samples without GO. The melting temperature and crystallinity of the hydrogels were increased by GO addition.	[128]
n.a/25 wt/v %	0.5, 0.8, 1.0, 1.5	Regenerated cellulose	n.d/0.52–0.73	103–238	n.d	Interestingly, increasing GO improved both tensile strength and elongation at break, simultaneously. The latter was attributed to PVA-GO interaction and the movement of GO sheets under extension, leading to straightening the PVA chains. The gels exhibited pH-sensitivity (i.e., increased swelling at higher pH) due to ionization of carboxylic acid of GO.	[129]

(3F-T cycles). Another study showed that GO was only effective up to 1.5 wt%, while higher contents deteriorated the mechanical properties [121]. It was also shown that the presence of poly(ethylene glycol) (PEG) improved GO exfoliation and results in a better GO dispersion. More importantly, increased crystallinity of the hydrogels was also demonstrated which was attributed to the nucleation effect of GO [121]. Interestingly, the addition of GO with HAp endowed the PVA solutions with printability due to weakened H-bonding and lowered entanglement, resulting in a low zero shear viscosity (η_0) and broad shear-thinning region [122]. Furthermore, double networks (i.e., IPNs) based on GO and PVA have recently been developed and found to significantly improve the mechanical properties [123]. To fabricate the double networks, the GO sheets were crosslinked with β-cyclodextrin aldehyde (β-CD-DA) in the presence of PVA followed by exposing the samples to 9F-T cycles. The GO network increased the compression modulus and elongation at break by 5.3, and 2.5-fold, respectively [123].

GO and its derivatives also have excellent electrical conductivity and thermal stability provided that the functional groups are reduced (referred to as graphene nanoplatelets (GNPs) or reduced graphene oxide (rGO)) [124,125]. However, in the reduced form, achieving a stable dispersion in aqueous media is extremely hard due to the absence of any polar functional group. Irreversible agglomerates may form by van der Waals interactions and π–π stacking [31]. This could be a reason why most studies related to PVA hydrogels focused on the use of GO rather than GNPs or rGO (Table 1). The use of DMSO for gel preparation could be regarded as a possible approach for achieving stable dispersions of rGO or GNPs and is highly encouraged to be studied as it has not yet to the best of our knowledge.

4. F-T PVA hydrogels with self-healing properties

Self-healing refers to the ability of spontaneous recovery of structure and properties after a damage, in the absence of human intervention. This attractive feature prolongs the material lifetime and lowers the cost. Such materials can be developed based on the release of a healing agent upon the damage or alternatively through activation of a specific molecular functionality triggered by a stimulus such as light [31,130–132].

Outstandingly, PVA hydrogels fabricated by the F-T process were found to possess self-healing ability in the absence of any external healing agent or stimulus (Fig. 6a), if they are provided with two main criteria: (i) sufficient hydroxyl groups and (ii) high chain mobility [131]. The combination of these two contributes to the formation of new H-bonding and repairing the damage spontaneously. The concentration of PVA solution used for gel preparation is the most important parameter, affecting the amount of hydroxyl group in the cut/damaged surface. Clearly, the lower the hydroxyl population, the lower the chance of H-bonding for self-healing [131]. Unanimously in different studies, self-healability was reported for the PVA concentrations of $>$ 25 wt% [131,133–135]. It was shown that under concentrated conditions, crystallinity percentage is greatly increased, whereas the crystallite size is decreased. Therefore, the lack of self-healability at low PVA concentrations (i.e., $<$25 wt%), aside from low hydroxyl population, could be due to the large crystallites too, hindering chain diffusion/re-entanglement.

The incorporation of melamine deteriorated self-healing ability of the F-T PVA hydrogels (35 wt% PVA). [134]. Melamine established strong H-bonding with PVA and strengthened the hydrogel. However, at the same time, this led to reduced chain movements and adversely affected chain inter-diffusion as well as the formation of new H-bonding

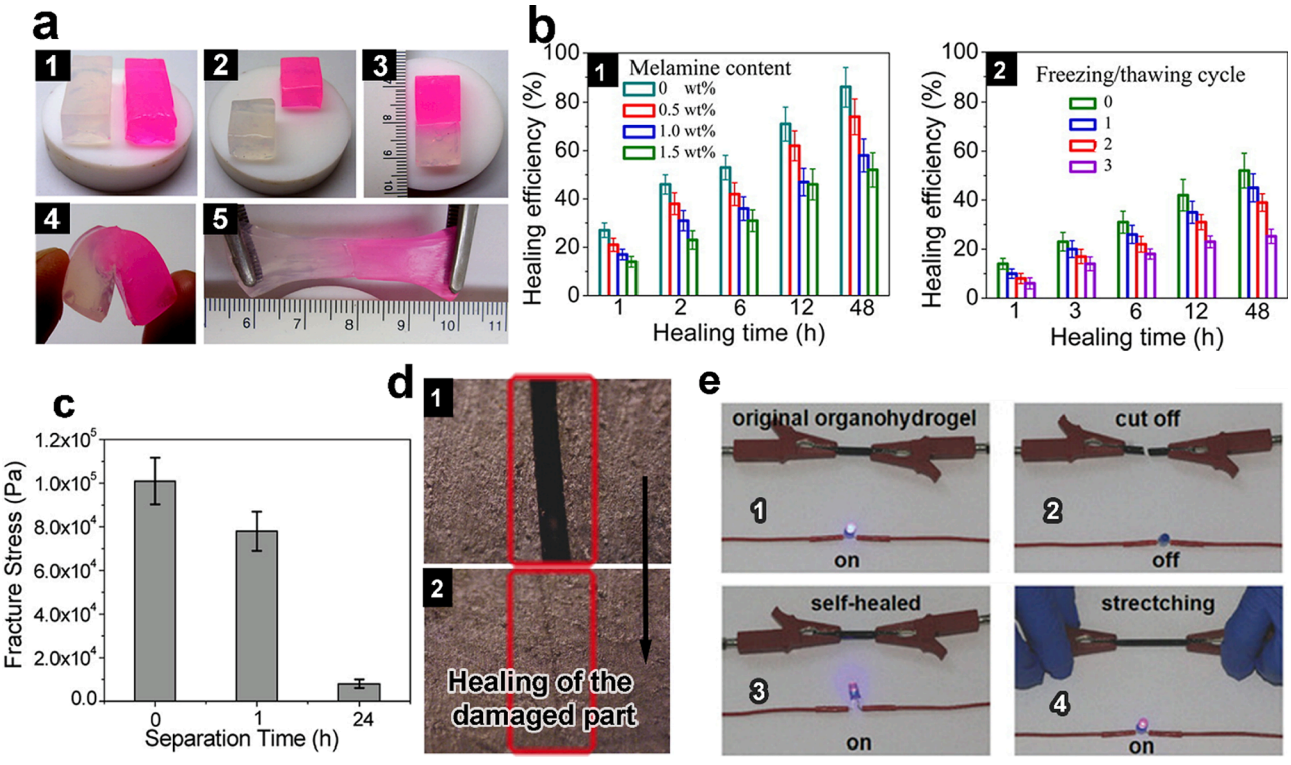

Fig. 6. Autonomous self-healing ability of the F-T PVA hydrogels: (a) Photographs show the self-healability without any intervention. **(1)** two pieces of original hydrogel (one pure, the other dyed for visualization); **(2)** the gels were cut into two, and one slice from each sample were put together quickly **(3)** the self-healed hydrogel after 12 h at room temperature; (4) the self-healed gel can withstand bending, and (5) 100 % extension [131]. **(b)** (1) Effect of melamine content, and (2) the number of the F-T cycles on self-healability of the F-T PVA hydrogels [134]. **(c)** Effects of separation time of the cut slices on fracture stress [131]. **(d)** The self-healing performance of the F-T PVA-polydopamine hydrogels after 3F-T cycles treatment. The optical microscopy photos of the cut surface **(1)** before and **(2)** after being heated after NIR irradiation (output power: 0.75 W cm^{-2}, irritation time: 30 s) [138]. **(e)** Circuit comprising self-healing anti-freezing conductive organohydrogels in series with a light emitting diode (LED) indicator: **(1)** undamaged, **(2)** furcated, **(3)** self-healed, and **(4)** stretched after healing [62].

at fractured surfaces (Fig. 6b-1). Similarly, a higher number of the F-T cycles, which has similar effect on the gel properties, reduced the self-healability (Fig. 6b-2). Similar results were also observed in PEG/PVA double networks when the cycle number increased [136]. Therefore, it can be concluded that self-healability has an inverse relationship with the gel strength. In fact, any parameter that decelerates or hinders the chain mobility could adversely affect the self-healing ability [131,135].

The effect of chain mobility was also illustrated by changing the healing and separation times in the PVA-based hydrogels prepared with only one F-T cycle and concentration of 35 wt% [135]. The recovery of mechanical properties (referred to as recovery ratio or healing efficiency) increased at longer healing time (i.e., the duration of putting the two cut pieces together). This is due to the fact that the formation of new H-bonding and chain diffusion as the main factors of self-healing are time-consuming processes [135]. The separation time of the two pieces before rejoining can also affect the recovery ratio [131]. The self-healability reduced continuously with prolonging separation time and lost completely after 24 h which could be attributed to the minimized surface energy as a result of partial drying and chains rearrangement (Fig. 6c). In other words, the cut surface after ageing does not have sufficient free hydroxyl groups for establishing new interactions [135]. Furthermore, if the cut surface is left to dry, the molecular motion of the chains is significantly lost and thus they are no longer able to re-arrange and re-entangle with the other chains to self-heal [131,135].

To enhance the self-healing properties, other complementing strategies have also been implemented as below [31,137,138]. For example, strong H-bonding interactions between PVA and polydopamine nanoparticles were exploited for self-healing of the ensuing composite hydrogels [138]. Polydopamine has an excellent photo-thermal conversion efficiency as it can convert light energy (i.e., infrared light 760–1500 nm) to heat energy. Upon laser irradiation (0.75 W cm^{-2}, for 30 s), the fractured surface was heated, which promoted macromolecular movements, H-bonding formation, and consequently healing of the damaged part (Fig. 6d).

Rong et al. [62] induced the healing by heating the cut surface (80 °C) and applying a freezing step at −20 °C. The gels were electrically conductive through loading with PEDOT:PSS [poly(3,4-ethylenedioxythiophene):polystyrene sulfonate] as conductive pair polymers. Although the healing cannot be classified as completely autonomous, it recovered the electrical circuit and lighted the LED indicator (Fig .6e). Heating of the damaged part contributed to the healing process as it melted the PVA crystallites which have low chain mobility, thereby facilitating the formation of new crystallites by one F-T cycle. Guo et al. [139] also prepared semi-IPN hydrogels of PVA and poly 6-acrylamidohexanoic acid by the F-T process and showed reversible pH responsive self-healing properties of the gels. Under acidic media, due to protonation of COOH groups of the latter polymer, H-bonding is formed, leading to self-healing whereas under alkaline condition, COOH groups become ionized (i.e., deprotonated), resulting in separation of the pieces.

In conclusion, in order for the F-T PVA hydrogels to spontaneously and autonomously heal themselves, they should meet certain criteria such as high concentration and availability of free hydroxyl groups. Having a stronger gel (e.g., by higher F-T cycles) may results in a lower healing efficiency. The healing process is typically time consuming which may be accelerated by complementing approaches such as iron-catechol, boron-based bonds, etc.

5. PVA hydrogels with shape memory properties

Shape memory polymers are defined as polymers with the ability to change and regulate their shape until reverting to the initial shape upon exposure to an external stimulus (e.g., temperature, light, and pH) [140–144]. Such polymers can have a variety of applications in soft robots, actuators, and specifically in biomedical areas where this feature can be exploited in vascular stents, and self-tightening sutures [145,146].

Shape memory process consists of three steps viz. deformation, fixation, and shape recovery. In the deformation stage, an external force is applied to the material to convert its permanent shape to a momentary shape. Then, in the fixation stage, the induced deformation is stabilized through a strong interaction (e.g., crosslinking). When the interactions are fully established and the second network is created, the applied force is released and as such the temporary shape is accomplished. The first two stages are collectively referred to as programming process [147]. Finally, in the shape recovery stage, an external stimulus such as temperature capable of disintegration of the second network is applied to break the interaction/crosslinking to return the material to its original shape [144,148,149].

Interestingly, the F-T-prepared PVA hydrogels exhibited shape memory behavior by the inclusion of a suitable compound functioning as primary crosslinker. The gelation by the F-T process is then performed in the fixation step which is served for the creation of secondary networks to fix the temporary shape. As the PVA crystallites are melted via increment of temperature (>50–60 °C), any stimuli generating heat (e.g., ultrasound) can be employed for disintegration of such networks and consequently for recovery of the original shape [148,150]. Fig. 7a shows the procedure of preparation of shape memory hydrogels.

The selection of an appropriate multifunctional agent for the formation of primary PVA network is of utmost importance. The primary network should have enough strength to withstand the stress/strains induced in the deformation step until the shape is fixed by the F-T cycles. The primary network should also be resistant to elevated temperatures at recovery step otherwise, the gel will be completely disintegrated. Basically, to ensure strong interaction with PVA and to have a structurally stable gel, the agent should bear abundant functional groups (e.g., NH_2, and COOH), as depicted in the Fig. 7b.

The incorporation of a small amount (0.5–2 wt%) of polydopamine particles to PVA provided the hydrogels with shape memory property (Fig. 7c1, 2, and 3). Polydopamine has abundant catechol and amine groups and thus can form strong interaction with the hydroxyl groups of PVA, inducing a physically cross-linked network. The shape recovery was triggered by NIR light (808 nm, 0.25–1.5 W/cm^2) which led to a huge temperature increment (60 and 90 °C, respectively for 0.5 and 2% as shown in Fig. 7c4), melting of the crystals, and consequently recovering to the original shape [138]. This is due to the photothermal ability of the particles as discussed above in section 4.

Similar to polydopamine, incorporation of polyaniline could also provide the F-T PVA hydrogels with shape memory property as it forms H-bonding with PVA through N-H groups [151]. The shape recovery was triggered by exposing the composite hydrogels to either water or NIR light (at 808 nm, and 4.2 W/cm^2) (Fig. 7d). In case of the former and latter, the shape recovery is respectively attributed to the water-induced plasticization, and melting of crystallites due to photothermal effect of polyaniline (similar to polydopamine particles) [151].

The use of multifunctional small molecules such as melamine [134] and tannic acid [152] has also shown promising results in terms of shape memory effect as they can form multiple and strong H-bonding with PVA, resulting in crosslinking. Therapeutic ultrasound (power output: 2.2 W/cm^2 and frequency 3 MHz) in the case of PVA-melamine, and simple hot water immersion at 60 °C in the PVA-tannic acid hydrogels were utilized to trigger the shape recovery. In the ultrasound process, the absorption of sound waves by the material generates thermal energy, thereby melting the crystallite regions formed in the fixation stage, and returning to the original shape [134,152]. Network formation by a second polymer can also be adopted for PVA-based shape-memory materials. For example, PVA-PEG double network hydrogels exhibited fast shape recovery at T > 60 °C (approx. 15 s) as well as superior mechanical properties [136].

Overall, whilst there may be other methods for the design of shape memory PVA hydrogels, the discussed approach herein is the most convenient and widely investigated in the literature. The establishment

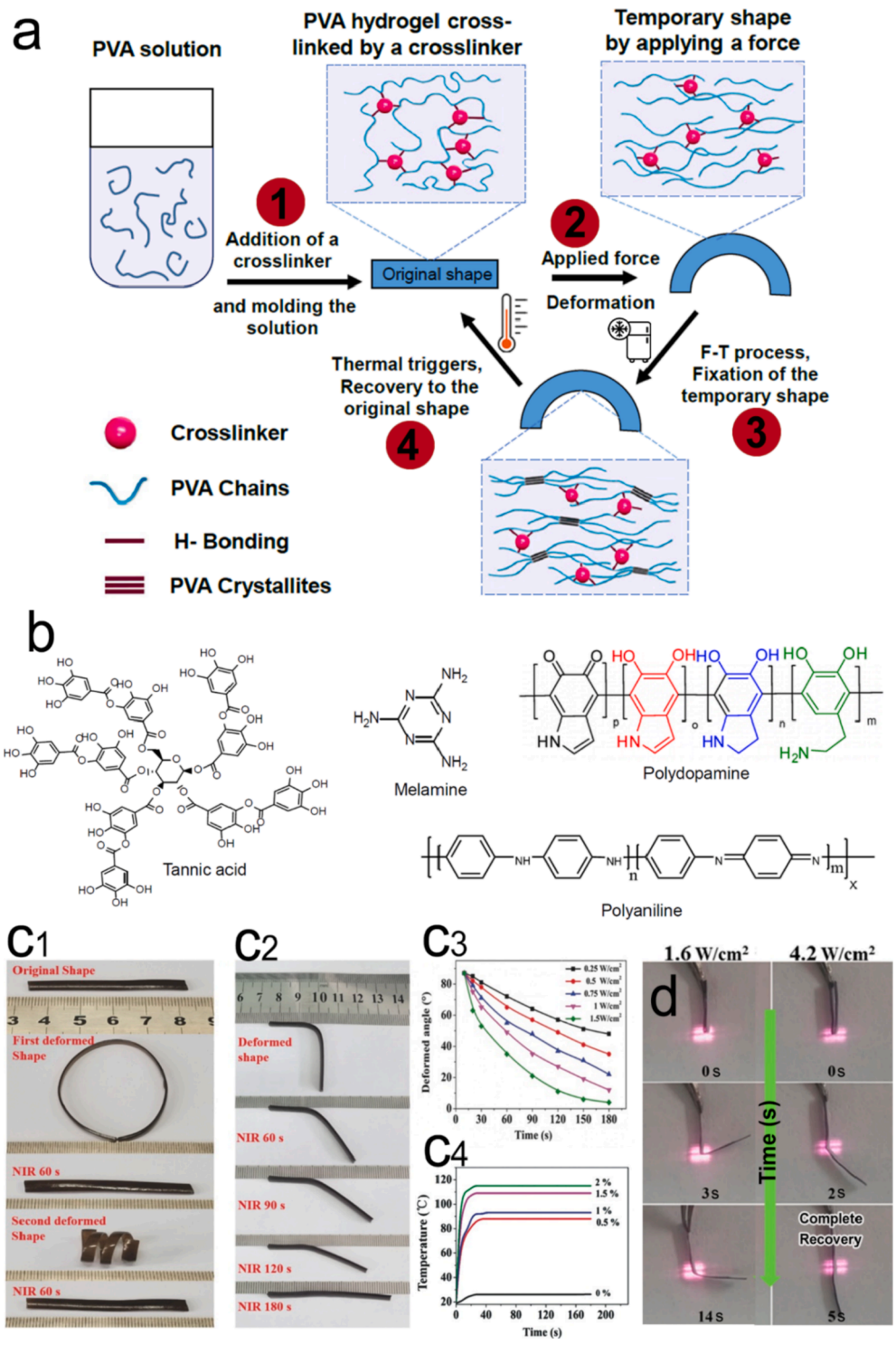

Fig. 7. Shape memory behavior of the F-T PVA hydrogels. (a) Schematic representation for development of F-T PVA-based hydrogel with shape memory ability. **(1)** Crosslinking (either physical or chemical) of PVA by adding a suitable agent. **(2)** Deformation of the primary gel by applying a force, **(3)** Fixation (i.e., the formation of the second network which is attained by F-T process) is carried out. The formed crystalline regions are able to retain the deformed shape (if not, more cycling is needed) **(4)** A thermal trigger is applied to melt crystalline domains and recover the temporary shape. **(b)** Chemical structure of multifunctional agents studied for shape memory PVA hydrogels. **(c1)** Shape memory behavior of the F-T PVA hydrogels loaded with polydopamine particles under NIR irradiation with different shapes. **(c2)** The decrease of deformed angle as a function of time at different output power for the samples on the right panel. **(c3)** Temperature change of the hydrogels as a function of time with different polydopamine particles contents [138]. **(d)** NIR light-induced shape memory behavior of PVA-polyaniline under different power density light irradiation (the number stands for the time in second required for complete shape recovery) [151].

of a robust primary network is vital for overall stability of the gels before fixation and after recovery, whereas the crystallites formed by the F-T are only served to maintain the temporary shape. Accordingly, shape memory parameters such as fixing ratio and recovery ratio could be tuned by changing F-T parameters. As an example, more F-T cycles resulted in higher fixing ratios and lower recovery ratios [134]. Last but not the least, the use of chemical cross-linker such as glutaraldehyde for primary network could be an interesting approach as it ensures the network stability even under harsh conditions. To the best of our knowledge, there is no report on utilizing such a strategy and thus future studies on this topic would be of great interest.

6. Emerging application of F-T based PVA hydrogels

Chemical modification of PVA is typically challenging due to low reactivity level of hydroxyl groups, making it difficult to provide the PVA-based hydrogels with a new functionality. However, the simplicity of gel formation by F-T, together with the ability to incorporate a wide variety of NPs (i.e., hydrogel nanocomposites) and polymers to PVA hydrogels (i.e., IPN and semi-IPNs) opens up a wide window of

opportunity for advanced areas which are discussed below.

6.1. Actuators based on the F-T PVA hydrogels

Soft actuator materials change their shape or size in response to a stimulus (e.g., electricity, light, and pH), presenting them highly suitable for soft mechatronics and robots [153–155]. Polyelectrolytes typically exhibit a response to DC (i.e., direct current) electric field in relatively low voltage (<24 V) as they carry ionic groups along the chain [155]. Despite being non-ionic, PVA hydrogels have shown electro-actuation under high voltage electric fields (up to a voltage of 1.6 KV) [156–159]. The displacement equal to 3600 ppm strain with an electric field strength of 0.4 V/μm was achieved for PVA-based hydrogels. The incorporation of cellulose nanocrystals [157,158] and/or polyacrylic acid [159] has improved electro-actuation. Poly(N-isopropylacrylamide) [poly(NIPAAm)] – a well-known polymer with lower critical solubility temperature (LCST) at 32 °C- was polymerized into the F-T PVA gels, yielding temperature-sensitive actuators capable of gripping objects as heavy as 20 times of the gel weight [160]. Magnetic field is another simple approach for actuation. The F-T PVA hydrogels loaded with iron oxide particles (Fe_3O_4) showed instantaneous deflection and recovery respectively upon application and removal of a magnetic field [161]. Considering the simplicity in the design of shape memory PVA hydrogel, providing actuation property particularly by polyelectrolytes could be of great interest on which minimal attention has been paid to the best of our knowledge.

6.2. Ionically conductive PVA-based gels for sensor applications

As compared to polyelectrolytes, the physiochemical properties (e.g., swelling) PVA is less/ moderately affected by media with high ionic strength, due to its nonionic nature [162]. On this basis, PVA-based gels loaded with electrolytes can be utilized as conductive gels for diverse applications. In this regard, PVA, as a non-ionic polymer, can serve as a suitable host for large quantities of ions to be accommodated with moderate impact on the structure. $FeCl_3$-loaded PVA-poly(acrylic acid) full IPNs exhibited ionic conductivity of ca. 0.14 S/m which was sufficiently high for sensor applications, in spite of low value when compared with metallic- or carbon-based conductive nanocomposites [163]. The hydrogel resistance had a linear relationship with tensile strain, with no hysteresis in stretching/relaxation cycles (due to gel elasticity), characterizing them as suitable strain sensors. Upon stretching, the distance of the conductive path increases, lowering the conductivity (Fig. 8a). Similarly, applying pressure was associated with an increase in

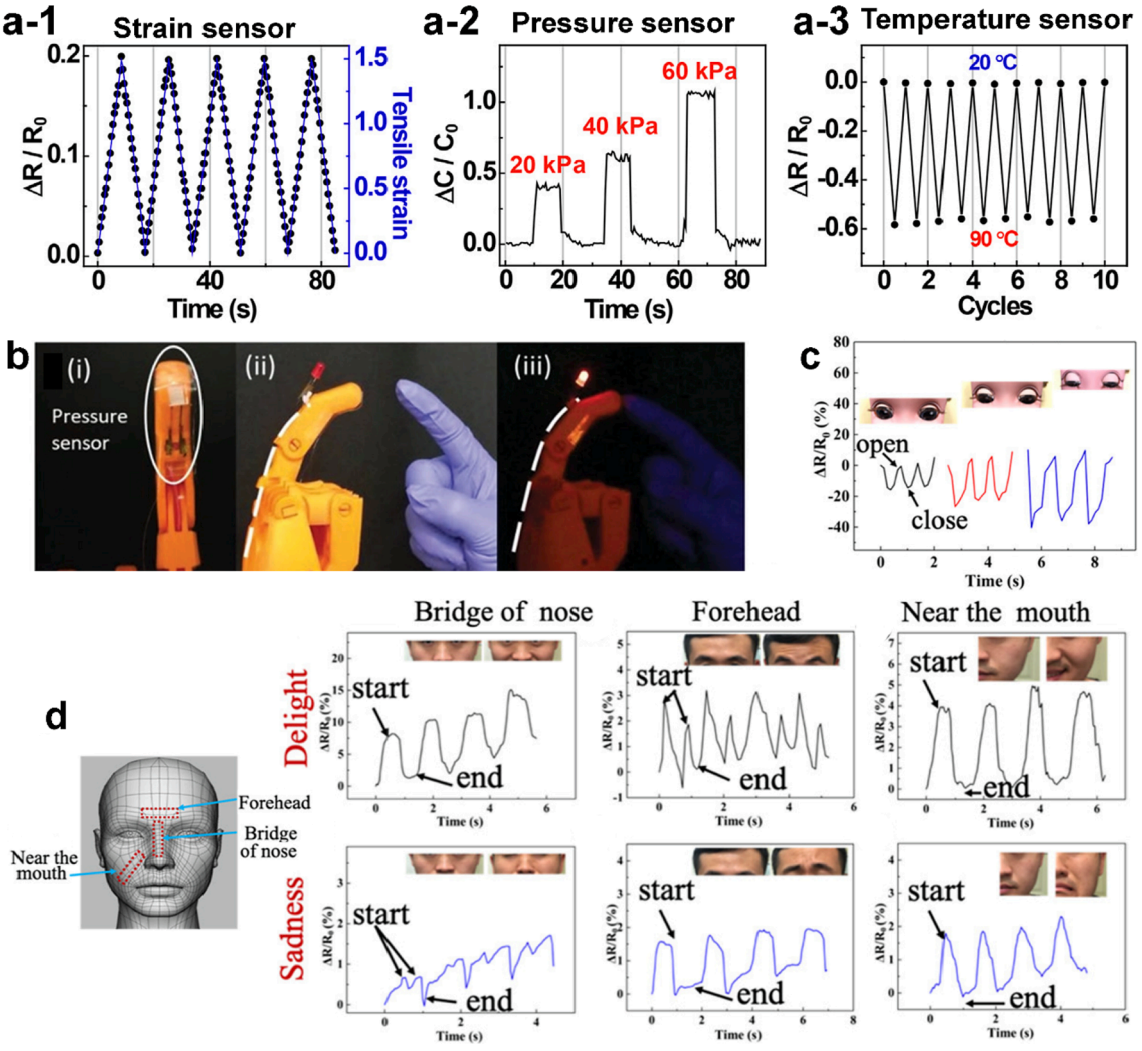

Fig. 8. Ionically conductive F-T PVA-based gels for sensing application. (a) Sensing performances of PVA/poly(acrylic acid) IPNs in terms of $\triangle R/R_0$ as a function of time for different **(a-1)** strain, **(a-2)** pressure, and **(a-3)** temperature [163]. **(b)** Demonstration of PVA-hydroxypropyl cellulose semi-IPN gels sensor on robotic hand with DC applied shows that a touch from human finger can trigger the LED [167]. **(c)** The change in resistance of ionically conductive PVA-based gels (soaked in NaCl) upon blinking [76]. **(d)** Attachment of the ionically conductive PVA gels to the forehead, near the mouth, and bridge of nose for detection of sadness and delight moods [76].

resistance with negligible hysteresis (Fig. 8b). Temperature was also successfully sensed by these gels due to the direct relationship of ionic conductivity to temperature (conductivity = ions mobility × ion concentration [164–166]) (Fig. 8c). Regarding the temperature sensing, the gels were exposed to temperatures as high as 90 °C. Such elevated temperatures could certainly disintegrate the F-T PVA gels (as discussed in section 2.2) which was not taken into consideration in the study.

In another study, sodium chloride (1 to 5 M) was incorporated into PVA-hydroxypropyl cellulose semi-IPN gels for the preparation of sensors [167]. Although detrimental to mechanical strength, the cellulosic polymer contributed to a more porous structure and electrical conductivity. The porous structures played an important role in sensor efficacy by providing space and path for ion migration [167,168]. The conductivity exhibited good sensitivity up to 400% strain. Under no pressure, the whole gel was open-circuited and thus the LED on the finger remained off (Fig. 8b (ii)). Once a human finger touched the gel which applies a certain level of pressure, the resistance is reduced, triggering the LED to turn on (Fig. 8b (iii)). A recent study simply soaked the F-T pure PVA hydrogel into 2 M sodium chloride and developed transparent ionically conductive sensors for smart contact lens applications where staring (i.e, eye blinking) is correlated to the gel resistance (Fig. 8c) [76]. The gels were capable of sensing the facial muscle movement as well, when they were attached to different parts of the face, enabling detection of sadness and delight moods (Fig. 8d).

Although interesting studies have been conducted on ionically conductive gels, their practical use is restricted due to the high content of ions which is far higher than that of biological conditions, leading to a plethora of issues for biomedical sensing applications. Even for non-biomedical purposes, if the gel come in contact with surfaces, this could potentially lead to corrosion. Therefore, manipulating the conductivity by other complementary methods (e.g., conductive NPs) is highly encouraged, while keeping the ion concentration low. Furthermore, another cause of concern is that the ion content may vary if it is exposed to other fluids and wet surfaces due to diffusion, which clearly changes the sensing parameters/values, and thus should be taken into consideration.

6.3. Photonic crystals based on F-T PVA hydrogels

The F-T PVA gels have also been employed for the preparation of photonic crystals [169–171]. Asher's group whose expertise is photonic crystals was the first who developed opals based on F-T PVA gels [170]. Typically, the ordered arrays of colloidal particles can generate specific colors depending on the inter-particle distance in the crystals. The idea behind the incorporation of colloidal crystals into hydrogels is to tune the inter-particle distance by the swelling change particularly through a stimulus (e.g., pH), which is then translated into distinguishable color change by the naked eye. Therefore, on the basis of such changes, sensors can be developed and designed [171]. Considering the nonionic nature of PVA, which makes it insensitive to pH in particular, a question is posed: where do the F-T PVA gels stand in the field of photonic crystals? The preparation of perfect photonic crystals is dependent upon the immaculate self-assembly of particles without any defect to generate uniform color in the opals. Such self-assembly, especially for non-close-packed structures is directly related to electrostatic repulsion of the particles. Small quantities of ions may disrupt the inter-particle electrostatic repulsion and in turn the crystal structure of colloids [172]. PVA or other non-ionic polymers are generally used to immobilize the photonic crystal with minimal impact on the structure. After fixation by the F-T PVA networks, polymerization of the desired monomer(s) is carried out. In other words, the PVA network can perfectly immobilize the colloidal crystal structure for further processes without any adverse effect on particle charge due to its non-ionic nature [173]. Finally, the PVA network can be optionally removed and dissolved by thermal disintegration [174,175]. However, if left in the structure, one can still take advantage of PVA features while its inertness should not adversely affect the opal color.

According to the above approach, several stimuli-responsive photonic crystal systems have been developed. Optical sensors for pH and metal cations (Cu^{2+}, Ni^{2+}, and Zn^{2+}) were prepared by PVA-poly(acrylic acid) hydrogels [176]. Polystyrene NPs (size: 186 nm) were fixed in the F-T PVA gels followed by polymerization of the acrylic acid monomer with a crosslinker. The IPNs were then chemically modified with 8-hydroxyquinoline which is a strong chelating agent for metal cations. The gels exhibited color change upon a variation in pH and/or nickel concentration (Fig. 9a, b, and c). The lower the swelling, the shorter the particle–particle distance, thereby shifting the diffraction peak to lower wavelength values. Low swelling for anionic polymers typically occurs in the acidic media and/or high metal ion content [177]. In addition to pH, another study revealed that PVA/poly(acrylic acid) photonic crystal gels respond to ethanol concentration (0 to 100% with respect to water) as well as compressive stress [178]. With the same concept, pH-sensitive photonic crystals based on PVA-chitosan semi-IPN were fabricated [179]. In contrast to the previous study [176], due to the cationic nature of chitosan, increasing the pH resulted in a decrease in the diffraction wavelength (Fig. 9d) [179]. Importantly, the change of diffracted wavelength versus pH in pH-responsive photonic crystals is not linear. However, as seen in Fig. 9e and f, the change is proportional to swelling, further confirming the relationship of diffraction to inter-particle distance and swelling. It should be noted that the swelling of an ionic hydrogel is governed by dissociation or protonation of its ionic groups and thus is not correlated to pH in a linear manner. In general, the change in swelling of pH sensitive hydrogels occurs around the pK of the ionic group [180].

Glucose sensors were developed through F-T gelation of chemically modified PVA on a monolayer of polystyrene colloid crystals [181]. 4-boronobenzaldehyde which has suitable complexation with glucose was conjugated to PVA. The films responded to glucose concentration up to 0.6 mM with suitable repeatability (Fig. 9g). Interestingly, pure F-T PVA hydrogel photonic crystals gels respond to strain (Fig. 9h) [169,182]. Upon stretching, as the interparticle distance increases, the diffraction wavelength shifted to higher values and thus the change in gel color was easily distinguishable by the naked eye (Fig. 9i) [182]. In conclusion, the F-T PVA hydrogels are regarded as a suitable platform for the design of stimuli-responsive photonic crystals through manipulation of the gel swelling.

6.4. Cleaning of paintings by F-T PVA hydrogels

Recent findings of an Italian group have revealed that the PVA gels are highly effective for safe cleaning of paintings (Fig. 10) [183,184]. Semi-IPNs of PVA with either poly(vinyl pyrrolidone) (PVP) [183] or low-M_w PVA (referred to as twin-chain polymer networks) [184] have been employed for such a purpose. The dirt removal from the paintings was attributed to suitable adhesion of the gel to the texture, and fluid release at the interface [184]. The F-T PVA/PVP semi-IPN hydrogels exhibited more efficiency in terms of dirt removal when compared with gellan gum -a widely-used gel for paint conservation [183]. The addition of PVP (25 wt%) lowered crystallization and yielded less elastic gels which were more suitable for this kind of cleaning especially on the rough surfaces. However, higher PVP (50 wt%) further deteriorated elasticity and gave rise to brittle gels which were not suitable for the application [183]. Overall, water release from the gel during the cleaning is of great importance in this field, which should be optimized according to the painting type to be between 12 and 24 mg/cm^2. Suitable gel stickiness, arising from the presence of unbounded OH groups of PVA is also necessary. The latter can be achieved at low F-T cycles. It was demonstrated that 3F-T cycles showed better cleaning compared to 7 cycles [183]. Collectively, it can be concluded that facile manipulation of gel characteristics enables the design of efficient dirt erasers for a variety of delicate surfaces.

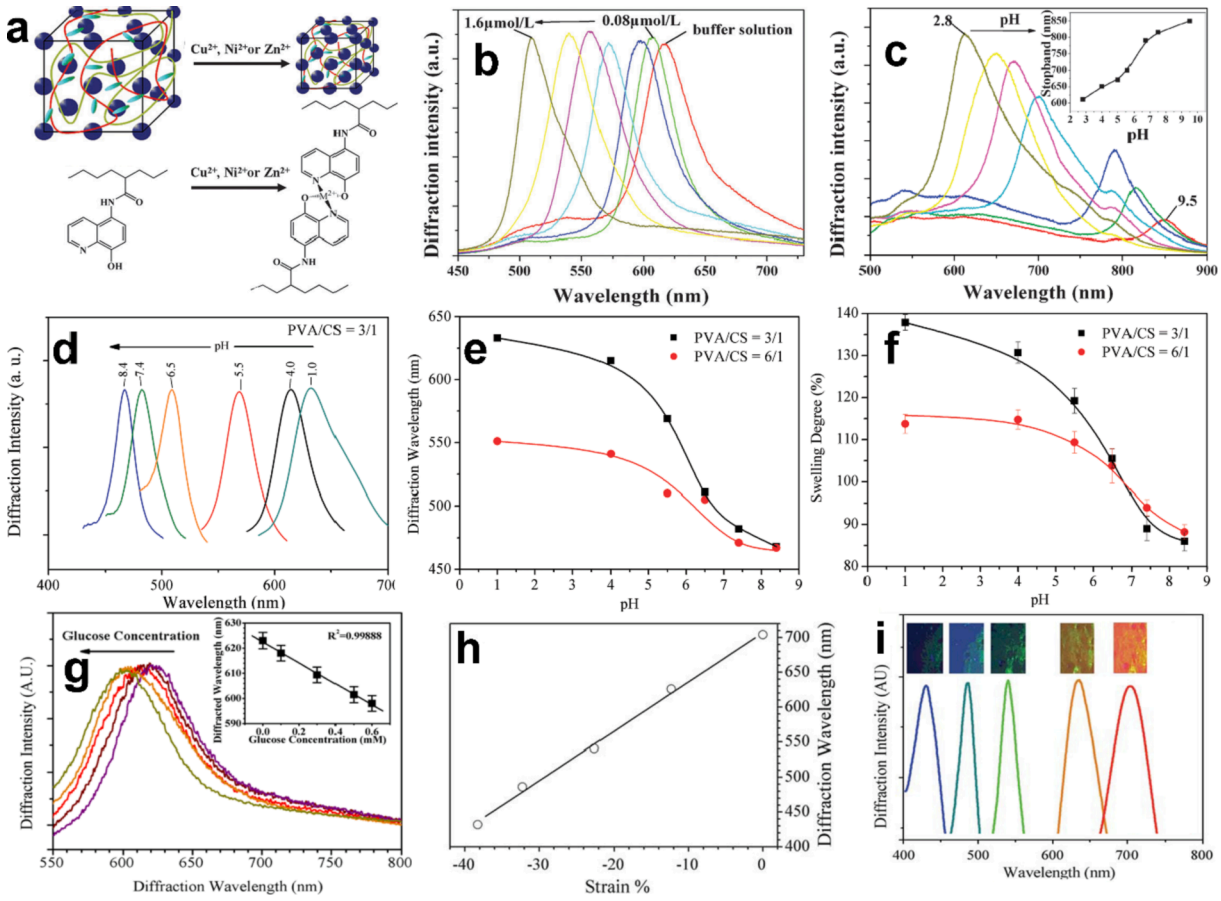

Fig. 9. Photonic crystals with the F-T PVA hydrogels. (a) The schematic representation of colloid crystals prepared in PVA/poly(acrylic acid) hydrogels functionalized by 8-hydroxyquinoline. Increase in metal ion concentration decreased the swelling and thus the interparticle distance, thereby shifting the diffracted peak to lower wavelengths [176]. **(b)** Diffraction peak of the corresponding gels as a function of nickel cation concentration [176]. **(c)** Change in the diffracted peak of the corresponding gels in different pH. The inset shows that at alkaline conditions due to anionic nature of gels, and higher swelling, the diffracted peak shifts to higher wavelengths [176]. **(d)** Diffraction spectra of PVA-chitosan hydrogels show that increasing the pH, shifts the diffraction to lower wavelengths [179]. **(e)** Nonlinear relationship of the diffraction with pH. It is also seen that as the ratio of PVA to chitosan is increased the sensitivity of sensors is decreased [179]. **(f)** Swelling degree vs. pH shows that diffraction strongly depends on swelling behavior as it affects interparticle distance [179]. **(g)** Shift of diffraction peak by increasing glucose for PVA-based photonic crystals. The inset shows linear relationship of the diffracted wavelength with glucose concentration (0.1–0.6 mM) [181]. **(h)** The change in diffracted wavelength vs. strain for the F-T pure PVA hydrogel photonic crystals shows linear relationship. [182] **(i)** Corresponding photographs and diffraction peaks of the films under strain [182].

6.5. Water purification by F-T based hydrogels

Typically, heavy metal ions are the main concern in water contamination due to their toxicity. To annihilate their toxic effect, complexation of metal ions -referred to as chelation- employing a suitable chelating agent is a viable strategy [185]. Due to its non-ionic nature, PVA by itself does not have the complexation ability with ionic species (e.g., metal cations such as Pb^{2+}, or anionic dyes). Therefore, either chemical modification or preferably introduction of an active agent needs to be conducted on PVA gels. For example, semi-IPNs of PVA/alginate were successfully utilized for removal of methylene blue cationic dyes from the contaminated water [126]. Similarly, the incorporation of cellulose nanocrystals and poly(N-methylene bisacrylamide) to PVA endowed the gels with the removal ability of both cationic and anionic dyes [186]. The F-T based PVA/alginate hydrogels in the form of beads also exhibited efficient capability for arsenic removal [187]. A recent study showed that the self-assembled F-T PVA beads impregnated with Zr(IV), Fe(III), and Cu(II) possess effective fluoride removal with several cycles of regeneration [188]. In addition, metal–organic framework-incorporated Cu-alginate/PVA beads have displayed high durability and efficient ion removal for seawater desalination [189]. Overall, although not effective by itself, advantageous properties of PVA such as robustness can be exploited for the introduction of active chelating agent. For instance, poly(aspartic acid) hydrogels have strong affinity with calcium ions, enabling efficient calcium removal, as well as prevention of deposition/mineralization of calcium-containing salts [190]. However, its inferior mechanical properties arising from its low M_w hinder its application to some extent [191]. Hence, more studies on such areas and alike are still highly encouraged.

7. Biomedical applications of the F-T PVA hydrogels

7.1. Biocompatibility of the F-T PVA hydrogels and scaffolds

High purity of the gels prepared by the F-T process results in excellent biocompatibility and thus several biomedical applications have been exploited accordingly. Various in-vitro studies have indicated non-toxicity of the F-T PVA hydrogels with different cell lines such as NIH-3 T3 (mouse embryonic fibroblast), hCHs (human chondrocytes) [123], MC3T3-E1 (mouse osteoblastic) [192], MSCs (mesenchymal stem) [193], SV40 (human osteoblast) [194], and MRC-5 (human fibroblast) [87]. However, these results should be interpreted as biologically inertness of the gels, since PVA does not independently stimulate cell adhesion and proliferation. In other words, hydrophilicity and non-ionic

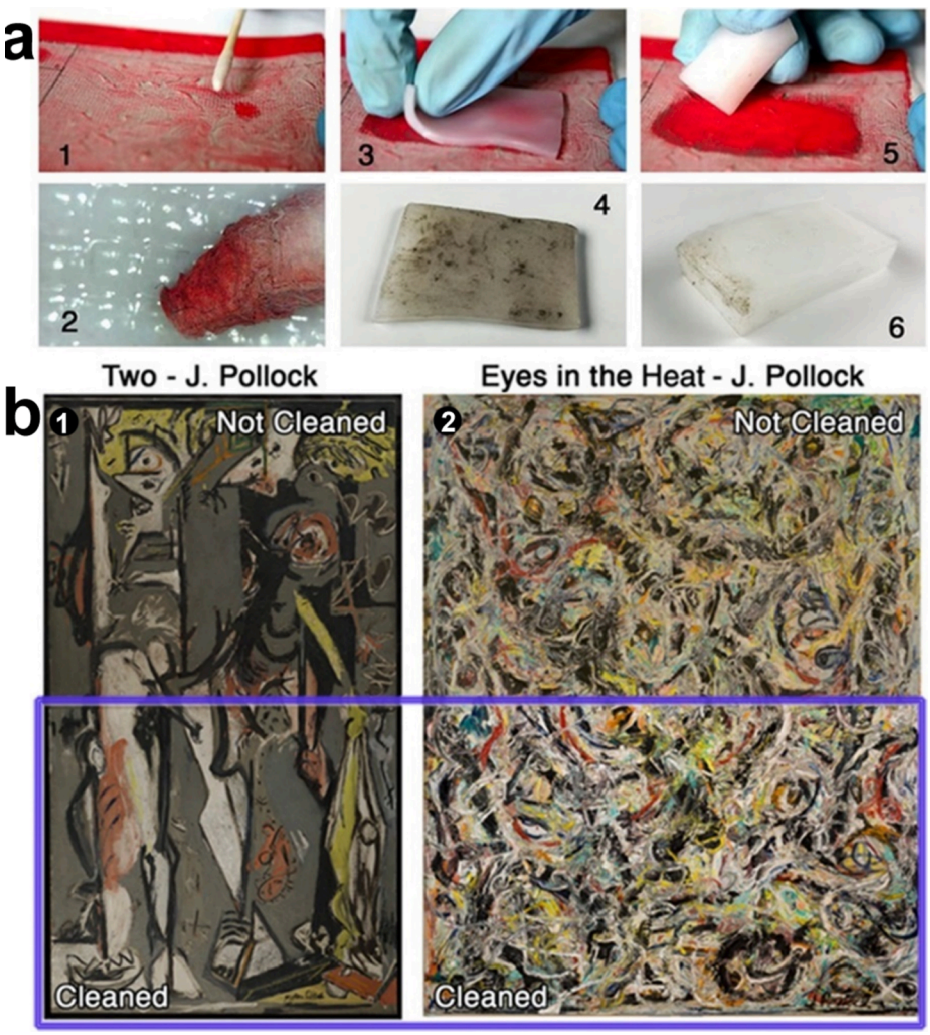

Fig. 10. Assessment of the F-T PVA gel cleaning. (a) Comparison of the gels with cotton swabs **(1)** Cleaning of soil by a swab soaked with a cleaning solution. **(2)** Closer look at the swab tip shows removal of some red pigments with soil. **(3)** Application of the PVA-based hydrogel sheet on the soiled painting **(4)** the gel surface shows the removal of only soil (not red pigment). **(5)** Cleaning of the painting by the PVA-based hydrogel shaped as an eraser gum; gentle application of the eraser leads to the complete soil removal, **(6)** with no red pigment detachment from the painting. [184]. **(b)** Cleaning of Pollock's masterpieces viz.: Two (1) Eyes in the Heat (2) before and after the cleaning, where the soil was removed using the PVA-based hydrogels [184].

nature of PVA cause low protein adsorption and low cell attachment to an extent that after 10 days of culture a very low level of cell attachment was observed [195,196].

To address such an issue, the introduction of active agents such as biopolymers has proved to be highly beneficial [195]. For instance, the addition of gelatin (optimum concentration of 30 wt%) to PVA was associated with enhanced biocompatibility, cell adhesion (MC3T3-E1), and calcium deposition [81]. Gelatin can improve cell adhesion as it contains a large amount of RGD (Arg-Gly-Asp) peptide motifs in its structure [197]. Introduction of Salecan as an extracellular water-soluble microbial polysaccharide to the F-T PVA gels also enhanced the adhesion of fibroblast [80]. Similarly, Curdlan as another microbial polysaccharide was found to be promising for improving biocompatibility [198]. Chitosan, a well-known cationic biopolymer, has also shown to endow the gels with anti-microbial properties, enhance bioactivity, and significantly increase the attachment of vascular smooth muscle and endothelial cells [199–202]. As discussed in semi-IPN (section 3.1), the introduction of the second polymer should be carried out cautiously since the high concentration deteriorates crystallinity and gel strength, as reported in several studies [77–81]. Surface treatment of the gel could be a viable strategy for enhancing the cell attachment without reducing the mechanical strength [200].

Biocompatibility, strength, and porosity make PVA-based gels suitable materials for the scaffold preparation. Scaffolds are typically utilized for cultivation of the cells derived from damaged tissue for the purpose of implantation and subsequent tissue regeneration. The gel porosity provides the cells with a suitable exchange of nutrients, and space to stretch, proliferate and function normally. Although hydrogels are inherently porous, further porosity may contribute to further cell proliferation and migration.

There are a variety of methods for changing the gel porosity. Most importantly, the gelation parameters such as F-T cycle numbers could affect the pore size greatly as discussed above in section 2.2 (Fig. 4b-d). The addition of PEG along with nHAp to PVA yielded highly porous sponge-like hydrogels [203]. Another study employed CO_2 as emulsion droplets dispersed in PVA solution, leaving large pores behind [204]. This is highly favorable for cell proliferation given the fact that neither emulsifier nor toxic foaming agents is used [204]. In another study, the porosity percentage and pore size (up to 200 μm) were increased through the addition of a high amount of baking soda (i.e., sodium bicarbonate) as a porogen (up to 9 times with respect to PVA), [205]. The porogen was then removed by acid washing. Overall, whilst high porosity improves cell growth and proliferation, it is accompanied with a reduction in mechanical strength, which should be taken into consideration.

The scaffold implantation should not induce inflammation, which could eventuate into its immune rejection by the body. Depending on the purpose, the scaffold could be either perishable or permanent. Due to its non-degradability, PVA is not suited for the former purpose, however this specific characteristic together with the aforementioned properties makes PVA a potential choice for artificial articular cartilage, and vascular stent which is explained below.

7.2. F-T PVA hydrogels for artificial cartilage

Cartilage-related damages such as osteoarthritis starts from physical injuries and degenerative joint diseases. Due to low blood flow and poor vascularization, treatment, and healing of such injuries is challenging [206], necessitating the joint replacement with a suitable biomaterial (Fig. 11a). In this regard, the F-T PVA gels have exhibited great promises in terms of biocompatibility, wear resistance, shock absorption, friction coefficient, flexibility, and lubrication (due to uptake/excretion of body fluid), thereby differentiating them from the widely studied polyethylene-based cartilages (Fig. 11b) [207–211]. A two-year implantation of the F-T PVA gels as artificial meniscus in rabbits showed that the gels remain intact without degradation, fracture, or loss of properties (Fig. 11c) [212].

Despite the similarities to cartilages, the F-T PVA hydrogels still suffer from inferior mechanical properties, osteoconductivity, protein adsorption, and cell attachment which may be addressed by the addition of (n)HAp (Table 2) [93,122,194,203,213–220]. Importantly, HAp is the main constituent of human bone, and thus is a top choice in studies related to bone regeneration [194,214]. (n)HAp can establish strong bonds with the bone and/or bone-forming proteins such as osteopontin which play a key role in osteoblast differentiation and biomineralization [215,221]. Such a bond originates from the fact that osteopontin contains approx. 30% aspartic acid motif which has a high affinity toward calcium and calcium-containing minerals such as HAp.

Improved osteoconductivity was shown in the PVA/HAp composite hydrogels as they mineralized in vitro in simulated body fluid, forming bone-like hydroxyl–carbonate–apatite deposit [222]. Furthermore, implantation of the gels in the rabbit knees for 3 months revealed that the gels are tightly combined with the surrounding tissues, contributing to the repair of articular cartilage defects. The growth of bone-like tissue and chondrocyte proliferation around the gel, as well as the absence of cartilage degeneration, was also indicated.

It should be noted that the addition of HAp is associated with the decreased PVA crystallinity which is in contrast with its improvement effect on the mechanical properties [216–219]. Although the PVA gelation and crystallinity are interrupted by the presence of HAp, the adverse effect is compensated by the reinforcing effect of HAp itself. Importantly, the enhanced properties are only achieved when the HAp NPs are dispersed in the PVA matrix uniformly, which could be challenging due to tendency of small sized NPs to aggregate. This issue could be addressed by *in-situ* HAp synthesis in PVA gel or solution, ensuring well-dispersion and fixation of the HAp NPs in the hydrogel matrix [93,223,224].

Aside from cell proliferation, porosity is also necessary for calcification and integration of the prosthetic cartilage into the surrounding tissues. The effect of porosity was evaluated ex vivo by implanting the gels in the torn meniscus [205]. The gels showed enough stability, mechanical and morphological characteristics comparable to those of native meniscus, and more importantly suitable integration. However, to perfectly mimic whole cartilage, gradient porosity is preferable. Articular cartilage covers the bone ends in diarthrodial joints, with a gradient layer structure ranging from a smooth but dense zone at the surface to a porous calcified core zone, providing concurrent high load-bearing and low-friction properties. In this regard, in an effort to simulate the multi-layer gradient porous structure of the cartilages, a recent study subjected the PVA/HAp-GO solution to the F-T with gradient temperature in the freezing step (Fig. 11d) [122]. This resulted in gradient pore size on two sides of the object, which can pave the way in the design of precisely customized cartilages. The porous side allows calcification as well as firm attachment to the bone over time, while the non-porous side provides smoothness, lubrication, and low friction.

Despite extensive studies, limited cell migration/attachment is still believed to be a challenge which could be attributed to inertness and lack of control over porosity of PVA. This could lead to a low level of calcification and loose attachment (even detachment) to the bone

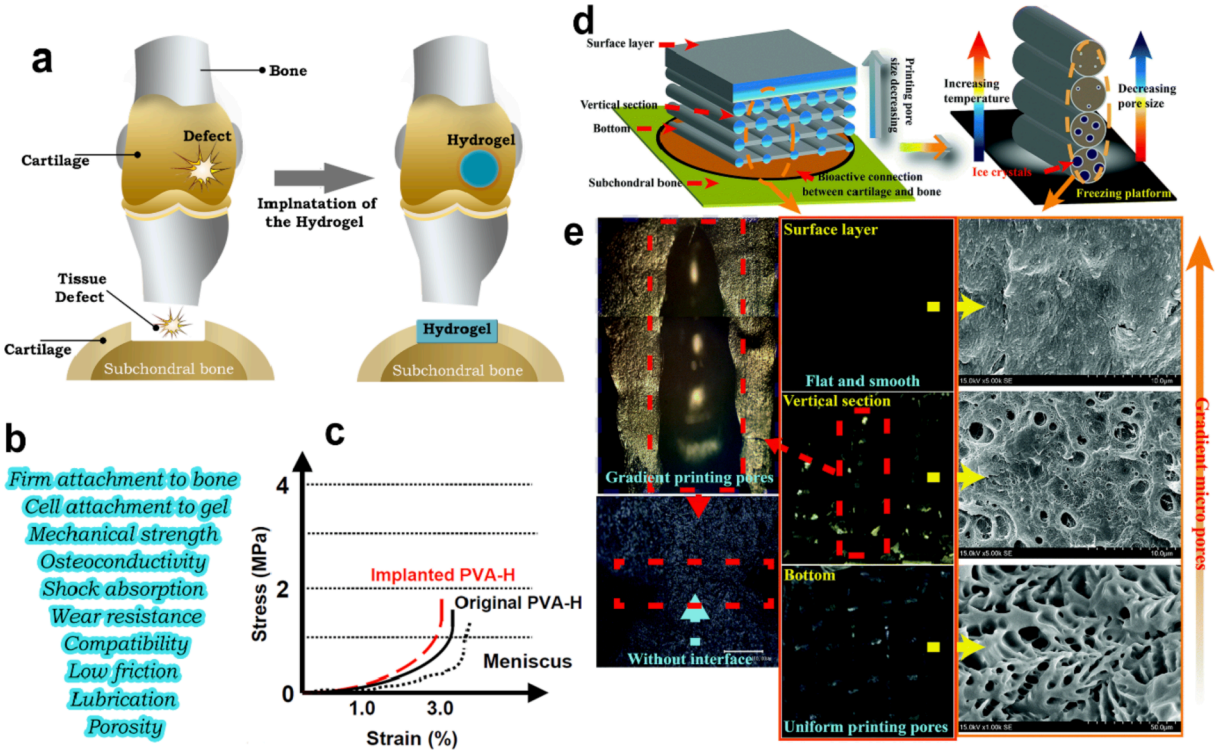

Fig. 11. F-T PVA hydrogels as artificial cartilage. **(a)** Schematic representation of replacement of the damaged part with PVA hydrogels. **(b)** The requirement for implantation of a hydrogel. **(c)** Compression stress–strain curves of the F-T PVA artificial meniscus before and after implantation and comparison with human natural meniscus [212]. **(d)** Design of PVA-based artificial cartilage with a gradient porous structure. Increase in temperature in the freezing step decreases the porosity. **(e)** Digital photograph and SEM micrographs of the PVA-based cartilages, showing gradient porosity [122].

Table 2
Properties and use of (nano)composites of the F-T PVA hydrogels with HAp and nHAp.

PVA M_w (kDa) /Conc. (wt. %)	HAp conc. (wt.%)	Other materials	Tensile modulus (MPa)/strength (MPa)/strain (%)	Compressive modulus (MPa)/strength (MPa)/ strain (%)	Remark	Ref
n.a/10	0, 1, 2, 5, and 8	γ-Fe2O3 (HAP-coated with γFe2O3)	n.d	n.d/19–30/n.d	Compared with PVA and nHAP/PVA hydrogels, incorporation of magnetic-nanoHAp promoted adhesion and proliferation of human SV40 osteoblast. Also, the magnetic-nanoHAp reinforced the hydrogel.	[194]
91.5/15	3 and 7.5		152–1074/ 14–721/169–223	73–149/12–29/43–92	Partial agglomeration of higher content of HAp showed direct influence on mechanical properties while general behaviour was consistent with the articular cartilage.	[217]
n.a/16	2	Poly(acrylic acid)	0.34–0.98/ 2.3–3.7/381–688	n.d	The addition of poly (acrylic acid) led to the formation of a compact 3-D network and enhanced mechanical and frictional properties. Furthermore, annealing treatment (the dehydrated hydrogel was placed at 120 °C for 1 hr) significantly improved crystallinity, thermal stability and mechanical strength as a result of increased degree of crosslinking.	[225]
72/10% (w/v)	n.a	Selenium-doped Titanium dioxide (Se-doped-TiO_2)	15000/n.d/n.d	n.d	Selenium has antimicrobial and chemo-preventive properties. Also, TiO_2 NPs are biocompatible, antibacterial and have excellent biomechanical properties. They also stimulate HAp formation via the Ti-OH sites and thus accelerate bone growth when incorporated in the implants. Due to these properties, Se-doped-TiO_2 together with HAp was added to PVA hydrogels. Such an addition was accompanied with a synergic reinforcing effect on both mechanical and structural properties.	[226]
n.a/15	1.5, 3, 6, 7.5		333–460/ 168–217/44–52	120–166/16–17/ 92–97	Pore size and gel fraction, thermal stability and mechanical properties increased as HAp content increased. At high contents of Hap, structural stability of PVA was improved, preventing the collapse of porous structure.	[227]
205/13	4, 7, 10, and 15	Collagen	n.d	n.d	Collagen along with HAp has the potential to mimic natural bone matrix. The hydrogels showed a bone-like ECM with excellent mechanical properties and enhanced adhesion, growth, and differentiation of mouse osteoblast (MC3T3).	[228]
n.a/10	5	Hydroxypropyl guar (HPG)	n.d	n.d	HPG was added to mimic ECM and to improve cell proliferation. The incorporation of the HPG and HAp promoted cell growth and differentiation when compared to PVA alone. Hap also improved the mechanical properties. However, it was not in favor of the cell proliferation (mouse osteoblast, MC3T3).	[229]
n.a/10, 15, 20	2, 3, 4	2-hydroxypropyltrimethyl ammonium chloride chitosan (HACC)	n.d/2.7–2.9/n.d	0.72–0.88 (Young's modulus) /40–55 (at 95% strain) /n.d	HACC as a polysaccharide has good biocompatibility and antibacterial activity. The addition of sodium citrate led to crosslinking of HACC due to the formation of citrate-N-glucosamine coordination. Together with F-T gelation, double network hydrogels were obtained. The addition of HAp decreased elongation at break, and toughness but improved the modulus and strength. The friction coefficient was also reduced by HAp incorporation, suggesting that HAp improves tribological performance. The hydrogel also had ant-fatigue, self-recovery and energy dissipation properties.	[230]
n.a/8	n.d	Carbon dots	n.d	n.d	Two sets of crosslinking (F-T, and glutaraldehyde as physical and chemical, respectively) were used to prepare double network PVA hydrogels. The incorporation of carbon dots provided the gel with fluorescence properties (for fluorescence-visible bone scaffold). The hydrogels showed biocompatibility against mouse osteoblast (MC3T3).	[231]

underneath, all making the implant less compatible for integration to the surrounding tissues.

7.3. Stent based on the F-T PVA hydrogels

The F-T PVA hydrogels have the potential for the design of different types of stents due to their elasticity and biocompatibility. This includes but not limited to endoscopic biliary stenting and cardiovascular stents [58,232]. Artificial heart valve stents have also been prepared by such hydrogels [53]. Detailed modeling/simulation of the valve leaflet were conducted on the basis of natural valves. [233,234]. Currently, prosthetic aortic valves (porcine- or bovine-based) are the most commonly used valves which undergoes calcification, or mechanical failure, and thus do not typically last>15 years [235]. Although mechanical valves can last a lifetime, the patient needs to take blood-thinner/anti-coagulant for the entire lifespan [236]. By changing the parameters of the F-T, the mechanical properties of the PVA-based valves matched those of porcine aortic root under physiological pressure [53].

Furthermore, through injection molding, artificial heart valve stents with desirable shape and geometry were successfully fabricated (Fig. 12a). Using injection molding, another study fabricated heart valves which showed the ability to be compressed temporarily into a small ball, enabling its insertion into the chest cavity through a keyhole incision (Fig. 12b) [237]. This is highly useful for the replacement of valves by closed-chest surgery. The valve could expand circumferentially in a synchronic manner with the aorta during systole when the valve is open.

In an effort to fabricate vessels for the purpose of coronary bypass graft surgery, the F-T PVA hydrogels were molded in the form of a conduit [238]. The conduits were designed in a way to closely match the tensile properties of the porcine aorta both in the circumferential and the axial directions (Fig. 12c). It should be added that the aortic tissues (largely made up of elastin and collagen) have an anisotropic nonlinear mechanical strength, in which the elastic modulus is higher in the circumferential vs. axial direction. To achieve such an anisotropic response, after the first F-T cycle, when the gels have sufficiently gained enough integrity, they were stretched by 75% of the initial strain [238].

After years of efforts, there are still limited synthetic materials for vessel replacement and grafting. Thus, surgeries are still relying on using the patient's saphenous vein, which has a high failure rate. The failure in both prosthetic and autologous grafting originates mainly from poor endothelialization, which consequently causes thrombosis, calcification, intimal hyperplasia (abnormal cell proliferation/accumulation), and atherosclerosis. Due to its characteristics, PVA-based hydrogels have the potential as vascular grafts. For instance, Atlan et al. [239], fabricated prosthetic rat aorta based on PVA-gelatin with thickness of 400 μm, and diameter of 1.4 mm. For gelation, only one cycle of F-T together with the use of a PVA chemical crosslinker (sodium trimetaphosphate) was applied which collectively satisfied the required strength for vessel application and for suture retention (Fig. 12d). The graft failure after two months was reported to be 50%. The failure was attributed to a change in mechanical properties. This highlighted the disadvantage of the F-T PVA hydrogels in terms of gel stability longitudinally for this specific application. Alternatively, in this regard, chemically crosslinked gels have drawn a great deal of attention [240–243]. Regardless of the crosslinking type, common cause of failure could be ascribed to poor endothelialization and hemocompatibility of the PVA-based gels. The addition of gelatin was found to be highly effective for these issues when compared to chitosan or starch [244].

7.4. Wound dressing based on F-T PVA hydrogels

Wound dressings with a proper biocompatible hydrogel can greatly contribute to accelerating the healing process particularly when it is not occurring under normal conditions (e.g., wounds of patients with diabetes, and wounds under arterial insufficiency [245]). As shown in Fig. 13a, the hydrogel dressing not only protects the wound from pathogens infecting it but also stimulates cell growth as well as tissue regeneration without the formation of scars. The dressing should also be able to completely absorb the fluid produced by the wound (i.e., exudates) while keeping the wound moist and allowing gas exchange so that oxygen reaches the wound for cell growth/proliferation [245,246]. It should be noted that exudate accumulation can lead to maceration and bacterial proliferation [247]. Hydrogel dressings can also reduce pain due to high water content leading to cooling and soothing effects [248]. Furthermore, elasticity, biocompatibility as well as easy and painless removal are of importance in the design of suitable hydrogel dressings [105,249,250].

Despite meeting the abovementioned requirements, due to non-bioactivity and inertness in the healing process, the pure F-T PVA hydrogels are rarely studied. Accordingly, they are typically incorporated with active agents with anti-microbial properties and/or stimulatory effects on growth factors [251]. The introduction of Curcumin as a natural polyphenolic with anti-inflammatory, and antioxidant activities contributed to considerable wound contraction after 2 weeks by stimulating collagen synthesis [252]. Collagen plays a key role in the healing and is typically synthesized by fibroblasts, forming an integral part in the extracellular matrix (ECM), and providing structural support and rigidity to the connective tissues [253].

Most commercial hydrogel dressings (e.g., Algisite, Kaltostat, and

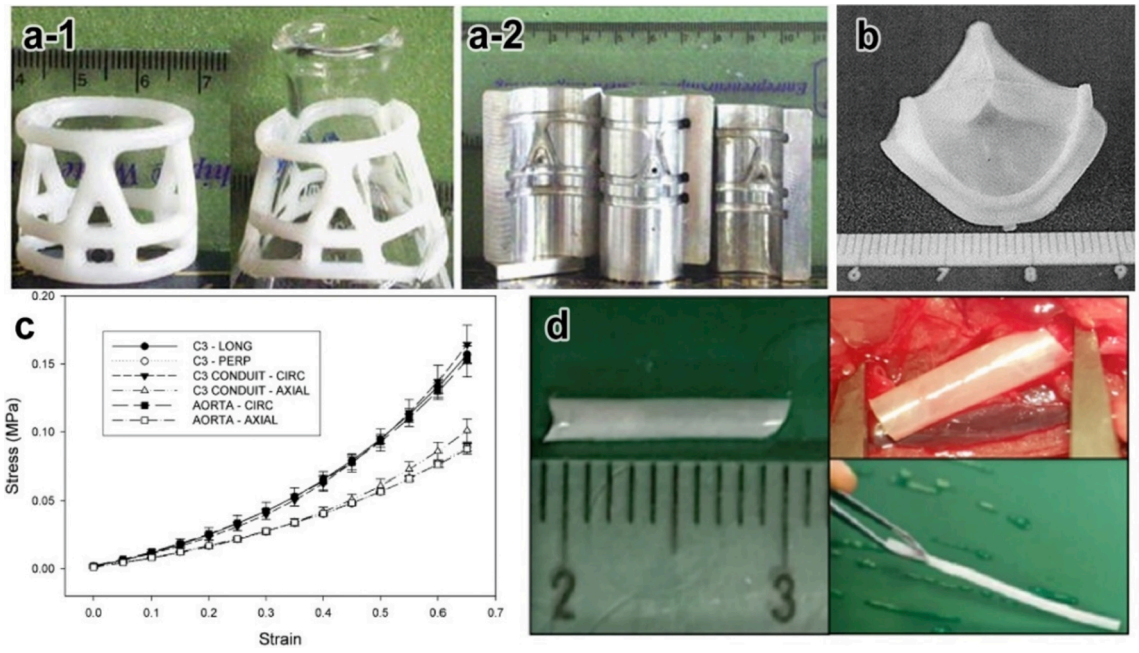

Fig. 12. PVA-based hydrogels for stent and artificial vessels. (a) Preparation of artificial heart valve stents with desirable shape and geometry. (1) The shape of the expansible heart valve stent under normal and deformed state. (2) The four-part injection mold. [53] **(b)** A heart valve fabricated by PVA hydrogels that integrates into a single part the 3 leaflets, stent, and sewing ring [237]. **(c)** Comparison of tensile curves for the PVA conduit with porcine aorta. The conduits were prepared by 1F-T cycle, followed by 75% stretching and finally 3 more F-T cycles [238] **(d)** PVA tube with 1 cm length, and handling of the grafts for the vascular replacement at the level of the abdominal aorta was easy and without collapse of the lumen [239].

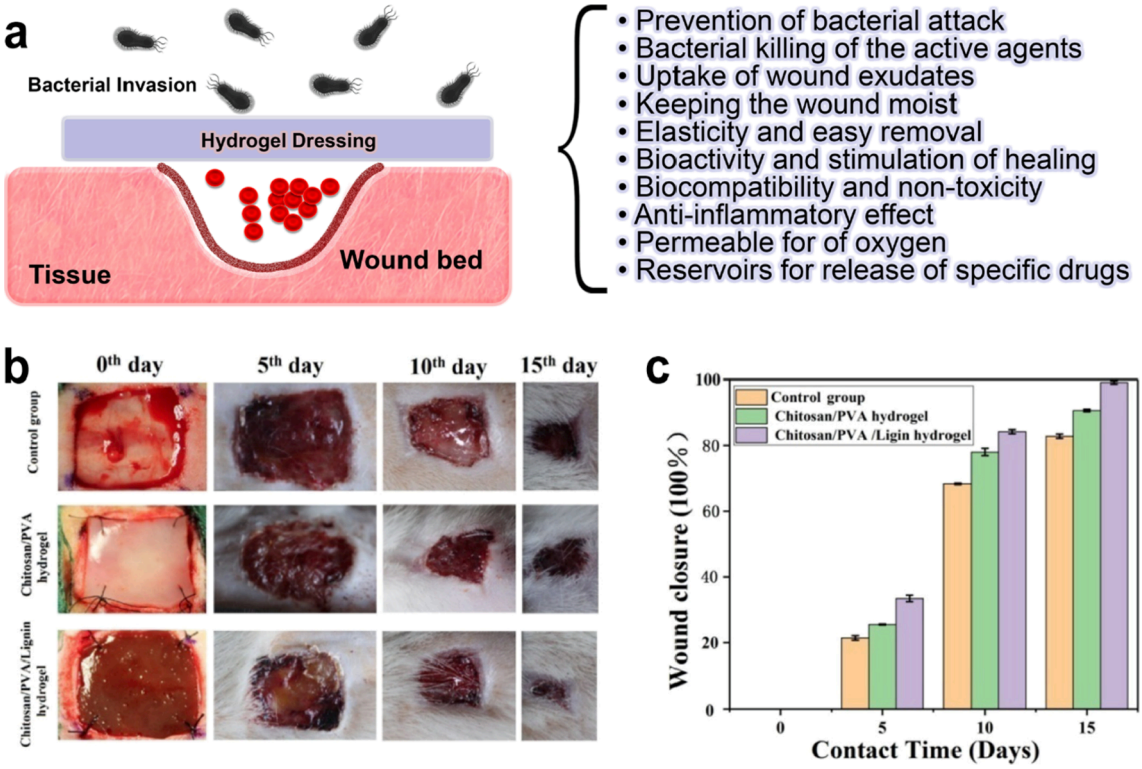

Fig. 13. Wound dressing based on the F-T PVA hydrogels. (a) Schematic representation that the hydrogel dressing protects the wound. **(b)** Macroscopic appearance of the wounds with, PVA -based hydrogel dressings and without dressing (control group) at different time points. **(c)** The wound closure (%) of the dressings calculated from the recovered area [260].

Condress) are based on polysaccharides particularly alginate and chitosan [254]. Alginate dressings significantly decrease wound secretions and bacterial contamination. They also accelerate the healing process through enhancing cell migration, stimulation of collagen synthesis, and the formation of granulation tissue [255,256]. In-vitro and in-vivo wound healing studies on the F-T PVA/sodium alginate hydrogels loaded with clindamycin (an antibiotic) revealed that the hybrids are more effective than pure PVA hydrogels [77]. More inflammatory cells

Table 3
Mechanical properties and applications of nanocomposites of the F-T PVA hydrogels with AgNPs.

PVA MW (kDa)/ PVA Conc. (wt %)	AgNPs (wt %)	Other materials	No. of F/ T cycles	Tensile Modulus (MPa)/ Tensile strength (MPa)/ Elongation (%)	Remark	Ref
60/20	0.5, 1, 2 wt%		5	n.d/0.75–1.26/400–586	Uniform distribution of NPs was achieved as a result of *in situ* synthesis of AgNPs by PVA. PVA was employed as both stabilizer and reducing agent of silver cations. Electrical conductivity, mechanical properties, and anti-bacterial activity was achieved by the introduction of AgNPs.	[86]
145/10	7.8 mM of Ag ion		3	n.d/0.8/273	The antimicrobial efficacy was retained even after 96 h of release of AgNPs, suggesting that they can be regarded as silver reservoir to provide a sterile environment in the long term. Slow release of silver into the medium reduced the systemic toxicity.	[263]
70–100/10	3.9 mM	Graphene	5	309–701/121–141/83	Slow release and large amount of silver after 28 days incubation in simulated body fluid was shown, suggesting that the gels are suitable for long-term sterility. The incorporation of graphene led to better mechanical, thermal and anti-microbial properties.	[88]
85–124/4	10 mM	Chitosan	n.a	n.d	The hydrogels were used as nano-reactors for AgNPs *in situ* synthesis. The higher amount of crosslinker (glutaraldehyde) and silver enhanced the porosity. The AgNP-hydrogel exhibited good antibacterial activity against *Escherichia coli* in 12 h.	[91]
70–100/10	0.25 and 3.9 mM	Graphene and Chitosan	5	n.d	Diffusion-controlled release of silver over 28 days was monitored. Strong anti-bacterial activity against *Staphylococcus aureus* and *Escherichia coli* bacterial strains was observed while no significant toxicity toward fibroblast cell lines (human and mice) was noticed.	[87]
89–98/n.d	5 mM	Sodium alginate	15	n.d	The double network hydrogels loaded with AgNPs exhibited high bactericidal activity against *Escherichia coli, and E. coli*	[273]
n.a/10	9.3 mM	Clay, activated carbon	3	n.d	The AgNPs synthesized by cabbage (*Brassica Oleracea Capitata*) plant extract was added to the hydrogels along with clay and activated carbon due to their wound healing and anti-bacterial activities, respectively. Excellent antibacterial activity and in vivo wound (scar on rabbit) healing efficiency was observed.	[264]

were observed in the hybrid hydrogels compared to pure PVA.

Chitosan, on the other hand, possesses inherent anti-bacterial effect as it interacts with toxins present inside a bacterial cell (i.e., endotoxins) [257]. The improved efficiency of PVA/chitosan with and without glycerol for wound healing was demonstrated in vivo due to inherent anti-microbial activity of chitosan [258]. In another study, the F-T PVA/hyaluronic acid hydrogels loaded with ampicillin (an antibiotic) were studied. Even in the absence of ampicillin, owning to the presence of hyaluronic acid, the hybrid gels showed anti-microbial activity against *Candida albicans,* a common cause of wound infections [78]. The addition of Glucan as another natural polymer to PVA has also led to accelerated wound healing [259]. Another study showed that lignin and chitosan introduction to the PVA hydrogels greatly improves absorption of bovine serum albumin as a model protein and accelerates the healing (Fig. 13 bc) [260].

Nevertheless, as explained above in section 3.1, the incorporation of the second polymer at high content may compromise the mechanical properties. The addition of suitable anti-microbial NPs can address this undesirable issue. Silver-based products have proven to possess low toxicity and antimicrobial activity against variety of antibiotic-resistant bacteria. Silver -both in the form of cation (Ag^{+}) or reduced form (Ag^{0})- is biologically active as it disrupts cell membranes of bacteria and blocks cellular respiration [261,262]. AgNPs are of top choices for the design and development of tough and strong wound healing and implants based on the F-T PVA hydrogels (Table 3). AgNPs contribute to the acceleration of wound healing, reduction of hypertrophic scar formation, and improvement of gels' elongation at break [263–265]. Sustained release of ionic and atomic silver from solid AgNPs provides the dressings with long-term sterilization activity [88,90,263].

Other nanoparticles such as zinc oxide [266], cerium oxide [109], GO [267], and HAp [203] have also exhibited promising results in the dressing based on PVA hydrogel. In-vivo and in-vitro studies showed that GO serves as a biologically active agent promoting cell growth when 2 wt% or lower was added to alginate-PVA gels loaded with norfloxacin (an antibiotic) [267]. The gels had suitable breathability which is defined as the moisture vapor transmission rate (MVTR) in the field of dressing, indicating the level of water loss. The higher the MVTR, the higher the water loss [268]. Very high and low WVTR may respectively lead to wound dehydration and exudates accumulation [269]. The MVTR in the PVA-based gels can be tuned by changing the gelation parameters. For instance, the deswelling ratio of PVA-AgNPs hydrogels was tuned by gelation parameters and found to decrease by increasing PVA conc., and F-T cycles [270].

Overall, despite their unique properties, PVA hydrogels have not yet adopted any stance in the dressing field which may be attributed to the long gelation process, slow water uptake, and lack of bioactivity. Importantly, polysaccharide-based dressings, despite their presence in the market, suffer from poor mechanical properties due to their monomer composition and batch-to-batch variation [254,271,272]. Hence, considering the advantages and drawbacks of both polysaccharides and PVA, their combination preferably together with AgNPs is highly encouraged for wound dressing.

7.5. Contact lens based F-T PVA hydrogels

As stated above in section 2.7, transparent PVA hydrogels can be prepared by changing the F-T gelation parameters. Highly transparent PVA gels were obtained by (i) the use of a proper co-solvent (e.g., glycerol or DMSO) [65], or (ii) application of at least 30F-T cycles with a freezing temperature of 0 °C [71]. Optimum DMSO content in terms of transmittance was determined to be 60–80 wt% [65,66]. DMSO removal by dialysis after the gel formation did not influence the gel transparency [65]. The prepared F-T PVA gels showed excellent self-standing, flexibility, stiffness, biocompatibility, and more importantly UV-blocking properties (Fig. 14 a-c). Flexibility and high strength allow the gels to be sutured too (Fig. 14d) [274]. The F-T PVA gels loaded with HAp, graphite, and hydroxyethyl cellulose have also been exploited for artificial cornea application. These additives were shown to enhance cell adhesion [220]. The composite gels were surrounded by a transparent PVA gel as the core.

All these features can be translated into the practical applicability of such gels as contact lenses. Hyon et al. [275] were the first to introduce the transparent F-T PVA hydrogels (prepared by aqueous DMSO) for contact lens application. The gels had exceptionally higher strength (ca. 5 times) and lower protein adsorption compared to commercial poly (hydroxyethyl methacrylate) (PHEMA) lenses. Biocompatibility of the PVA gels has been shown in vitro by the adhesion of dermal fibroblasts and human lens epithelial cells [71]. Analysis of corneal epithelium of the rabbit eyes worn with the PVA-based lenses for 3 months showed no significant difference when compared to the control group (i.e., non-wearing eyes) [275]. Ophthalmic drugs can be loaded into the PVA gels for sustained release [276,277]. Drug loading/release has widely been studied using commercial lenses for diverse diseases such as glaucoma [278], and cystinosis [279].

The commercial lenses are mostly based on either PHEMA [280] and silicone hydrogels [281] and have a water content ranging from 30 to 80% [280]. Comfort, safety, high optical clarity, suitable mechanical properties, high oxygen permeability, and water content are important parameters for contact lenses and should be precisely controlled. The properties of the F-T PVA-based gels can be easily tuned by changing the gelation parameters, thereby presenting promising prospects for the development of next generation contact lenses. However, special efforts are still required in order to further improve gel transparency and maintain gel stability over time in terms of swelling in particular.

7.6. Drug-loaded F-T PVA hydrogels

Sustained release of drugs is a viable strategy specifically for wound dressing application. The gentle and mild F-T process enables efficient loading of susceptible and degradable therapeutic compounds into the

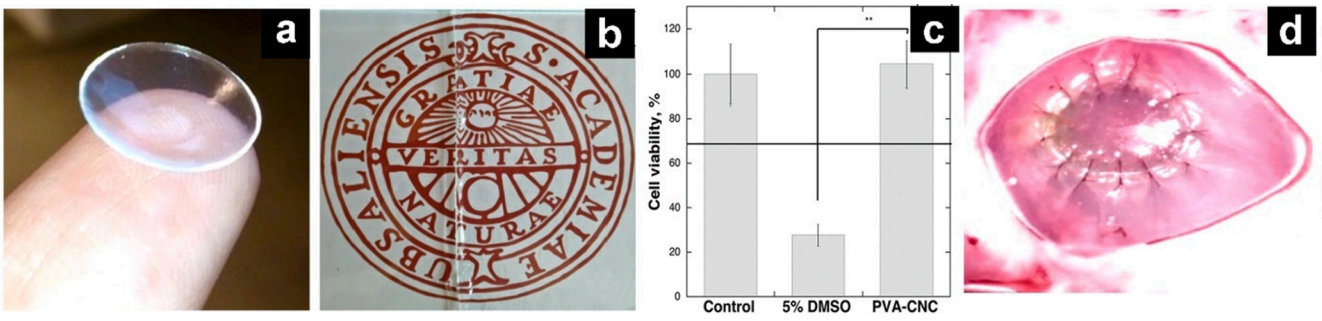

Fig. 14. Application of the transparent F-T-based PVA gels for contact lens. (a) Self-standing **(b)** transparency, **(c)** biocompatibility, and **(d)** ex-vivo implantation of the gels by suturing on porcine cornea. CNC stands for carboxylated nanocellulose whiskers where its addition to the gels improved mechanical properties, while maintaining the high optical transparency [274].

PVA hydrogels for slow and sustained release. The release profile is not affected by pH due to the non-ionic nature of PVA. However, the PVA gel characteristics may affect the release as shown by Peppas et al. [46] who found that at higher F-T cycles, a slower release rate of theophylline and oxprenolol hydrochloride was obtained. This was attributed to the presence of more crystalline regions in the gel structure. Given the relationship of crystallinity with swelling, which was explained above in section 2, it can be concluded that the lower the swelling, the slower the release.

Although loading/release of a variety of therapeutic compounds into/from the F-T PVA hydrogels has been studied [46,282–284], little attention has been paid to the delivery routes. To the best of our knowledge, with regards to oral or intravenous administration, a few studies with limited information on the potential and characterization has been reported. This is possibly due to non-degradability as well as difficulty in particle preparation of PVA hydrogels. Even if the former is not an issue (e.g., for oral administration purposes), the latter could be extremely challenging. Particle formation of a water-soluble polymer can be typically conducted by inverse emulsification (i.e., emulsion evaporation or diffusion) where an aqueous solution of PVA is emulsified in an organic phase (e.g., cyclohexane or liquid paraffin) as a medium with the aid of a lipophilic stabilizer/emulsifier (e.g., Span 80). The emulsion should be followed by F-T, which is proved to be highly detrimental to a variety of emulsions to an extent that it is usually employed for deliberate destabilization of emulsions and colloids [285,286]. Manipulation of the emulsion formulation (e.g., change of medium to an anti-freezing solvent) for maintaining stability under a prolonged F-T process is necessary for F-T PVA gel particles.

Other approaches for particle formation if feasible such as nano-precipitation or salting-out result in direct solidification of PVA chains. This requires precipitation of PVA chains in a controlled manner, leading to separation of the particles from water by the use of an anti-solvent that is water miscible. Inducing such a controlled phase separation for the purpose of particle formation makes the F-T process, and thus PVA gelation impossible. As another disadvantage, the low reactivity of hydroxyl groups in PVA makes conjugation of targeting agents such as peptides or antibodies to the resulting particles difficult. Overall, in light of the aforementioned, the potential of using F-T PVA hydrogel particles (i.e., micro- or nanogels) for targeted delivery is highly limited especially when they are compared with other biodegradable natural polymers such as chitosan [287], alginate [288], polypeptides [191], etc.

Despite these limitations, Li et al. [289] reported high loading of bovine serum albumin in the F-T PVA microgels (average size of 670 nm with wide size distribution). Firstly, PVA solution (3 mL, ca. 16 wt%) was dispersed in silicone oil (100 mL). The emulsion was then subjected to 3F-T cycles (F: −20 °C for 20 h, and T: RT for 4 h), to convert emulsion to nanogel. Suitable emulsion stability was achieved despite the lack of an emulsifier/stabilizer which was ascribed to the high viscosity and thermal properties of silicone oil at freezing temperatures. Importantly, it was suggested that the F-T process itself plays a positive role in emulsion stability [289]. In another study, PVA micro-particles (size 30–90 μm, with high polydispersity) were prepared and served for the entrapment of nano-sized polyethyleneimine-based polyplexes and their corresponding liposome analogues [290]. The PEI-based polymers due to their cationic nature are widely used for condensation and transfection of nucleic acids with high efficiency [291]. PVA hydrogel shell protected the polyethyleneimine-based NPs against intestinal fluid and improved mucoadhesion in the gastrointestinal tract, thereby improving uptake of NPs via oral administration. The issues associated with PVA particle formation were not however mentioned in the study. Success in their microgel preparation could be attributed to the use of very high stabilizer content, which is 22 wt% with respect to total components of the emulsion [290].

As stated above in section 2.2, a low F-T cycle number lead to incomplete gelation and stickiness [292,293]. Although it is indicative of inferior mechanical strength, such stickiness can be highly useful in terms of mucoadhesion. The adhesion to mucus is mainly attributed to the presence of abundant free OH groups (not still involved in the gelation) which are capable of establishing strong interactions with polar groups (e.g., thiol: S-H) of mucus glycoproteins [294,295]. Thus, due to the inherent mucoadhesion and stickiness, PVA gels with low F-T cycles number can also have a great potential for transdermal, buccal, and rectal delivery routes [296,297]. As an example, loading of fluconazole in PVA gels (3F-T cycles), and its subsequent transdermal application was found to be more efficient than the orally administered free fluconazole for cutaneous *candidal* infection in pigs [298]. Overall, following the interesting study of Schulze et al. [290], the encapsulation of drug-loaded NPs into F-T PVA hydrogel particles seems to offer promising prospects for oral administration of highly unstable and degradable drugs such as insulin. Besides its mucoadhesion, PVA could also serve as a protective layer as it has good resistance to the harsh medium in the microenvironment in the stomach.

8. Conclusion and Remark

This paper provides a comprehensive review on the physically crosslinked PVA hydrogels by the freezing-thawing (F-T) process. Not every polymer has the ability to gel by the F-T, and not every F-T gel offers the features that PVA does. The F-T gelation allows the preparation of highly pure hydrogels free from any trace of crosslinker or related agents, which is highly beneficial for biomedical applications. Tuning the characteristics of the PVA hydrogels is explained on the basis of the gelation mechanism by changing the gelation parameters. The hydrogels can gain excellent mechanical strength through adopting appropriate gelation parameters, as thoroughly discussed. Despite that, recent efforts have been directed to further enhance the gels strength through inducing crystallization by gel stretching, which can provide anisotropic properties as well. Increasing the PVA concentration beyond its solubility and processing limit (>25 wt%) is expected to yield highly tough gels as well. The use of energy-intensive instruments such as extruders for such a purpose is highly encouraged. In terms of large-scale production, the gel can be prepared in areas where temperature constantly fluctuates above and below the freezing point during the night and daytime. Although it has not been stated in the literature to the best of our knowledge, this feature could provide a cost-free and facile way to prepare extremely useful and pure hydrogels at industrial levels.

As time goes on, more novel applications are successfully exploited on the basis of the gel features. As an attractive feature, the F-T PVA hydrogels possess inherent self-healing without the need for any sort of healing agent. Despite being spontaneous, the self-healability may still require more investigations to attain faster and more efficient recovery. Furthermore, the development of shape-memory materials based on the F-T PVA hydrogels has rapidly advanced. The fundamentals, procedure, and the whys and wherefores of shape memory were also explained. Shape recovery is generally triggered by the application of heat (T > 50–60 °C), which melts the crystalline zones, and disintegrates the F-T gel points. Such a gel-to-sol transition of the F-T PVA hydrogels, though undesirable for some areas, could potentially be taken advantage of, in a variety of applications (e.g., drug delivery/release systems).

Difficulty in chemical modification of PVA has led a special attention towards semi-IPNs which also permit taking advantage of the second polymer's benefits. Nevertheless, the inclusion of the second polymer particularly at high content was found to disturb PVA crystallinity, thereby deteriorating mechanical properties. Therefore, preparation of semi-IPNs based on PVA is not recommended unless the presence of the second polymer is really vital and beneficial. Introducing natural polymer (e.g., gelatin) has shown to well compensate low bioactivity of the PVA hydrogels such as low cell adhesion. Besides semi-IPNs, the incorporation of nanomaterials can also be regarded as a versatile tool not only for manipulating the properties but also for presenting a new feature. For instance, silver and hydroxyapatite nanoparticles could

confer anti-bacterial and osteoconductivity properties to the gels, respectively.

Accordingly, by complementing different strategies, the F-T PVA-based hydrogels have been employed for diverse biomedical applications such as wound dressings, drug delivery/release systems, scaffolds, and prosthetic materials. Regarding the latter, such strategies allow the gels to be designed soft enough for vascular stents, hard enough for artificial cartilages, or transparent enough for contact lenses. Recent findings have revealed the suitability of PVA gels with low F-T cycles (yields incomplete gelation and sticky gels) for oral drug delivery purposes due to their high muco-adhesive property. Such types of gels are highly efficient for dirt removal from different delicate substrates including precious paintings. The reducing ability of PVA enables an efficient in-situ synthesis of nanoparticles inside the PVA hydrogels as templates. Loading of high amounts of ions has also enabled the preparation of ionically conductive PVA-based hydrogels for sensing applications. In light of the discussed potentials of the F-T PVA hydrogels, as we move ahead, there will certainly be more opportunities to be seized and more challenges to be solved.

Declaration of Competing Interest

The authors declare that they have no known competing financial interests or personal relationships that could have appeared to influence the work reported in this paper.

Acknowledgement

The authors acknowledge the support from National Health and Medical Research Council (HTT: APP1037310, APP1182347, APP2002827), and Heart Foundation (HTT: 102761).

References

[1] V.S. Meka, M.K. Sing, M.R. Pichika, S.R. Nali, V.R. Kolapalli, P. Kesharwani, A comprehensive review on polyelectrolyte complexes, Drug Discovery Today 22 (11) (2017) 1697–1706.
[2] M. Aslam, M.A. Kalyar, Z.A. Raza, Polyvinyl alcohol: A review of research status and use of polyvinyl alcohol based nanocomposites, Polym. Eng. Sci. 58 (12) (2018) 2119–2132.
[3] M.I. Baker, S.P. Walsh, Z. Schwartz, B.D. Boyan, A review of polyvinyl alcohol and its uses in cartilage and orthopedic applications, J. Biomed. Mater. Res. B Appl. Biomater. 100 (5) (2012) 1451–1457.
[4] N.A. Peppas, E.W. Merrill, Crosslinked poly (vinyl alcohol) hydrogels as swollen elastic networks, J. Appl. Polym. Sci. 21 (7) (1977) 1763–1770.
[5] E.A. Kamoun, X. Chen, M.S.M. Eldin, E.-R.-S. Kenawy, Crosslinked poly (vinyl alcohol) hydrogels for wound dressing applications: A review of remarkably blended polymers, Arabian J. Chem. 8 (1) (2015) 1–14.
[6] M. Teodorescu, M. Bercea, S. Morariu, Biomaterials of PVA and PVP in medical and pharmaceutical applications: Perspectives and challenges, Biotechnol. Adv. 37 (1) (2019) 109–131.
[7] M. Hamidi, A. Azadi, P. Rafiei, Hydrogel nanoparticles in drug delivery, Adv. Drug Deliv. Rev. 60 (15) (2008) 1638–1649.
[8] W.E. Hennink, C.F. van Nostrum, Novel crosslinking methods to design hydrogels, Adv. Drug Deliv. Rev. 64 (2012) 223–236.
[9] A.d.A. Morandim-Giannetti, S.R. Rubio, R.F. Nogueira, F.d.S. Ortega, O. Magalhães Junior, P. Schor, P.A. Bersanetti, Characterization of PVA/glutaraldehyde hydrogels obtained using Central Composite Rotatable Design (CCRD), Journal of Biomedical Materials Research Part B: Applied Biomaterials 106(4) (2018) 1558-1566.
[10] T. Mehrotra, M.N. Zaman, B.B. Prasad, A. Shukla, S. Aggarwal, R. Singh, Rapid immobilization of viable Bacillus pseudomycoides in polyvinyl alcohol/glutaraldehyde hydrogel for biological treatment of municipal wastewater, Environ. Sci. Pollut. Res. (2020) 1–14.
[11] N. Teramoto, M. Saitoh, J. Kuroiwa, M. Shibata, R. Yosomiya, Morphology and mechanical properties of pullulan/poly (vinyl alcohol) blends crosslinked with glyoxal, J. Appl. Polym. Sci. 82 (9) (2001) 2273–2280.
[12] B. Karaman, A. Bozkurt, Enhanced performance of supercapacitor based on boric acid doped PVA-H2SO4 gel polymer electrolyte system, Int. J. Hydrogen Energy 43 (12) (2018) 6229–6237.
[13] B. Lu, F. Lin, X. Jiang, J. Cheng, Q. Lu, J. Song, C. Chen, B. Huang, One-pot assembly of microfibrillated cellulose reinforced PVA–borax hydrogels with self-healing and pH-responsive properties, ACS Sustainable Chem. Eng. 5 (1) (2017) 948–956.
[14] A.W.M. El-Naggar, M.M. Senna, T.A. Mostafa, R.H. Helal, Radiation synthesis and drug delivery properties of interpenetrating networks (IPNs) based on poly (vinyl alcohol)/methylcellulose blend hydrogels, Int. J. Biol. Macromol. 102 (2017) 1045–1051.
[15] S.M. Nasef, E.E. Khozemy, E.A. Kamoun, H. El-Gendi, Gamma radiation-induced crosslinked composite membranes based on polyvinyl alcohol/chitosan/AgNO3/vitamin E for biomedical applications, Int. J. Biol. Macromol. 137 (2019) 878–885.
[16] H.S. Mansur, C.M. Sadahira, A.N. Souza, A.A. Mansur, FTIR spectroscopy characterization of poly (vinyl alcohol) hydrogel with different hydrolysis degree and chemically crosslinked with glutaraldehyde, Mater. Sci. Eng., C 28 (4) (2008) 539–548.
[17] C. Chang, A. Lue, L. Zhang, Effects of crosslinking methods on structure and properties of cellulose/PVA hydrogels, Macromol. Chem. Phys. 209 (12) (2008) 1266–1273.
[18] H. Park, K. Park, W.S. Shalaby, Biodegradable hydrogels for drug delivery, CRC Press, 1993.
[19] Y. Liu, L.M. Geever, J.E. Kennedy, C.L. Higginbotham, P.A. Cahill, G. B. McGuinness, Thermal behavior and mechanical properties of physically crosslinked PVA/Gelatin hydrogels, J. Mech. Behav. Biomed. Mater. 3 (2) (2010) 203–209.
[20] J.L. Holloway, A.M. Lowman, G.R. Palmese, The role of crystallization and phase separation in the formation of physically cross-linked PVA hydrogels, Soft Matter 9 (3) (2013) 826–833.
[21] S. Bi, P. Wang, S. Hu, S. Li, J. Pang, Z. Zhou, G. Sun, L. Huang, X. Cheng, S. Xing, Construction of physical-crosslink chitosan/PVA double-network hydrogel with surface mineralization for bone repair, Carbohydr. Polym. 224 (2019), 115176.
[22] T. Miao, E.J. Miller, C. McKenzie, R.A. Oldinski, Physically crosslinked polyvinyl alcohol and gelatin interpenetrating polymer network theta-gels for cartilage regeneration, J. Mater. Chem. B 3 (48) (2015) 9242–9249.
[23] C. Hu, M.X. Wang, L. Sun, J.H. Yang, M. Zrínyi, Y.M. Chen, Dual-Physical Cross-Linked Tough and Photoluminescent Hydrogels with Good Biocompatibility and Antibacterial Activity, Macromol. Rapid Commun. 38 (10) (2017) 1600788.
[24] N.A. Peppas, Turbidimetric studies of aqueous poly (vinyl alcohol) solutions, Die Makromolekulare Chemie: Macromolecular Chemistry and Physics 176 (11) (1975) 3433–3440.
[25] E.-R. Kenawy, E.A. Kamoun, M.S.M. Eldin, M.A. El-Meligy, Physically crosslinked poly (vinyl alcohol)-hydroxyethyl starch blend hydrogel membranes: Synthesis and characterization for biomedical applications, Arabian J. Chem. 7 (3) (2014) 372–380.
[26] O. Moscoso-Londoño, J.S. Gonzalez, D. Muraca, C.E. Hoppe, V.A. Alvarez, A. López-Quintela, L.M. Socolovsky, K. Pirota, Structural and magnetic behavior of ferrogels obtained by freezing thawing of polyvinyl alcohol/poly (acrylic acid) (PAA)-coated iron oxide nanoparticles, Eur. Polym. J. 49 (2) (2013) 279–289.
[27] S.R. Van Tomme, M.J. van Steenbergen, S.C. De Smedt, C.F. van Nostrum, W. E. Hennink, Self-gelling hydrogels based on oppositely charged dextran microspheres, Biomaterials 26 (14) (2005) 2129–2135.
[28] F. Yokoyama, I. Masada, K. Shimamura, T. Ikawa, K. Monobe, Morphology and structure of highly elastic poly (vinyl alcohol) hydrogel prepared by repeated freezing-and-melting, Colloid Polym. Sci. 264 (7) (1986) 595–601.
[29] J.Y. Chang, D. Godovsky, M. Han, C. Hassan, J. Kim, B. Lee, Y. Lee, N. Peppas, R. Quirk, T. Yoo, Biopolymers· PVA Hydrogels Anionic Polymerisation Nanocomposites, Springer Science & Business Media, 2000.
[30] W. Wan, A.D. Bannerman, L. Yang, H. Mak, Poly (vinyl alcohol) cryogels for biomedical applications, Polymeric Cryogels (2014) 283–321.
[31] Y. Zhuang, Y. Kong, K. Han, H. Hao, B. Shi, A physically cross-linked self-healable double-network polymer hydrogel as a framework for nanomaterial, New J. Chem. 41 (24) (2017) 15127–15135.
[32] R. Hernández, A. Sarafian, D. López, C. Mijangos, Viscoelastic properties of poly (vinyl alcohol) hydrogels and ferrogels obtained through freezing–thawing cycles, Polymer 45 (16) (2004) 5543–5549.
[33] S. Gupta, A.K. Pramanik, A. Kailath, T. Mishra, A. Guha, S. Nayar, A. Sinha, Composition dependent structural modulations in transparent poly (vinyl alcohol) hydrogels, Colloids Surf., B 74 (1) (2009) 186–190.
[34] T. Abitbol, T. Johnstone, T.M. Quinn, D.G. Gray, Reinforcement with cellulose nanocrystals of poly (vinyl alcohol) hydrogels prepared by cyclic freezing and thawing, Soft Matter 7 (6) (2011) 2373–2379.
[35] J.L. Holloway, A.M. Lowman, G.R. Palmese, Mechanical evaluation of poly (vinyl alcohol)-based fibrous composites as biomaterials for meniscal tissue replacement, Acta Biomater. 6 (12) (2010) 4716–4724.
[36] N. Joshi, K. Suman, Y.M. Joshi, Rheological behavior of aqueous poly (vinyl alcohol) solution during a freeze–thaw gelation process, Macromolecules 53 (9) (2020) 3452–3463.
[37] Y. Chen, C. Jiao, X. Peng, T. Liu, Y. Shi, M. Liang, H. Wang, Biomimetic anisotropic poly (vinyl alcohol) hydrogels with significantly enhanced mechanical properties by freezing–thawing under drawing, J. Mater. Chem. B 7 (20) (2019) 3243–3249.
[38] B.S. Chee, G.G. de Lima, D.M. Devine, M.J. Nugent, Investigation of the effects of orientation on freeze/thawed Polyvinyl alcohol hydrogel properties, Materials Today, Communications 17 (2018) 82–93.
[39] T. Yamamoto, Molecular dynamics simulation of stretch-induced crystallization in polyethylene: Emergence of fiber structure and molecular network, Macromolecules 52 (4) (2019) 1695–1706.
[40] H. Adelnia, H.C. Bidsorkhi, A. Ismail, T. Matsuura, Gas permeability and permselectivity properties of ethylene vinyl acetate/sepiolite mixed matrix membranes, Sep. Purif. Technol. 146 (2015) 351–357.
[41] N.A. Peppas, J.E. Scott, Controlled release from poly (vinyl alcohol) gels prepared by freezing-thawing processes, J. Control. Release 18 (2) (1992) 95–100.

[42] U. Fumio, Y. Hiroshi, N. Kumiko, N. Sachihiko, S. Kenji, M. Yasunori, Swelling and mechanical properties of poly (vinyl alcohol) hydrogels, Int. J. Pharm. 58 (2) (1990) 135–142.

[43] C.M. Hassan, N.A. Peppas, Structure and morphology of freeze/thawed PVA hydrogels, Macromolecules 33 (7) (2000) 2472–2479.

[44] J.L. Holloway, K.L. Spiller, A.M. Lowman, G.R. Palmese, Analysis of the in vitro swelling behavior of poly (vinyl alcohol) hydrogels in osmotic pressure solution for soft tissue replacement, Acta Biomater. 7 (6) (2011) 2477–2482.

[45] S.R. Stauffer, N.A. Peppast, Poly (vinyl alcohol) hydrogels prepared by freezing-thawing cyclic processing, Polymer 33 (18) (1992) 3932–3936.

[46] N.A. Peppas, N.K. Mongia, Ultrapure poly (vinyl alcohol) hydrogels with mucoadhesive drug delivery characteristics, Eur. J. Pharm. Biopharm. 43 (1) (1997) 51–58.

[47] C.M. Hassan, N.A. Peppas, Structure and applications of poly (vinyl alcohol) hydrogels produced by conventional crosslinking or by freezing/thawing methods, Biopolymers· PVA Hydrogels, Anionic Polymerisation Nanocomposites, Springer2000, pp. 37-65.

[48] M. Figueroa-Pizano, I. Vélaz, F. Penas, P. Zavala-Rivera, A. Rosas-Durazo, A. Maldonado-Arce, M. Martínez-Barbosa, Effect of freeze-thawing conditions for preparation of chitosan-poly (vinyl alcohol) hydrogels and drug release studies, Carbohydr. Polym. 195 (2018) 476–485.

[49] T. Hatakeyama, A. Yamauchi, H. Hatakeyama, Effect of thermal hysteresis on structural change of water restrained in poly (vinyl alcohol) pseudo-gel, Eur. Polym. J. 23 (5) (1987) 361–365.

[50] V. Lozinsky, F. Plieva, Poly (vinyl alcohol) cryogels employed as matrices for cell immobilization. 3. Overview of recent research and developments, Enzyme Microb. Technol. 23 (3–4) (1998) 227–242.

[51] V.I. Lozinsky, A.L. Zubov, I.N. Savina, F.M. Plieva, Study of cryostructuration of polymer systems. XIV. Poly (vinyl alcohol) cryogels: Apparent yield of the freeze–thaw-induced gelation of concentrated aqueous solutions of the polymer, J. Appl. Polym. Sci. 77 (8) (2000) 1822–1831.

[52] V.I. Lozinsky, L.G. Damshkaln, Study of cryostructuration of polymer systems. XVII. Poly (vinyl alcohol) cryogels: Dynamics of the cryotropic gel formation, J. Appl. Polym. Sci. 77 (9) (2000) 2017–2023.

[53] W. Wan, G. Campbell, Z. Zhang, A. Hui, D. Boughner, Optimizing the tensile properties of polyvinyl alcohol hydrogel for the construction of a bioprosthetic heart valve stent, Journal of Biomedical Materials Research: An Official Journal of the Society for Biomaterials, the Japanese Society for Biomaterials, and the Australian Society for Biomaterials and the Korean Society for, Biomaterials 63 (6) (2002) 854–861.

[54] T. Hatakeyema, J. Uno, C. Yamada, A. Kishi, H. Hatakeyama, Gel–sol transition of poly (vinyl alcohol) hydrogels formed by freezing and thawing, Thermochim Acta 431 (1–2) (2005) 144–148.

[55] M. Nugent, C. Higginbotham, Investigation of the influence of freeze-thaw processing on the properties of polyvinyl alcohol/polyacrylic acid complexes, J. Mater. Sci. 41 (8) (2006) 2393–2404.

[56] S. Butylina, S. Geng, K. Oksman, Properties of as-prepared and freeze-dried hydrogels made from poly (vinyl alcohol) and cellulose nanocrystals using freeze-thaw technique, Eur. Polym. J. 81 (2016) 386–396.

[57] A. Takamura, F. Ishii, H. Hidaka, Drug release from poly (vinyl alcohol) gel prepared by freeze-thaw procedure, J. Control. Release 20 (1) (1992) 21–27.

[58] Y. Nagakawa, S. Fujita, S. Yunoki, T. Tsuchiya, S.i. Suye, T. Itoi, Self-expandable hydrogel biliary stent design utilizing the swelling property of poly (vinyl alcohol) hydrogel, Journal of Applied Polymer Science 137(28) (2020) 48851.

[59] M. Watase, K. Nishinari, Rheological and DSC changes in poly (vinyl alcohol) gels induced by immersion in water, Journal of Polymer Science: Polymer Physics Edition 23 (9) (1985) 1803–1811.

[60] V. Lozinsky, E. Vainerman, L. Domotenko, A. Mamtsis, E. Titova, E. Belavtseva, S. Rogozhin, Study of cryostructurization of polymer systems VII. Structure formation under freezing of poly (vinyl alcohol) aqueous solutions, Colloid Polym. Sci. 264 (1) (1986) 19–24.

[61] J. Stasko, M. Kalniņš, A. Dzene, V. Tupureina, Poly (vinyl alcohol) hydrogels, Proc. Est. Acad. Sci. 58 (1) (2009).

[62] Q. Rong, W. Lei, L. Chen, Y. Yin, J. Zhou, M. Liu, Anti-freezing, conductive self-healing organohydrogels with stable strain-sensitivity at subzero temperatures, Angew. Chem. Int. Ed. 56 (45) (2017) 14159–14163.

[63] J. Tavakoli, J. Gascooke, N. Xie, B.Z. Tang, Y. Tang, Enlightening Freeze-Thaw Process of Physically Cross-Linked Poly (vinyl alcohol) Hydrogels by Aggregation-Induced Emission Fluorogens, ACS Applied Polymer Materials 1 (6) (2019) 1390–1398.

[64] S.J. Hong, H.T. Huang, P.D. Hong, Effects of solvent adsorption on solution properties of poly (vinyl alcohol)/dimethylsulfoxide/water ternary systems, J. Appl. Polym. Sci. 92 (5) (2004) 3211–3217.

[65] G.K. Tummala, R. Rojas, A. Mihranyan, Poly (vinyl alcohol) hydrogels reinforced with nanocellulose for ophthalmic applications: general characteristics and optical properties, J. Phys. Chem. B 120 (51) (2016) 13094–13101.

[66] Y. Hou, C. Chen, K. Liu, Y. Tu, L. Zhang, Y. Li, Preparation of PVA hydrogel with high-transparence and investigations of its transparent mechanism, RSC Adv. 5 (31) (2015) 24023–24030.

[67] S.-H. Hyon, W.-I. Cha, Y. Ikada, Preparation of transparent poly (vinyl alcohol) hydrogel, Polym. Bull. 22 (2) (1989) 119–122.

[68] P. Yusong, D. Jie, C. Yan, S. Qianqian, Study on mechanical and optical properties of poly (vinyl alcohol) hydrogel used as soft contact lens, Mater. Technol. 31 (5) (2016) 266–273.

[69] H. Hoshino, S. Okada, H. Urakawa, K. Kajiwara, Gelation of poly (vinyl alcohol) in dimethyl sulfoxide/water solvent, Polym. Bull. 37 (2) (1996) 237–244.

[70] R.N. Havemeyer, Freezing point curve of dimethyl sulfoxide—water solutions, J. Pharm. Sci. 55 (8) (1966) 851–853.

[71] S. Gupta, T.J. Webster, A. Sinha, Evolution of PVA gels prepared without crosslinking agents as a cell adhesive surface, J. Mater. Sci. - Mater. Med. 22 (7) (2011) 1763–1772.

[72] T. Kanaya, M. Ohkura, K. Kaji, M. Furusaka, M. Misawa, Structure of poly (vinyl alcohol) gels studied by wide-and small-angle neutron scattering, Macromolecules 27 (20) (1994) 5609–5615.

[73] S.-J. Hong, P.-D. Hong, J.-C. Chen, K.-S. Shih, Effect of mixed solvent on solution properties and gelation behavior of poly (vinyl alcohol), Eur. Polym. J. 45 (4) (2009) 1158–1168.

[74] N. Takahashi, T. Kanaya, K. Nishida, K. Kaji, Effects of cononsolvency on gelation of poly (vinyl alcohol) in mixed solvents of dimethyl sulfoxide and water, Polymer 44 (15) (2003) 4075–4078.

[75] P. He, J. Wu, X. Pan, L. Chen, K. Liu, H. Gao, H. Wu, S. Cao, L. Huang, Y. Ni, Anti-freezing and moisturizing conductive hydrogels for strain sensing and moist-electric generation applications, J. Mater. Chem. A 8 (6) (2020) 3109–3118.

[76] X.-J. Zha, S.-T. Zhang, J.-H. Pu, X. Zhao, K. Ke, R.-Y. Bao, L. Bai, Z.-Y. Liu, M.-B. Yang, W. Yang, Nanofibrillar Poly (vinyl alcohol) Ionic Organohydrogels for Smart Contact Lens and Human-Interactive Sensing, ACS Appl. Mater. Interfaces 12 (20) (2020) 23514–23522.

[77] J.O. Kim, J.Y. Choi, J.K. Park, J.H. Kim, S.G. Jin, S.W. Chang, D.X. Li, M.-R. Hwang, J.S. Woo, J.-A. Kim, Development of clindamycin-loaded wound dressing with polyvinyl alcohol and sodium alginate, Biol. Pharm. Bull. 31 (12) (2008) 2277–2282.

[78] A. Fahmy, E.A. Kamoun, R. El-Eisawy, E.M. El-Fakharany, T.H. Taha, B.K. El-Damhougy, F. Abdelhai, Poly (vinyl alcohol)-hyaluronic acid membranes for wound dressing applications: synthesis and in vitro bio-evaluations, J. Braz. Chem. Soc. 26 (7) (2015) 1466–1474.

[79] M.G. Cascone, S. Maltinti, N. Barbani, M. Laus, Effect of chitosan and dextran on the properties of poly (vinyl alcohol) hydrogels, J. Mater. Sci. - Mater. Med. 10 (7) (1999) 431–435.

[80] X. Qi, X. Hu, W. Wei, H. Yu, J. Li, J. Zhang, W. Dong, Investigation of Salecan/poly (vinyl alcohol) hydrogels prepared by freeze/thaw method, Carbohydr. Polym. 118 (2015) 60–69.

[81] A. Thangprasert, C. Tansakul, N. Thuaksubun, J. Meesane, Mimicked hybrid hydrogel based on gelatin/PVA for tissue engineering in subchondral bone interface for osteoarthritis surgery, Mater. Des. 183 (2019), 108113.

[82] J. Kundu, L.A. Poole-Warren, P. Martens, S.C. Kundu, Silk fibroin/poly (vinyl alcohol) photocrosslinked hydrogels for delivery of macromolecular drugs, Acta Biomater. 8 (5) (2012) 1720–1729.

[83] X.Y. Wu, S.W. Huang, J.T. Zhang, R.X. Zhuo, Preparation and characterization of novel physically cross-linked hydrogels composed of poly (vinyl alcohol) and amine-terminated polyamidoamine dendrimer, Macromol. Biosci. 4 (2) (2004) 71–75.

[84] W.J. Koshut, D. Smoot, C. Rummel, A. Kirillova, K. Gall, Tensile Fatigue of Poly (Vinyl Alcohol) Hydrogels with Bio-Friendly Toughening Agents, Macromol. Mater. Eng. 305 (3) (2020) 1900784.

[85] X. Niu, Y. Wang, C. Xu, Z. Fu, S. Bai, J. Wang, Y. Wang, X. Guo, Access to Highly Tough Hydrogels by Polymer Modules for Application of Catalytic Reactors, Ind. Eng. Chem. Res. 59 (11) (2020) 4977–4986.

[86] A. Golabdar, H. Adelnia, N. Moshtzan, J. Nasrollah Gavgani, H. Izadi-Vasafi, Anti-bacterial poly (vinyl alcohol) nanocomposite hydrogels reinforced with in situ synthesized silver nanoparticles, Polym. Compos. 40 (4) (2019) 1322–1328.

[87] K. Nešović, A. Janković, V. Kojić, M. Vukašinović-Sekulić, A. Perić-Grujić, K. Y. Rhee, V. Mišković-Stanković, Silver/poly (vinyl alcohol)/chitosan/graphene hydrogels–Synthesis, biological and physicochemical properties and silver release kinetics, Compos. B Eng. 154 (2018) 175–185.

[88] R. Surudžić, A. Janković, N. Bibić, M. Vukašinović-Sekulić, A. Perić-Grujić, V. Mišković-Stanković, S.J. Park, K.Y. Rhee, Physico–chemical and mechanical properties and antibacterial activity of silver/poly (vinyl alcohol)/graphene nanocomposites obtained by electrochemical method, Compos. B Eng. 85 (2016) 102–112.

[89] K. Nešović, A. Janković, T. Radetić, M. Vukašinović-Sekulić, V. Kojić, L. Živković, A. Perić-Grujić, K.Y. Rhee, V. Mišković-Stanković, Chitosan-based hydrogel wound dressings with electrochemically incorporated silver nanoparticles–In vitro study, Eur. Polym. J. 121 (2019), 109257.

[90] M. Abudabbus, I. Jevremović, A. Janković, A. Perić-Grujić, I. Matić, M. Vukašinović-Sekulić, D. Hui, K. Rhee, V. Mišković-Stanković, Biological activity of electrochemically synthesized silver doped polyvinyl alcohol/graphene composite hydrogel discs for biomedical applications, Compos. B Eng. 104 (2016) 26–34.

[91] S. Agnihotri, S. Mukherji, S. Mukherji, Antimicrobial chitosan–PVA hydrogel as a nanoreactor and immobilizing matrix for silver nanoparticles, Applied Nanoscience 2 (3) (2012) 179–188.

[92] J.S. Gonzalez, C.E. Hoppe, P. Mendoza Zélis, L. Arciniegas, G.A. Pasquevich, F. H. Sánchez, V.A. Alvarez, Simple and efficient procedure for the synthesis of ferrogels based on physically cross-linked PVA, Ind. Eng. Chem. Res. 53 (1) (2014) 214–221.

[93] W. Li, D. Wang, W. Yang, Y. Song, Compressive mechanical properties and microstructure of PVA–HA hydrogels for cartilage repair, RSC Adv. 6 (24) (2016) 20166–20172.

[94] X. He, C. Zhang, M. Wang, Y. Zhang, L. Liu, W. Yang, An electrically and mechanically autonomic self-healing hybrid hydrogel with tough and thermoplastic properties, ACS Appl. Mater. Interfaces 9 (12) (2017) 11134–11143.

[95] Z. Mbhele, M. Salemane, C. Van Sittert, J. Nedeljković, V. Djoković, A. Luyt, Fabrication and characterization of silver– polyvinyl alcohol nanocomposites, Chem. Mater. 15 (26) (2003) 5019–5024.
[96] H. Yu, X. Xu, X. Chen, T. Lu, P. Zhang, X. Jing, Preparation and antibacterial effects of PVA-PVP hydrogels containing silver nanoparticles, J. Appl. Polym. Sci. 103 (1) (2007) 125–133.
[97] H.C. Bidsorkhi, H. Adelnia, N. Naderi, N. Moazeni, Z. Mohamad, Ethylene vinyl acetate copolymer nanocomposites based on (un) modified sepiolite: Flame retardancy, thermal, and mechanical properties, Polym. Compos. 38 (7) (2017) 1302–1310.
[98] A. Karimi, W.M.A. Wan Daud, Harmless hydrogels based on PVA/Na+-MMT nanocomposites for biomedical applications: fabrication and characterization, Polym. Compos. 38 (6) (2017) 1135–1143.
[99] C. Yu, X. Tang, S. Liu, Y. Yang, X. Shen, C. Gao, Laponite crosslinked starch/polyvinyl alcohol hydrogels by freezing/thawing process and studying their cadmium ion absorption, Int. J. Biol. Macromol. 117 (2018) 1–6.
[100] G. Sharifzadeh, M. Soheilmoghaddam, H. Adelnia, M.U. Wahit, M.R.D. Arzhandi, A. Moslehyani, Biocompatible regenerated cellulose/halloysite nanocomposite fibers, Polym. Eng. Sci. 60 (6) (2020) 1169–1176.
[101] L.M. Sanchez, P.S. Shuttleworth, C. Waiman, G. Zanini, V.A. Alvarez, R.P. Ollier, Physically-crosslinked polyvinyl alcohol composite hydrogels containing clays, carbonaceous materials and magnetic nanoparticles as fillers, J. Environ. Chem. Eng. 8 (3) (2020), 103795.
[102] L.M. Sanchez, R.P. Ollier, V.A. Alvarez, Sorption behavior of polyvinyl alcohol/bentonite hydrogels for dyes removal, J. Polym. Res. 26 (6) (2019) 1–8.
[103] E. Ghanaatian, M. Entezam, Mechanical properties and drug release rate of poly (vinyl alcohol)/poly (ethylene glycol)/clay nanocomposite hydrogels: Correlation with structure and physical properties, J. Appl. Polym. Sci. 136 (32) (2019) 47843.
[104] B. Rezazadeh, M. Sirousazar, V. Abbasi-Chianeh, F. Kheiri, Polymer-clay nanocomposite hydrogels for molecular irrigation application, J. Appl. Polym. Sci. 137 (18) (2020) 48631.
[105] M. Kokabi, M. Sirousazar, Z.M. Hassan, PVA–clay nanocomposite hydrogels for wound dressing, Eur. Polym. J. 43 (3) (2007) 773–781.
[106] M. Sirousazar, M. Kokabi, Z. Hassan, A. Bahramian, Mineral kaolinite clay for preparation of nanocomposite hydrogels, J. Appl. Polym. Sci. 125 (S1) (2012) E122–E130.
[107] M. Sirousazar, M. Kokabi, Z. Hassan, Swelling behavior and structural characteristics of polyvinyl alcohol/montmorillonite nanocomposite hydrogels, J. Appl. Polym. Sci. 123 (1) (2012) 50–58.
[108] L. Jing, H. Li, R.Y. Tay, B. Sun, S.H. Tsang, O. Cometto, J. Lin, E.H.T. Teo, A.I. Y. Tok, Biocompatible hydroxylated boron nitride nanosheets/poly (vinyl alcohol) interpenetrating hydrogels with enhanced mechanical and thermal responses, ACS Nano 11 (4) (2017) 3742–3751.
[109] K. Kalantari, E. Mostafavi, B. Saleh, P. Soltantabar, T.J. Webster, Chitosan/PVA hydrogels incorporated with green synthesized cerium oxide nanoparticles for wound healing applications, Eur. Polym. J. 134 (2020), 109853.
[110] G. Du, L. Nie, G. Gao, Y. Sun, R. Hou, H. Zhang, T. Chen, J. Fu, Tough and biocompatible hydrogels based on in situ interpenetrating networks of dithiol-connected graphene oxide and poly (vinyl alcohol), ACS Appl. Mater. Interfaces 7 (5) (2015) 3003–3008.
[111] L. Zhang, Z. Wang, C. Xu, Y. Li, J. Gao, W. Wang, Y. Liu, High strength graphene oxide/polyvinyl alcohol composite hydrogels, J. Mater. Chem. 21 (28) (2011) 10399–10406.
[112] S. Baseghi, H. Garmabi, J.N. Gavgani, H. Adelnia, Lightweight high-density polyethylene/carbonaceous nanosheets microcellular foams with improved electrical conductivity and mechanical properties, J. Mater. Sci. 50 (14) (2015) 4994–5004.
[113] J.W. Suk, R.D. Piner, J. An, R.S. Ruoff, Mechanical properties of monolayer graphene oxide, ACS Nano 4 (11) (2010) 6557–6564.
[114] C. Lee, X. Wei, J.W. Kysar, J. Hone, Measurement of the elastic properties and intrinsic strength of monolayer graphene, Science 321 (5887) (2008) 385–388.
[115] J.N. Gavgani, H. Adelnia, M.M. Gudarzi, Intumescent flame retardant polyurethane/reduced graphene oxide composites with improved mechanical, thermal, and barrier properties, J. Mater. Sci. 49 (1) (2014) 243–254.
[116] J.N. Gavgani, H. Adelnia, D. Zaarei, M.M. Gudarzi, Lightweight flexible polyurethane/reduced ultralarge graphene oxide composite foams for electromagnetic interference shielding, RSC Adv. 6 (33) (2016) 27517–27527.
[117] M. Soheilmoghaddam, H. Adelnia, H.C. Bidsorkhi, G. Sharifzadeh, M.U. Wahit, N. I. Akos, A.A. Yussuf, Development of ethylene-vinyl acetate composites reinforced with graphene platelets, Macromol. Mater. Eng. 302 (2) (2017) 1600260.
[118] R. Xue, X. Xin, L. Wang, J. Shen, F. Ji, W. Li, C. Jia, G. Xu, A systematic study of the effect of molecular weights of polyvinyl alcohol on polyvinyl alcohol–graphene oxide composite hydrogels, PCCP 17 (7) (2015) 5431–5440.
[119] H. Bai, C. Li, X. Wang, G. Shi, A pH-sensitive graphene oxide composite hydrogel, Chem. Commun. 46 (14) (2010) 2376–2378.
[120] H. Bai, C. Li, X. Wang, G. Shi, On the gelation of graphene oxide, The Journal of Physical Chemistry C 115 (13) (2011) 5545–5551.
[121] Y. Meng, L. Ye, P. Coates, P. Twigg, In situ cross-linking of poly (vinyl alcohol)/graphene oxide–polyethylene glycol nanocomposite hydrogels as artificial cartilage replacement: intercalation structure, unconfined compressive behavior, and biotribological behaviors, The Journal of Physical Chemistry C 122 (5) (2018) 3157–3167.
[122] Y. Meng, J. Cao, Y. Chen, Y. Yu, L. Ye, 3D printing of a poly (vinyl alcohol)-based nano-composite hydrogel as an artificial cartilage replacement and the improvement mechanism of printing accuracy, J. Mater. Chem. B 8 (4) (2020) 677–690.
[123] J. Chen, X. Shi, L. Ren, Y. Wang, Graphene oxide/PVA inorganic/organic interpenetrating hydrogels with excellent mechanical properties and biocompatibility, Carbon 111 (2017) 18–27.
[124] F.A. Tabr, F. Salehiravesh, H. Adelnia, J.N. Gavgani, M. Mahyari, High sensitivity ammonia detection using metal nanoparticles decorated on graphene macroporous frameworks/polyaniline hybrid, Talanta 197 (2019) 457–464.
[125] M. Soheilmoghaddam, H. Adelnia, G. Sharifzadeh, M.U. Wahit, T.W. Wong, A. A. Yussuf, Bionanocomposite regenerated cellulose/single-walled carbon nanotube films prepared using ionic liquid solvent, Cellulose 24 (2) (2017) 811–822.
[126] C. Liu, H. Liu, T. Xiong, A. Xu, B. Pan, K. Tang, Graphene oxide reinforced alginate/PVA double network hydrogels for efficient dye removal, Polymers 10 (8) (2018) 835.
[127] Y. Huang, M. Zhang, W. Ruan, High-water-content graphene oxide/polyvinyl alcohol hydrogel with excellent mechanical properties, J. Mater. Chem. A 2 (27) (2014) 10508–10515.
[128] Y. Shi, D. Xiong, J. Li, N. Wang, The water-locking and cross-linking effects of graphene oxide on the load-bearing capacity of poly (vinyl alcohol) hydrogel, RSC Adv. 6 (86) (2016) 82467–82477.
[129] X. Rui-Hong, R. Peng-Gang, H. Jian, R. Fang, R. Lian-Zhen, S. Zhen-Feng, Preparation and properties of graphene oxide-regenerated cellulose/polyvinyl alcohol hydrogel with pH-sensitive behavior, Carbohydr. Polym. 138 (2016) 222–228.
[130] C.H. Li, J.L. Zuo, Self-Healing Polymers Based on Coordination Bonds, Adv. Mater. 1903762 (2019).
[131] H. Zhang, H. Xia, Y. Zhao, Poly (vinyl alcohol) hydrogel can autonomously self-heal, ACS Macro Lett. 1 (11) (2012) 1233–1236.
[132] A.J. Amaral, G. Pasparakis, Stimuli responsive self-healing polymers: gels, elastomers and membranes, Polym. Chem. 8 (42) (2017) 6464–6484.
[133] H. Hong, H. Liao, S. Chen, H. Zhang, Facile method to prepare self-healable PVA hydrogels with high water stability, Mater. Lett. 122 (2014) 227–229.
[134] G. Li, Q. Yan, H. Xia, Y. Zhao, Therapeutic-ultrasound-triggered shape memory of a melamine-enhanced poly (vinyl alcohol) physical hydrogel, ACS Appl. Mater. Interfaces 7 (22) (2015) 12067–12073.
[135] Z. Zhang, T. Li, B. Chen, S. Wang, Z. Guo, Self-healing supramolecular hydrogel of poly (vinyl alcohol)/chitosan carbon dots, J. Mater. Sci. 52 (17) (2017) 10614–10623.
[136] G. Li, H. Zhang, D. Fortin, H. Xia, Y. Zhao, Poly (vinyl alcohol)–poly (ethylene glycol) double-network hydrogel: a general approach to shape memory and self-healing functionalities, Langmuir 31 (42) (2015) 11709–11716.
[137] K. Song, W. Zhu, X. Li, Z. Yu, A novel mechanical robust, self-healing and shape memory hydrogel based on PVA reinforced by cellulose nanocrystal, Mater. Lett. 260 (2020), 126884.
[138] L. Yang, Z. Wang, G. Fei, H. Xia, Polydopamine particles reinforced poly (vinyl alcohol) hydrogel with NIR light triggered shape memory and self-healing capability, Macromol. Rapid Commun. 38 (23) (2017) 1700421.
[139] P. Guo, J. Liang, Y. Li, X. Lu, H. Fu, H. Jing, S. Guan, D. Han, L. Niu, High-strength and pH-responsive self-healing polyvinyl alcohol/poly 6-acrylamidohexanoic acid hydrogel based on dual physically cross-linked network, Colloids Surf., A 571 (2019) 64–71.
[140] A. Lendlein, H. Jiang, O. Jünger, R. Langer, Light-induced shape-memory polymers, Nature 434 (7035) (2005) 879–882.
[141] T. Xie, Recent advances in polymer shape memory, Polymer 52 (22) (2011) 4985–5000.
[142] Y. Osada, A. Matsuda, Shape memory in hydrogels, Nature 376(6537) (1995) 219-219.
[143] G. Li, G. Fei, H. Xia, J. Han, Y. Zhao, Spatial and temporal control of shape memory polymers and simultaneous drug release using high intensity focused ultrasound, J. Mater. Chem. 22 (16) (2012) 7692–7696.
[144] A. Lendlein, S. Kelch, Shape-memory polymers, Angew. Chem. Int. Ed. 41 (12) (2002) 2034–2057.
[145] M. Zarek, N. Mansour, S. Shapira, D. Cohn, 4D printing of shape memory-based personalized endoluminal medical devices, Macromol. Rapid Commun. 38 (2) (2017) 1600628.
[146] S.O. Omid, Z. Goudarzi, L.M. Kangarshahi, A. Mokhtarzade, F. Bahrami, Self-expanding stents based on shape memory alloys and shape memory polymers, Journal of Composites and Compounds 2 (3) (2020) 92–98.
[147] A. Lendlein, O.E. Gould, Reprogrammable recovery and actuation behaviour of shape-memory polymers, Nat. Rev. Mater. 4 (2) (2019) 116–133.
[148] J. Shang, X. Le, J. Zhang, T. Chen, P. Theato, Trends in polymeric shape memory hydrogels and hydrogel actuators, Polym. Chem. 10 (9) (2019) 1036–1055.
[149] C. Löwenberg, M. Balk, C. Wischke, M. Behl, A. Lendlein, Shape-memory hydrogels: evolution of structural principles to enable shape switching of hydrophilic polymer networks, Acc. Chem. Res. 50 (4) (2017) 723–732.
[150] R. Liang, L. Wang, H. Yu, A. Khan, B.U. Amin, R.U. Khan, Molecular design, synthesis and biomedical applications of stimuli-responsive shape memory hydrogels, Eur. Polym. J. 114 (2019) 380–396.
[151] Y. Bai, J. Zhang, X. Chen, A thermal-, water-, and near-infrared light-induced shape memory composite based on polyvinyl alcohol and polyaniline fibers, ACS Appl. Mater. Interfaces 10 (16) (2018) 14017–14025.
[152] Y.-N. Chen, L. Peng, T. Liu, Y. Wang, S. Shi, H. Wang, Poly (vinyl alcohol)–tannic acid hydrogels with excellent mechanical properties and shape memory behaviors, ACS Appl. Mater. Interfaces 8 (40) (2016) 27199–27206.

[153] J. Kim, J.W. Kim, H.C. Kim, L. Zhai, H.-U. Ko, R.M. Muthoka, Review of soft actuator materials, Int. J. Precis. Eng. Manuf. 20 (12) (2019) 2221–2241.
[154] Q. Shi, H. Liu, D. Tang, Y. Li, X. Li, F. Xu, Bioactuators based on stimulus-responsive hydrogels and their emerging biomedical applications, NPG Asia Mater. 11 (1) (2019) 1–21.
[155] S. Murdan, Electro-responsive drug delivery from hydrogels, J. Control. Release 92 (1–2) (2003) 1–17.
[156] T. Jayaramudu, H.-U. Ko, H.C. Kim, J.W. Kim, R.M. Muthoka, J. Kim, Electroactive hydrogels made with polyvinyl alcohol/cellulose nanocrystals, Materials 11 (9) (2018) 1615.
[157] T. Jayaramudu, H.-U. Ko, L. Zhai, Y. Li, J. Kim, Preparation and characterization of hydrogels from polyvinyl alcohol and cellulose and their electroactive behavior, Soft Mater. 15 (1) (2017) 64–72.
[158] J. Kim, T. Jayaramudu, L. Zhai, H.C. Kim, D.O. Agumba, Preparation of Cellulose Nanocrystal-Reinforced Physical Hydrogels for Actuator Application, Crystals 10 (11) (2020) 969.
[159] T. Jayaramudu, Y. Li, H.-U. Ko, I.R. Shishir, J. Kim, Poly (acrylic acid)-Poly (vinyl alcohol) hydrogels for reconfigurable lens actuators, International Journal of Precision Engineering and Manufacturing-Green Technology 3 (4) (2016) 375–379.
[160] T.H. Lee, J.Y. Jho, Temperature-Responsive Actuators Fabricated with PVA/PNIPAAm Interpenetrating Polymer Network Bilayers, Macromol. Res. 26 (7) (2018) 659–664.
[161] R. Ramanujan, L. Lao, The mechanical behavior of smart magnet–hydrogel composites, Smart Mater. Struct. 15 (4) (2006) 952.
[162] H. Omidian, K. Park, Hydrogels, in: J. Siepmann, R.A. Siegel, M.J. Rathbone (Eds.), Fundamentals and Applications of Controlled Release Drug Delivery, Springer, US, Boston, MA, 2012, pp. 75–105.
[163] S.-H. Shin, W. Lee, S.-M. Kim, M. Lee, J.M. Koo, S.Y. Hwang, D.X. Oh, J. Park, Ion-conductive self-healing hydrogels based on an interpenetrating polymer network for a multimodal sensor, Chem. Eng. J. 371 (2019) 452–460.
[164] H. Adelnia, J.N. Gavgani, M. Soheilmoghaddam, Fabrication of composite polymer particles by stabilizer-free seeded polymerization, Colloid Polym. Sci. 293 (8) (2015) 2445–2450.
[165] H. Adelnia, S. Pourmahdian, Soap-free emulsion polymerization of poly (methyl methacrylate-co-butyl acrylate): effects of anionic comonomers and methanol on the different characteristics of the latexes, Colloid Polym. Sci. 292 (1) (2014) 197–205.
[166] H. Adelnia, J.N. Gavgani, H. Riazi, H.C. Bidsorkhi, Transition behavior, surface characteristics and film formation of functionalized poly (methyl methacrylate-co-butyl acrylate) particles, Prog. Org. Coat. 77 (11) (2014) 1826–1833.
[167] Y. Zhou, C. Wan, Y. Yang, H. Yang, S. Wang, Z. Dai, K. Ji, H. Jiang, X. Chen, Y. Long, Highly stretchable, elastic, and ionic conductive hydrogel for artificial soft electronics, Adv. Funct. Mater. 29 (1) (2019) 1806220.
[168] Z. Zhao, H. Chen, H. Zhang, L. Ma, Z. Wang, Polyacrylamide-phytic acid-polydopamine conducting porous hydrogel for rapid detection and removal of copper (II) ions, Biosens. Bioelectron. 91 (2017) 306–312.
[169] X. Wang, Y. Qiu, G. Chen, Z. Chu, A. Shadike, C. Chen, C. Chen, Z. Zhu, Self-healable poly (vinyl alcohol) photonic crystal hydrogel, ACS Applied Polymer Materials 2 (5) (2020) 2086–2092.
[170] S.A. Asher, K.W. Kimble, J.P. Walker, Enabling thermoreversible physically cross-linked polymerized colloidal array photonic crystals, Chem. Mater. 20 (24) (2008) 7501–7509.
[171] X. Sun, S. Agate, K.S. Salem, L. Lucia, L. Pal, Hydrogel-Based Sensor Networks: Compositions, Properties, and Applications—A Review, ACS Applied Bio Materials (2020).
[172] J.J. Bohn, M. Ben-Moshe, A. Tikhonov, D. Qu, D.N. Lamont, S.A. Asher, Charge stabilized crystalline colloidal arrays as templates for fabrication of non-close-packed inverted photonic crystals, J. Colloid Interface Sci. 344 (2) (2010) 298–307.
[173] H. Jiang, X. Yang, C. Chen, Y. Zhu, C. Li, Facile and controllable fabrication of three-dimensionally quasi-ordered macroporous TiO 2 for high performance lithium-ion battery applications, New J. Chem. 37 (5) (2013) 1578–1583.
[174] J. Qin, B. Dong, L. Cao, W. Wang, Photonic hydrogels for the ultratrace sensing of divalent beryllium in seawater, J. Mater. Chem. C 6 (15) (2018) 4234–4242hild::* [last()])">.
[175] A.E. Coukouma, N.L. Smith, S.A. Asher, Removable interpenetrating network enables highly-responsive 2-D photonic crystal hydrogel sensors, Analyst 140 (19) (2015) 6517–6521.
[176] H. Jiang, Y. Zhu, C. Chen, J. Shen, H. Bao, L. Peng, X. Yang, C. Li, Photonic crystal pH and metal cation sensors based on poly (vinyl alcohol) hydrogel, New J. Chem. 36 (4) (2012) 1051–1056.
[177] S.M. Molaei, H. Adelnia, A.M. Seif, J.N. Gavgani, Sulfonate-functionalized polyacrylonitrile-based nanoparticles; synthesis, and conversion to pH-sensitive nanogels, Colloid Polym. Sci. 297 (9) (2019) 1245–1253.
[178] C. Chen, Z. Zhu, X. Zhu, W. Yu, M. Liu, Q. Ge, W.-H. Shih, A composite hydrogels-based photonic crystal multi-sensor, Mater. Res. Express 2 (4) (2015), 046201.
[179] C. Chen, Y. Zhu, H. Bao, X. Yang, C. Li, Physically controlled cross-linking in gelated crystalline colloidal array photonic crystals, ACS Appl. Mater. Interfaces 2 (5) (2010) 1499–1504.
[180] N.A. Peppas, A.S. Hoffman, 1.3.2E - Hydrogels, in: W.R. Wagner, S.E. Sakiyama-Elbert, G. Zhang, M.J. Yaszemski (Eds.), Biomaterials Science (Fourth Edition), Academic Press2020, pp. 153-166.
[181] C. Chen, Z.-Q. Dong, J.-H. Shen, H.-W. Chen, Y.-H. Zhu, Z.-G. Zhu, 2D photonic crystal hydrogel sensor for tear glucose monitoring, ACS Omega 3 (3) (2018) 3211–3217.
[182] C. Chen, Y. Zhu, H. Bao, P. Zhao, H. Jiang, L. Peng, X. Yang, C. Li, Solvent-assisted poly (vinyl alcohol) gelated crystalline colloidal array photonic crystals, Soft Matter 7 (3) (2011) 915–921.
[183] N. Bonelli, G. Poggi, D. Chelazzi, R. Giorgi, P. Baglioni, Poly (vinyl alcohol)/poly (vinyl pyrrolidone) hydrogels for the cleaning of art, J. Colloid Interface Sci. 536 (2019) 339–348.
[184] R. Mastrangelo, D. Chelazzi, G. Poggi, E. Fratini, L.P. Buemi, M.L. Petruzzellis, P. Baglioni, Twin-chain polymer hydrogels based on poly (vinyl alcohol) as new advanced tool for the cleaning of modern and contemporary art, Proc. Natl. Acad. Sci. 117 (13) (2020) 7011–7020.
[185] R. Mehrandish, A. Rahimian, A. Shahriary, Heavy metals detoxification: A review of herbal compounds for chelation therapy in heavy metals toxicity, Journal of Herbmed Pharmacology 8 (2) (2019) 69–77.
[186] H. Bai, Z. Li, S. Zhang, W. Wang, W. Dong, Interpenetrating polymer networks in polyvinyl alcohol/cellulose nanocrystals hydrogels to develop absorbent materials, Carbohydr. Polym. 200 (2018) 468–476.
[187] E. Baigorria, L.A. Cano, L.M. Sanchez, V.A. Alvarez, R.P. Ollier, Bentonite-composite polyvinyl alcohol/alginate hydrogel beads: Preparation, characterization and their use as arsenic removal devices, Environ. Nanotechnol. Monit. Manage. 14 (2020), 100364.
[188] S.K. Mani, R. Bhandari, A. Nehra, Self-assembled cylindrical Zr (IV), Fe (III) and Cu (II) impregnated polyvinyl alcohol-based hydrogel beads for real-time application in fluoride removal, Colloids Surf., A 610 (2021), 125751.
[189] S.J. Lee, H.W. Lim, S.H. Park, Adsorptive seawater desalination using MOF-incorporated Cu-alginate/PVA beads: Ion removal efficiency and durability, Chemosphere 268 (2021), 128797.
[190] H. Adelnia, I. Blakey, P.J. Little, H.T. Ta, Hydrogels Based on Poly (aspartic acid): Synthesis and Applications, Front. Chem. 7 (2019) 755.
[191] H. Adelnia, H.D. Tran, P.J. Little, I. Blakey, H.T. Ta, Poly (aspartic acid) in Biomedical Applications: From Polymerization, Modification, Properties, Degradation, and Biocompatibility to Applications, ACS Biomaterials Science & Engineering 7 (6) (2021) 2083–2105.
[192] W. Lan, X. Zhang, M. Xu, L. Zhao, D. Huang, X. Wei, W. Chen, Carbon nanotube reinforced polyvinyl alcohol/biphasic calcium phosphate scaffold for bone tissue engineering, RSC Adv. 9 (67) (2019) 38998–39010.
[193] N. Alexandre, J. Ribeiro, A. Gärtner, T. Pereira, I. Amorim, J. Fragoso, A. Lopes, J. Fernandes, E. Costa, A. Santos-Silva, Biocompatibility and hemocompatibility of polyvinyl alcohol hydrogel used for vascular grafting—In vitro and in vivo studies, J. Biomed. Mater. Res. Part A 102 (12) (2014) 4262–4275.
[194] R. Hou, G. Zhang, G. Du, D. Zhan, Y. Cong, Y. Cheng, J. Fu, Magnetic nanohydroxyapatite/PVA composite hydrogels for promoted osteoblast adhesion and proliferation, Colloids Surf., B 103 (2013) 318–325.
[195] C.R. Nuttelman, D.J. Mortisen, S.M. Henry, K.S. Anseth, Attachment of fibronectin to poly (vinyl alcohol) hydrogels promotes NIH3T3 cell adhesion, proliferation, and migration, Journal of Biomedical Materials Research: An Official Journal of The Society for Biomaterials, The Japanese Society for Biomaterials, and The Australian Society for Biomaterials and the Korean Society for, Biomaterials 57 (2) (2001) 217–223.
[196] R.S. Del Guerra, M.G. Cascone, N. Barbani, L. Lazzeri, Biological characterization of hydrogels of poly (vinyl alcohol) and hyaluronic acid, J. Mater. Sci. - Mater. Med. 5 (9–10) (1994) 613–616.
[197] W.-H. Lin, J. Yu, G. Chen, W.-B. Tsai, Fabrication of multi-biofunctional gelatin-based electrospun fibrous scaffolds for enhancement of osteogenesis of mesenchymal stem cells, Colloids Surf., B 138 (2016) 26–31.
[198] L. Ding, S. Song, L. Chen, J. Shi, B. Zhao, G. Teng, J. Zhang, A freeze-thawing method applied to the fabrication of 3-d curdlan/polyvinyl alcohol hydrogels as scaffolds for cell culture, Int. J. Biol. Macromol. (2021).
[199] M.T. Khorasani, A. Joorabloo, H. Adeli, Z. Mansoori-Moghadam, A. Moghaddam, Design and optimization of process parameters of polyvinyl (alcohol)/chitosan/nano zinc oxide hydrogels as wound healing materials, Carbohydr. Polym. 207 (2019) 542–554.
[200] N.E. Vrana, Y. Liu, G.B. McGuinness, P.A. Cahill, Characterization of poly (vinyl alcohol)/chitosan hydrogels as vascular tissue engineering scaffolds, Macromolecular symposia, Wiley Online Library, 2008, pp. 106-110.
[201] W. Yang, E. Fortunati, F. Bertoglio, J. Owczarek, G. Bruni, M. Kozanecki, J. Kenny, L. Torre, L. Visai, D. Puglia, Polyvinyl alcohol/chitosan hydrogels with enhanced antioxidant and antibacterial properties induced by lignin nanoparticles, Carbohydr. Polym. 181 (2018) 275–284.
[202] R. Ensandoost, H. Izadi-Vasafi, H. Adelnia, Anti-Bacterial Activity of Chitosan-Alginate-Poly (Vinyl Alcohol) Hydrogel Containing Entrapped Peppermint Essential Oil, Journal of Macromolecular Science, Part B (2021) 1–13.
[203] R. Feng, R. Fu, Z. Duan, C. Zhu, X. Ma, D. Fan, X. Li, Preparation of sponge-like macroporous PVA hydrogels via n-HA enhanced phase separation and their potential as wound dressing, J. Biomater. Sci. Polym. Ed. 29 (12) (2018) 1463–1481.
[204] W. Luo, S. Zhang, P. Li, R. Xu, Y. Zhang, L. Liang, C.D. Wood, Q. Lu, B. Tan, Surfactant-free CO2-in-water emulsion-templated poly (vinyl alcohol)(PVA) hydrogels, Polymer 61 (2015) 183–191.
[205] L. Coluccino, R. Gottardi, F. Ayadi, A. Athanassiou, R.S. Tuan, L. Ceseracciu, Porous Poly (vinyl alcohol)-based hydrogel for knee meniscus functional repair, ACS Biomater. Sci. Eng. 4 (5) (2018) 1518–1527.
[206] J. Wang, F. Zhang, W.P. Tsang, C. Wan, C. Wu, Fabrication of injectable high strength hydrogel based on 4-arm star PEG for cartilage tissue engineering, Biomaterials 120 (2017) 11–21.
[207] L.E. Millon, C.J. Oates, W. Wan, Compression properties of polyvinyl alcohol–bacterial cellulose nanocomposite, Journal of Biomedical Materials

Research Part B: Applied Biomaterials: An Official Journal of The Society for Biomaterials, The Japanese Society for Biomaterials, and The Australian Society for Biomaterials and the Korean Society for, Biomaterials 90 (2) (2009) 922–929.
[208] J.A. Stammen, S. Williams, D.N. Ku, R.E. Guldberg, Mechanical properties of a novel PVA hydrogel in shear and unconfined compression, Biomaterials 22 (8) (2001) 799–806.
[209] M. Oka, K. Ushio, P. Kumar, K. Ikeuchi, S. Hyon, T. Nakamura, H. Fujita, Development of artificial articular cartilage, Proc. Inst. Mech. Eng. [H] 214 (1) (2000) 59–68.
[210] Y.-S. Pan, D.-S. Xiong, R.-Y. Ma, A study on the friction properties of poly (vinyl alcohol) hydrogel as articular cartilage against titanium alloy, Wear 262 (7–8) (2007) 1021–1025.
[211] W. Święszkowski, D.N. Ku, H.E. Bersee, K.J. Kurzydlowski, An elastic material for cartilage replacement in an arthritic shoulder joint, Biomaterials 27 (8) (2006) 1534–1541.
[212] M. Kobayashi, Y.-S. Chang, M. Oka, A two year in vivo study of polyvinyl alcohol-hydrogel (PVA-H) artificial meniscus, Biomaterials 26 (16) (2005) 3243–3248.
[213] D. Zhang, J. Duan, D. Wang, S. Ge, Effect of preparation methods on mechanical properties of PVA/HA composite hydrogel, J. Bionic Eng. 7 (3) (2010) 235–243.
[214] J. Venkatesan, S.-K. Kim, Nano-hydroxyapatite composite biomaterials for bone tissue engineering—a review, J. Biomed. Nanotechnol. 10 (10) (2014) 3124–3140.
[215] Y. Pan, D. Xiong, Friction properties of nano-hydroxyapatite reinforced poly (vinyl alcohol) gel composites as an articular cartilage, Wear 266 (7–8) (2009) 699–703.
[216] X. Huang, Y. Zuo, J. Li, Y. Li, Study on crystallisation of nano-hydroxyapatite/polyvinyl alcohol composite hydrogel, Mater. Res. Innovations 13 (2) (2009) 98–102.
[217] A.S. Maiolo, M.N. Amado, J.S. Gonzalez, V.A. Alvarez, Development and characterization of poly (vinyl alcohol) based hydrogels for potential use as an articular cartilage replacement, Mater. Sci. Eng., C 32 (6) (2012) 1490–1495.
[218] Y. Ma, T. Bai, F. Wang, The physical and chemical properties of the polyvinylalcohol/polyvinylpyrrolidone/hydroxyapatite composite hydrogel, Mater. Sci. Eng., C 59 (2016) 948–957.
[219] X. Fenglan, L. Yubao, W. Xuejiang, W. Jie, Y. Aiping, Preparation and characterization of nano-hydroxyapatite/poly (vinyl alcohol) hydrogel biocomposite, J. Mater. Sci. 39 (18) (2004) 5669–5672.
[220] D. Kharaghani, D. Dutta, K.K. Ho, K.-Q. Zhang, W. Kai, X. Ren, M.D. Willcox, I. S. Kim, Active loading graphite/hydroxyapatite into the stable hydroxyethyl cellulose scaffold nanofibers for artificial cornea application, Cellulose (2020) 1–16.
[221] J. Holzinger, H. Kotisch, K.W. Richter, R. Konrat, Binding Mode Characterization of Osteopontin on Hydroxyapatite by Solution NMR Spectroscopy, ChemBioChem (2021).
[222] Y. Zheng, H. Lv, Y. Wang, H. Lu, L. Qing, T. Xi, Performance of novel bioactive hybrid hydrogels in vitro and in vivo used for artificial cartilage, Biomed. Mater. 4 (1) (2008), 015015.
[223] S.A. Poursamar, M. Azami, M. Mozafari, Controllable synthesis and characterization of porous polyvinyl alcohol/hydroxyapatite nanocomposite scaffolds via an in situ colloidal technique, Colloids Surf., B 84 (2) (2011) 310–316.
[224] A. Sinha, A. Guha, Biomimetic patterning of polymer hydrogels with hydroxyapatite nanoparticles, Mater. Sci. Eng., C 29 (4) (2009) 1330–1333.
[225] K. Chen, G. Chen, S. Wei, X. Yang, D. Zhang, L. Xu, Preparation and property of high strength and low friction PVA-HA/PAA composite hydrogel using annealing treatment, Mater. Sci. Eng., C 91 (2018) 579–588.
[226] S. Cavalu, L. Fritea, M. Brocks, K. Barbaro, G. Murvai, T.O. Costea, I. Antoniac, C. Verona, M. Romani, A. Latini, Novel Hybrid Composites Based on PVA/SeTiO2 Nanoparticles and Natural Hydroxyapatite for Orthopedic Applications: Correlations between Structural, Morphological and Biocompatibility Properties, Materials 13 (9) (2020) 2077.
[227] J.S. Gonzalez, V.A. Alvarez, Mechanical properties of polyvinylalcohol/hydroxyapatite cryogel as potential artificial cartilage, J. Mech. Behav. Biomed. Mater. 34 (2014) 47–56.
[228] W. Song, D.C. Markel, X. Jin, T. Shi, W. Ren, Poly (vinyl alcohol)/collagen/hydroxyapatite hydrogel: Properties and in vitro cellular response, J. Biomed. Mater. Res. Part A 100 (11) (2012) 3071–3079.
[229] A. Parameswaran-Thankam, Q. Al-Anbaky, Z. Al-karakooly, A.B. RanguMagar, B. P. Chhetri, N. Ali, A. Ghosh, Fabrication and characterization of hydroxypropyl guar-poly (vinyl alcohol)-nano hydroxyapatite composite hydrogels for bone tissue engineering, J. Biomater. Sci. Polym. Ed. 29 (17) (2018) 2083–2105.
[230] S. Gan, W. Lin, Y. Zou, B. Xu, X. Zhang, J. Zhao, J. Rong, Nano-hydroxyapatite enhanced double network hydrogels with excellent mechanical properties for potential application in cartilage repair, Carbohydr. Polym. 229 (2020), 115523.
[231] Y. Wang, Y. Xue, J. Wang, Y. Zhu, X. Wang, X. Zhang, Y. Zhu, J. Liao, X. Li, X. Wu, Biocompatible and photoluminescent carbon dots/hydroxyapatite/PVA dual-network composite hydrogel scaffold and their properties, J. Polym. Res. 26 (11) (2019) 248.
[232] T. Itoi, H. Isayama, A. Sofuni, F. Itokawa, T. Kurihara, T. Tsuchiya, S. Tsuji, K. Ishii, N. Ikeuchi, R. Tanaka, Stent selection and tips on placement technique of EUS-guided biliary drainage: transduodenal and transgastric stenting, Journal of hepato-biliary-pancreatic sciences 18 (5) (2011) 664–672.
[233] H. Mohammadi, D. Boughner, L. Millon, W. Wan, Design and simulation of a poly (vinyl alcohol)—bacterial cellulose nanocomposite mechanical aortic heart valve prosthesis, Proc. Inst. Mech. Eng. [H] 223 (6) (2009) 697–711.
[234] H. Mohammadi, Nanocomposite biomaterial mimicking aortic heart valve leaflet mechanical behaviour, Proc. Inst. Mech. Eng. [H] 225 (7) (2011) 718–722.
[235] L. Musumeci, N. Jacques, A. Hego, A. Nchimi, P. Lancellotti, C. Oury, Prosthetic aortic valves: challenges and solutions, Frontiers in cardiovascular medicine 5 (2018) 46.
[236] J.-Y. Qian, Z.-X. Gao, C.-W. Hou, Z.-J. Jin, A comprehensive review of cavitation in valves: mechanical heart valves and control valves, Bio-Design and Manufacturing 2 (2) (2019) 119–136.
[237] H. Jiang, G. Campbell, D. Boughner, W.-K. Wan, M. Quantz, Design and manufacture of a polyvinyl alcohol (PVA) cryogel tri-leaflet heart valve prosthesis, Med. Eng. Phys. 26 (4) (2004) 269–277.
[238] L.E. Millon, M.-P. Nieh, J.L. Hutter, W. Wan, SANS characterization of an anisotropic poly (vinyl alcohol) hydrogel with vascular applications, Macromolecules 40 (10) (2007) 3655–3662.
[239] M. Atlan, T. Simon-Yarza, J. Ino, V. Hunsinger, L. Corté, P. Ou, R. Aid-Launais, M. Chaouat, D. Letourneur, Design, characterization and in vivo performance of synthetic 2 mm-diameter vessel grafts made of PVA-gelatin blends, Sci. Rep. 8 (1) (2018) 1–12.
[240] C.J. Boyer, M. Boktor, H. Samant, L.A. White, Y. Wang, D.H. Ballard, R. C. Huebert, J.E. Woerner, G.E. Ghali, J.S. Alexander, 3D printing for bio-synthetic biliary stents, Bioengineering 6 (1) (2019) 16.
[241] M.-C. Lin, C.-W. Lou, J.-Y. Lin, T.A. Lin, Y.-S. Chen, J.-H. Lin, Fabrication of a biodegradable multi-layered polyvinyl alcohol stent, Fibers Polym. 19 (8) (2018) 1596–1604.
[242] M.-Y. Xing, C.-L. Yu, Y.-F. Wu, L. Wang, G.-P. Guan, Preparation and characterization of a polyvinyl alcohol/polyacrylamide hydrogel vascular graft reinforced with a braided fiber stent, Text. Res. J. 90 (13–14) (2020) 1537–1548.
[243] M.-C. Lin, C.-W. Lou, J.-Y. Lin, T.A. Lin, Y.-S. Chen, J.-H. Lin, Biodegradable polyvinyl alcohol vascular stents: structural model and mechanical and biological property evaluation, Mater. Sci. Eng., C 91 (2018) 404–413.
[244] Y. Liu, N. Vrana, P. Cahill, G. McGuinness, Physically crosslinked composite hydrogels of PVA with natural macromolecules: structure, mechanical properties, and endothelial cell compatibility, Journal of Biomedical Materials Research Part B: Applied Biomaterials: An Official Journal of The Society for Biomaterials, The Japanese Society for Biomaterials, and The Australian Society for Biomaterials and the Korean Society for, Biomaterials 90 (2) (2009) 492–502.
[245] I. George Broughton, J.E. Janis, C.E. Attinger, The basic science of wound healing, Plast. Reconstr. Surg. 117 (7S) (2006) 12S–34S.
[246] J.S. Boateng, K.H. Matthews, H.N. Stevens, G.M. Eccleston, Wound healing dressings and drug delivery systems: a review, J. Pharm. Sci. 97 (8) (2008) 2892–2923.
[247] S. Cascone, G. Lamberti, Hydrogel-based commercial products for biomedical applications: A review, Int. J. Pharm. 573 (2020), 118803.
[248] M. Madaghiele, C. Demitri, A. Sannino, L. Ambrosio, Polymeric hydrogels for burn wound care: Advanced skin wound dressings and regenerative templates, Burns & trauma 2(4) (2014) 2321-3868.143616.
[249] S.-Y. Lin, K.-S. Chen, L. Run-Chu, Design and evaluation of drug-loaded wound dressing having thermoresponsive, adhesive, absorptive and easy peeling properties, Biomaterials 22 (22) (2001) 2999–3004.
[250] M. Babu, Collagen based dressings—a review, Burns 26 (1) (2000) 54–62.
[251] E.A. Kamoun, E.-R.-S. Kenawy, X. Chen, A review on polymeric hydrogel membranes for wound dressing applications: PVA-based hydrogel dressings, J. Adv. Res. 8 (3) (2017) 217–233.
[252] A.A. Shefa, T. Sultana, M.K. Park, S.Y. Lee, J.-G. Gwon, B.-T. Lee, Curcumin incorporation into an oxidized cellulose nanofiber-polyvinyl alcohol hydrogel system promotes wound healing, Mater. Des. 186 (2020), 108313.
[253] S. Ray, H. Adelnia, H.T. Ta, Collagen and the Effect of Poly-L-lactic Acid based Materials on its Synthesis, Biomaterials, Science (2021).
[254] S. Tavakoli, A.S. Klar, Advanced Hydrogels as Wound Dressings, Biomolecules 10 (8) (2020) 1169.
[255] O. Catanzano, V. D'esposito, S. Acierno, M. Ambrosio, C. De Caro, C. Avagliano, P. Russo, R. Russo, A. Miro, F. Ungaro, Alginate–hyaluronan composite hydrogels accelerate wound healing process, Carbohydr. Polym. 131 (2015) 407–414.
[256] J. Koehler, F.P. Brandl, A.M. Goepferich, Hydrogel wound dressings for bioactive treatment of acute and chronic wounds, Eur. Polym. J. 100 (2018) 1–11.
[257] S. Ahmed, S. Ikram, Chitosan based scaffolds and their applications in wound healing, Achiev. Life Sci. 10 (1) (2016) 27–37.
[258] X. Yang, K. Yang, S. Wu, X. Chen, F. Yu, J. Li, M. Ma, Z. Zhu, Cytotoxicity and wound healing properties of PVA/ws-chitosan/glycerol hydrogels made by irradiation followed by freeze–thawing, Radiat. Phys. Chem. 79 (5) (2010) 606–611.
[259] M.-H. Huang, M.-C. Yang, Evaluation of glucan/poly (vinyl alcohol) blend wound dressing using rat models, Int. J. Pharm. 346 (1–2) (2008) 38–46.
[260] Y. Zhang, M. Jiang, Y. Zhang, Q. Cao, X. Wang, Y. Han, G. Sun, Y. Li, J. Zhou, Novel lignin–chitosan–PVA composite hydrogel for wound dressing, Mater. Sci. Eng., C 104 (2019), 110002.
[261] G. Franci, A. Falanga, S. Galdiero, L. Palomba, M. Rai, G. Morelli, M. Galdiero, Silver nanoparticles as potential antibacterial agents, Molecules 20 (5) (2015) 8856–8874.
[262] S. Tang, J. Zheng, Antibacterial activity of silver nanoparticles: structural effects, Adv. Healthcare Mater. 7 (13) (2018) 1701503.
[263] S. Bhowmick, V. Koul, Assessment of PVA/silver nanocomposite hydrogel patch as antimicrobial dressing scaffold: Synthesis, characterization and biological evaluation, Mater. Sci. Eng., C 59 (2016) 109–119.

[264] A. Ahsan, M.A. Farooq, Therapeutic potential of green synthesized silver nanoparticles loaded PVA hydrogel patches for wound healing, J. Drug Delivery Sci. Technol. 54 (2019), 101308.
[265] W. Yang, F. Xu, X. Ma, J. Guo, C. Li, S. Shen, D. Puglia, J. Chen, P. Xu, J. Kenny, Highly-toughened PVA/nanocellulose hydrogels with anti-oxidative and antibacterial properties triggered by lignin-Ag nanoparticles, Mater. Sci. Eng., C 129 (2021), 112385.
[266] A. Chaturvedi, A.K. Bajpai, J. Bajpai, S.K. Singh, Evaluation of poly (vinyl alcohol) based cryogel–zinc oxide nanocomposites for possible applications as wound dressing materials, Mater. Sci. Eng., C 65 (2016) 408–418.
[267] R. Ma, Y. Wang, H. Qi, C. Shi, G. Wei, L. Xiao, Z. Huang, S. Liu, H. Yu, C. Teng, Nanocomposite sponges of sodium alginate/graphene oxide/polyvinyl alcohol as potential wound dressing: In vitro and in vivo evaluation, Compos. B Eng. 167 (2019) 396–405.
[268] L. Wang, Performance Testing of Textiles: Methods, Technology and Applications, Woodhead Publishing, 2016.
[269] R. Xu, H. Xia, W. He, Z. Li, J. Zhao, B. Liu, Y. Wang, Q. Lei, Y. Kong, Y. Bai, Controlled water vapor transmission rate promotes wound-healing via wound re-epithelialization and contraction enhancement, Sci. Rep. 6 (1) (2016) 1–12.
[270] A. Chaturvedi, A. Bajpai, J. Bajpai, Preparation and characterization of poly (vinyl alcohol) cryogel-silver nanocomposites and evaluation of blood compatibility, cytotoxicity, and antimicrobial behaviors, Polym. Compos. 36 (11) (2015) 1983–1997.
[271] M.C. Catoira, L. Fusaro, D. Di Francesco, M. Ramella, F. Boccafoschi, Overview of natural hydrogels for regenerative medicine applications, J. Mater. Sci. - Mater. Med. 30 (10) (2019) 1–10.
[272] K.I. Draget, C. Taylor, Chemical, physical and biological properties of alginates and their biomedical implications, Food Hydrocolloids 25 (2) (2011) 251–256.
[273] K.B. Narayanan, S.S. Han, Dual-crosslinked poly (vinyl alcohol)/sodium alginate/silver nanocomposite beads–A promising antimicrobial material, Food Chem. 234 (2017) 103–110.
[274] G.K. Tummala, T. Joffre, V.R. Lopes, A. Liszka, O. Buznyk, N. Ferraz, C. Persson, M. Griffith, A. Mihranyan, Hyperelastic nanocellulose-reinforced hydrogel of high water content for ophthalmic applications, ACS Biomater. Sci. Eng. 2 (11) (2016) 2072–2079.
[275] S.-H. Hyon, W.-I. Cha, Y. Ikada, M. Kita, Y. Ogura, Y. Honda, Poly (vinyl alcohol) hydrogels as soft contact lens material, J. Biomater. Sci. Polym. Ed. 5 (5) (1994) 397–406.
[276] M. Åhlén, G.K. Tummala, A. Mihranyan, Nanoparticle-loaded hydrogels as a pathway for enzyme-triggered drug release in ophthalmic applications, Int. J. Pharm. 536 (1) (2018) 73–81.
[277] D. Kharaghani, D. Dutta, P. Gitigard, Y. Tamada, A. Katagiri, D.-N. Phan, M. D. Willcox, I.S. Kim, Development of antibacterial contact lenses containing metallic nanoparticles, Polym. Test. 79 (2019), 106034.
[278] P. Sekar, A. Chauhan, Effect of vitamin-E integration on delivery of prostaglandin analogs from therapeutic lenses, J. Colloid Interface Sci. 539 (2019) 457–467.
[279] P. Dixon, R.C. Fentzke, A. Bhattacharya, A. Konar, S. Hazra, A. Chauhan, In vitro drug release and in vivo safety of vitamin E and cysteamine loaded contact lenses, Int. J. Pharm. 544 (2) (2018) 380–391.
[280] X. Fan, C. Torres-Luna, M. Azadi, R. Domszy, N. Hu, A. Yang, A.E. David, Evaluation of commercial soft contact lenses for ocular drug delivery: a review, Acta Biomater. (2020).
[281] F. Stapleton, S. Stretton, E. Papas, C. Skotnitsky, D.F. Sweeney, Silicone hydrogel contact lenses and the ocular surface, The ocular surface 4 (1) (2006) 24–43.
[282] C. Peng, J. Xu, G. Chen, J. Tian, M. He, The preparation of α-chitin nanowhiskers-poly (vinyl alcohol) hydrogels for drug release, Int. J. Biol. Macromol. 131 (2019) 336–342.
[283] Y. Jiang, Y. Yang, X. Zheng, Y. Yi, X. Chen, Y. Li, D. Sun, L. Zhang, Multifunctional load-bearing hybrid hydrogel with combined drug release and photothermal conversion functions, NPG Asia Mater. 12 (1) (2020) 1–11.
[284] I. Galeska, T.-K. Kim, S.D. Patil, U. Bhardwaj, D. Chatttopadhyay, F. Papadimitrakopoulos, D.J. Burgess, Controlled release of dexamethasone from PLGA microspheres embedded within polyacid-containing PVA hydrogels, The AAPS journal 7 (1) (2005) E231–E240.
[285] A. Zhang, J. Yu, G. Wang, X. Wang, L. Zhang, Improving the emulsion freeze-thaw stability of soy protein hydrolysate-dextran conjugates, LWT 116 (2019), 108506.
[286] H. Feng, H. Jin, Y. Gao, S. Yan, Y. Zhang, Q. Zhao, J. Xu, Effects of freeze-thaw cycles on the structure and emulsifying properties of peanut protein isolates, Food Chem. 330 (2020), 127215.
[287] Y. Wu, R. Zhang, H.D. Tran, N.D. Kurniawan, S.S. Moonshi, A.K. Whittaker, H. T. Ta, Chitosan Nanococktails Containing Both Ceria and Superparamagnetic Iron Oxide Nanoparticles for Reactive Oxygen Species-Related Theranostics, ACS Applied Nano Materials 4 (4) (2021) 3604–3618.
[288] P. Severino, C.F. da Silva, L.N. Andrade, D. de Lima Oliveira, J. Campos, E. B. Souto, Alginate nanoparticles for drug delivery and targeting, Curr. Pharm. Des. 25 (11) (2019) 1312–1334.
[289] J.K. Li, N. Wang, X.S. Wu, Poly (vinyl alcohol) nanoparticles prepared by freezing–thawing process for protein/peptide drug delivery, J. Control. Release 56 (1–3) (1998) 117–126.
[290] J. Schulze, S. Hendrikx, M. Schulz-Siegmund, A. Aigner, Microparticulate poly (vinyl alcohol) hydrogel formulations for embedding and controlled release of polyethylenimine (PEI)-based nanoparticles, Acta Biomater. 45 (2016) 210–222.
[291] A. Zakeri, M.A.J. Kouhbanani, N. Beheshtkhoo, V. Beigi, S.M. Mousavi, S.A. R. Hashemi, A. Karimi Zade, A.M. Amani, A. Savardashtaki, E. Mirzaei, Polyethylenimine-based nanocarriers in co-delivery of drug and gene: a developing horizon, Nano reviews & experiments 9 (1) (2018) 1488497.
[292] N.K. Mongia, K.S. Anseth, N.A. Peppas, Mucoadhesive poly (vinyl alcohol) hydrogels produced by freezing/thawing processes: applications in the development of wound healing systems, J. Biomater. Sci. Polym. Ed. 7 (12) (1996) 1055–1064.
[293] C.F. Vecchi, R.S. Dos Santos, M.L. Bruschi, Technological development of mucoadhesive film containing poloxamer 407, polyvinyl alcohol and polyvinylpyrrolidone for buccal metronidazole delivery, Therapeutic delivery 11 (7) (2020) 431–446.
[294] S. Zadeh, S. Rajabnezhad, M. Zandkarimi, S. Dahmardeh, L. Mir, M. Darbandi, M. Rajabnejad, Mucoadhesive microspheres of chitosan and polyvinyl alcohol as a carrier for intranasal delivery of insulin: in vitro and in vivo studies, MOJ Bioequiv Availab 3 (2) (2017) 00030.
[295] N. Niknia, R. Kadkhodaee, Gum tragacanth-polyvinyl alcohol cryogel and xerogel blends for oral delivery of silymarin: Structural characterization and mucoadhesive property, Carbohydr. Polym. 177 (2017) 315–323.
[296] B. Gajra, S.S. Pandya, S. Singh, H.A. Rabari, Mucoadhesive hydrogel films of econazole nitrate: formulation and optimization using factorial design, Journal of drug delivery 2014 (2014).
[297] K. Tsutsumi, K. Takayama, Y. Machida, C. Ebert, I. Nakatomi, Formulation of buccal mucoadhesive dosage form of ergotamine tartrate, STP pharma sciences 4 (3) (1994) 230–234.
[298] M.M. Abdel-Mottaleb, N. Mortada, A. El-Shamy, G. Awad, Physically cross-linked polyvinyl alcohol for the topical delivery of fluconazole, Drug Dev. Ind. Pharm. 35 (3) (2009) 311–320.